FREEFORM FABRICATION OF MULTI-FUNCTIONAL COMPOSITE STRUCTURES

By

DAVID ERIC ROBERTS

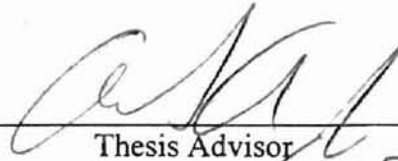Bachelor of Science

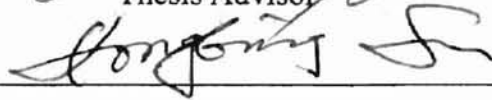Oklahoma State University

Stillwater, Oklahoma

1999

Submitted to the Faculty of the
Graduate College of
Oklahoma State University
in partial fulfillment of
the requirements for
the Degree of
MASTER OF SCIENCE
August, 2001

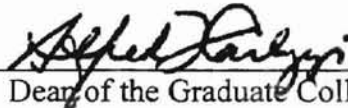# FREEFORM FABRICATION OF MULTI-FUNCTIONAL COMPOSITE STRUCTURES

Thesis Approved:

_____
Thesis Advisor

_____

_____
C.E. Price

_____
Dean of the Graduate College

ACKNOWLEDGEMENTS

TABLE OF CONTENTS

LIST OF TABLES

LIST OF FIGURES

NOMENCLATURE

CAD	Computer-Aided Design
C_D	Drag Coefficient
C_L	Lift Coefficient
CNC	Computer Numeric Controlled
CTD	Cold Temperature/Dry
DPM	Di-Propylene Glycol Monomethyl Ether
ETW	Elevated Temperature/Wet
FDM	Fused Deposition Modeling
GFM	Green Flexural Modulus
HTM	High Temperature Moulding
HX	Heat Exchanger
LOM	Laminated Object Manufacturing
LTM	Low Temperature Moulding
MTM	Medium Temperature Moulding
PAN	Polyacrylonitrile
QC	QuickCast™
RP	Rapid Prototyping
RTD	Room Temperature/Dry

SL	Stereolithography
SLA	Stereolithography Apparatus
SLS	Selective Laser Sintering
T_{bath}	Temperature of Water Bath
$T_{curing\ fixture}$	Surface Temperature of Curing Fixture
T_g	Glass Transition Temperature
t_{nom}	Nominal Ply Thickness
TPM	Tri-Propylene Glycol Monomethyl Ether
UV	Ultraviolet
α	Angle of Attack
$\Delta\theta$	Change in Angle
ΔT	Change in Temperature
θ_i	Initial Angle
ρ	Density

CHAPTER 1

1. INTRODUCTION

1.1   Background

1.1.1   Advanced Composites

Advanced composites have been researched by the aerospace industry since the 1960s. Manufacturers became aware that they needed to find new materials that were durable, strong, pliable, and inexpensive. Mankind has not yet found the absolutely ideal material, and whereas composites have their flaws, they still offer an enticing package to the aerospace community.

Advanced composites consist of high strength, high modulus reinforcement fibers suspended in a homogeneous resin matrix. Reinforcement fibers are typically graphite, aramid, or fiberglass, while typical resins include polyester and a variety of epoxies. Carbon or graphite fiber composites may be prefabricated as either unidirectional tape or multidirectional weave fabric. Mechanical properties are not equivalent in all directions of the tape or fabric. Thus, composites are "anisotropic," whereas metals, for example, are isotropic.

A resin matrix is necessary to bond the composite fibers securely to a surface and to each other. It is the matrix that transfers load from fiber to fiber. Commonly, graphite

fiber fabrics will be produced as "prepreg," composite fabrics that are run through an epoxy bath and ready for immediate application to a surface. Once the carbon fiber is applied to a surface, it must be cured at a higher temperature for a predetermined length of time, where the length of time depends on the cure temperature and the type of prepreg being applied. Furthermore, it must have a constant force applied to it, as carbon fiber tends to straighten as it cures. The most common method of curing is by way of an autoclave or oven and vacuum bag. The oven provides the cure temperature, and the vacuum bag allows air pressure to apply constant force throughout the curing process. This results in a cured composite laminate that adheres to the contours of a surface.

1.1.2   Stereolithography

Stereolithography (SL) is just one form of rapid prototyping (RP). Other methods include Laminated Object Manufacturing (LOM), Fused Deposition Modeling (FDM), and Selective Laser Sintering (SLS). SL is a liquid-based RP method, which means that it relies on the curing of a liquid to form a recognizable 3D model, and this is done using a stereolithography apparatus (SLA).

The SL technique was developed by Charles Hull in the late 1970's and early 1980's and commercialized by 3D Systems between 1986 and 1988. [Jacobs, 1992] Although the first SLA model was introduced in 1988, newer models have been released as time has passed. An early model was the SLA-250, which employed a 16 mW He:Cd laser scanning in the x-y plane at 0.762 m/s. [Fai and Kai, 1997] One of the most current models is the SLA-7000, which employs an 800 mW solid state Nd: YVO_4 laser scanning in the x-y plane at up to 9.52 m/s (depending on the beam diameter). [3D Systems, 2001]

2

As SLA products increase in accuracy, so do their usefulness. The most obvious was use within the manufacturing middle. To create a prototype using SLA may result in time and money savings of up to 80%. [Jacobs, 1996] With the introduction of Quick-Cast^{TM} – a quasi-hollow build style – in 1993, SLA parts became useful for creating ceramic shell molds. SLA models could be covered by a ceramic shell and eliminated by means of flash firing, resulting in a functional mold for molten metal. [Jacobs, 1996]

Since the inception of QuickCast^{TM}, SLA parts have become available for many applications. Furthermore, development of stronger, more durable resins have made SLA models candidates for usable parts beyond the prototyping phase. Many aerospace companies employ SL for model development, ranging from wind-tunnel testing to early-phase conceptualization. Current research is now underway that will pave the way for SLA parts to be used in final products, not just prototypes. The marriage of SLA and carbon fiber composites along with imbedded functionality is a step in that direction.

1.2   Research Objective

The objective of this research is to take the advantages of advanced composites, which include high strength-to-weight ratio and high corrosion resistance, and the advantages of stereolithography, which include swift part production and cost-efficiency, and combine them.

Early stages of this research explore the application of carbon fiber fabric to SLA substructures and the design of multifunctional SLA parts. SLA parts can be designed to house a variety of functionalities. The imbedded functions examined here include pressure taps, heat exchanger tubing, and thermocouple grooves. Imbedded pressure taps are

useful for measure pressure distribution over a variety of surfaces within a flow. Imbedded heat exchangers are useful for both heating and cooling applications. An example of this would be a deicing mechanism on the leading edge of a wing. Imbedded thermocouples are useful for recording temperature data on a part, but without the need to externally fasten the wire to the part. Later stages of this research involve the implementation of imbedded functionality to explore a new method of curing composites – a method that would not require an oven and vacuum bag. Furthermore, this method would allow for easy monitoring of a composite while it cures.

It is hoped that the results of this research will show the viability of the designs and methods explored, and that the imbedding of multiple functionalities into a part will prove to be useful for many applications. Furthermore, successful marriage of advanced composites and stereolithography will result in a new domain of research, development, and manufacturing. Please note that this process and the studies performed in this research effort are part of a patent-pending effort, owned by Freeform Composites, Inc. and its parent company, SharedReplicators, Inc. [Jones, 2000]

CHAPTER 2

2. LITERATURE SURVEY

In the study of composite laminates used in conjunction with rapid prototyping, there are a variety of factors to be considered at the onset. One must select from a myriad of rapid prototyping (RP) methods, and accordingly, choose the appropriate material to be used within that method. Also, the type of composite laminate must be considered.

The literature review covers stereolithography (SL) and advanced composites. In the review of SL, advancements in the apparatus and materials, the build process, and product applications are explored. In the review of composites, the materials and curing procedures are discussed.

2.1   Stereolithography

The RP method of choice for this project was stereolithography, a liquid-based method. The word itself is derived from the words *stereo-*, which means "solid body" or "having or dealing with three dimensions of space," and *lithography*, which means "the process of printing." [*Merriam-Webster*, 1993] Combining the two words results in *stereolithography*, which means "3-D printing." Thus, the resulting product of a stereo-lithography apparatus (SLA) is a 3-D solid model.

2.1.1   SLA Technological Advancements

Among the first SLA models was the SLA-250. It could produce parts with a layer resolution of approximately 0.004 inches. It utilized a He:Cd laser beam that had a beam diameter with a resolution of approximately 0.0078 inches. [Fai and Kai, 1997] Since the introduction of the SLA-250, a variety of newer SLA models have been introduced. One of the most current models is the SLA-7000. This model can produce parts that have a layer thickness as thin as 0.001 inches. It implements a high-resolution solid state Nd: YVO_4 laser with a beam diameter as short as 0.009 inches. [3D Systems, 2001] Table 2.1 shows a comparison of some of the more popular models.

Table 2.1 Comparison of selected SLA models

Model	SLA-250	SLA-500	SLA-3500	SLA-5000	SLA-7000
Laser Type	He:Cd	Argon Ion	Solid State Nd: YVO_4	Solid State triple freq. Nd: YVO_4	Solid State triple freq. Nd: YVO_4
Max Laser Power (mW)	16	264	160	218	800
Min Spot Size (in)	0.008	0.008	0.008	0.008	0.009
Max XY Scan Speed (ft/s)	2.5	16.4	8.33	16.4	31.2
Elevator Vertical Resolution (in)	0.0001	0.00007	0.00007	0.00007	0.00004
Minimum Layer Thickness (in)*	0.004	0.004	0.002	0.002	0.001
Work Volume XYZ (in x in x in)	9.8 x 9.8 x 9.8	20 x 20 x 23	13.8 x 13.8 x 15.7	20 x 20 x 23	20 x 20 x 23.62

* Minimum layer thickness is dependent upon part geometry, build parameters, and material.

Table 2.1 shows the evolution from the SLA-250 to the SLA-7000. The only characteristic that does not seem to improve from model to model is the minimum laser spot size. However, for each model the spot size may vary depending upon the build

mission. Spot size is also related to the drawing speed. For example, on the SLA-7000, a maximum XY drawing speed of 31.2 ft/s can be achieved if the beam diameter is considered a "large spot" (0.027 in – 0.033 in). If the beam diameter is within the "small spot" range (0.009 in – 0.011 in), then the maximum achievable XY drawing speed is 8.33 ft/s. [3D Systems, 2001] The SLA model evolution shows that improvements have been made since the first model was released in 1988. Over time, models with faster drawing speeds, improved beam and layer resolution, and faster recoating systems will likely be developed.

2.1.2   SLA Photopolymers and Resins

There are many companies that produce a myriad of resins that may be used in an SLA. Each resin has its own properties. Thus, differing applications may require use of different resins. This section covers the chemistry and properties of photopolymers and resins, and it lists some of the current resins available.

2.1.2.1   Chemistry of Photopolymers

Polymerization is defined as the process of linking monomers into polymers comprised of many monomers. [Jacobs, 1992] If a monomer has more than one reactive per molecule, it is said to be "multifunctional." Polymerization of these multifunctional monomers results in a cross-linked polymer, a continuous insoluble network of molecules.

Photopolymerization occurs when photoinitiator molecules are mixed with monomers. As the photoinitiators are exposed to a UV source, they become excited and

7

activate nearby monomers. This begins a complex chain reaction that results in the cross-linking of the activated monomers. The reaction propagates until a chain inhibition process terminates it. [Jacobs, 1996] Such polymerization at the molecular level results in solidification of a liquid. In SL, the covalent bonds within the cross-linked polymer must be strong enough so that it does not redissolve into the constituent liquid monomers.

Relevant to SL are acrylate chemistry and cationic photopolymerization. Acrylate systems use a free-radical mechanism during the polymerization process, and the photo speed of these photopolymers is high. However, if the UV exposure is insufficient during the cure process, then the surfaces may not be fully cured. Furthermore, free-radical systems are prone to oxygen inhibition, which results in surfaces that are not fully cured if UV exposure is insufficient. [Jacobs, 1996]

Cationic photopolymerization has been used more recently in SL. Here, the reactions are not inhibited by ambient oxygen but may be inhibited by humidity and bases. Also, photopolymers resulting from this reaction show a continued thermal curing following the photocure. However, these resins generally have a slower photospeed than the free-radical resins. [Jacobs, 1996]

SL photopolymers can be classified as acrylate, vinylester, or epoxy. This classification is based on the type of reaction that enables cross-linking. The acrylate system incorporates the free-radical reaction. The vinylester and epoxy systems utilize the cationic reaction. The difference between vinylester and epoxy systems stems from the molecular structure of the two monomers. Although both monomers are of the form C_2H_3OR, epoxy monomers are characterized by a ring structure, whereas vinylester monomers are characterized by a double bond between the carbon atoms. [Jacobs, 1996]

8

2.1.2.2   Properties of Photopolymers

Each type of resin system has its own unique chemistry, and therefore, each system exhibits its own unique properties. However, regardless of which resin is being used, there are general property issues that apply to all resins used in SL applications.

The first property is "green strength," named so because the state of the resin immediately after it is laser-cured is known as the "green state." Green strength is a general property that includes Young's modulus, tensile and flexural strengths, strain, hardness, and layer-to-layer adhesion. [Jacobs, 1996] Without sufficient green strength, the cured layers would be unable to resist the viscous forces of the uncured resin during the building process.

This property is a function of several factors including beam diameter, layer thickness, hatch spacing, and cure depth. Previously, tests using strips built with epoxy and acrylate resins demonstrated that epoxies have a green flexural modulus (GFM) 5 to 12 times greater than that of acrylates. [Jacobs, 1996] The results from these tests, however, are only specific to the resins used for them. The general conclusion is that epoxy GFM is greater than acrylate GFM.

Another property is volumetric shrinkage. As a resin is cured during the SL process, it undergoes a finite amount of shrinkage. Generally, the total shrinkage over the entire cure process (including post-cure) is roughly 6%, but it could easily vary from system to system and resin to resin. [Jacobs, 1996] Experiments run in the early 1990s have demonstrated that total volumetric shrinkage was somewhat dependent upon part geometry, but in those tests, the total shrinkage was never more than 1.5%. [Daily, 1991] Some

other factors that affected the shrinkage in these tests were build orientation, layer thickness, cross-hatch size, shrinkage factor, and post-curing time.

Another property to consider is curl. "Curl" is a type of distortion that can occur in any RP process that builds successive layers and in which the solidifying material undergoes shrinkage. Typically, the first of any cantilevered layer will bend upward after the addition of more layers due to an induced bending moment derived from the tendency for a layer to shrink. This can happen during a laser-curing process. Similar to curl is "green creep." Green creep is a phenomenon that occurs between the laser cure and the post-cure. If a part is laser-cured but left out for a period of time before post-cure, it may begin to bend much like the warping of wood. Hatching reduces the tendency of a part to curl.

2.1.2.3   Comparison of Resins

There are several different SLA machines available, and with each machine, many different resins are available from several different vendors. Recently, there has been some exploration of liquid crystal resins. [Ullett, Schultz, and Chartoff, 2000] Though this is a relatively new development, there is potential for these resins, particularly due to their ability to withstand temperatures in excess of 212°F. This section, however, only discusses the resins available for the SLA-7000. Table 2.2 shows a comparison of these resins.

Note from Table 2.2 that the minimum layer thickness is the same for all resins. This particular property pertains to the build phase. It describes the minimum layer thickness of liquid resin that may be coated over a recently cured layer during the build

10

process. Also, note the differences in properties of the resins used in the SLA-7000. With such a wide array of resins available, any may selected for parts as the applications change.

Table 2.2 Comparison of selected resins for use in SLA-7000

Resin	Min. Layer Thickness (in.)	Tensile Strength (psi)*	Tensile Modulus (ksi)*	Flexural Modulus (ksi)*	Glass Transition Temp, T_g (°F)
SL 7540[†]	0.001	5200	222	183	136
SL 7520[†]	0.001	9400	458	421	154
SL 7510[†]	0.001	7340	331	271	144
SL 5530[†]	0.001	9200	454	492	180
300 ND[‡]	Not Available	8700	435	406	176
700 ND[‡]	Not Available	10200	363	348	178

* Based on a 90-minute UV post-cure
[†] Vantico, Ltd resins
[‡] Rapid Prototyping Chemicals, Ltd resins

2.1.3   Building a Model in SLA

Stereolithography is a series of processes that begins with product design in a CAD environment and ends with a physical 3-D object. Figure 2.1 is an overview of the SL process.
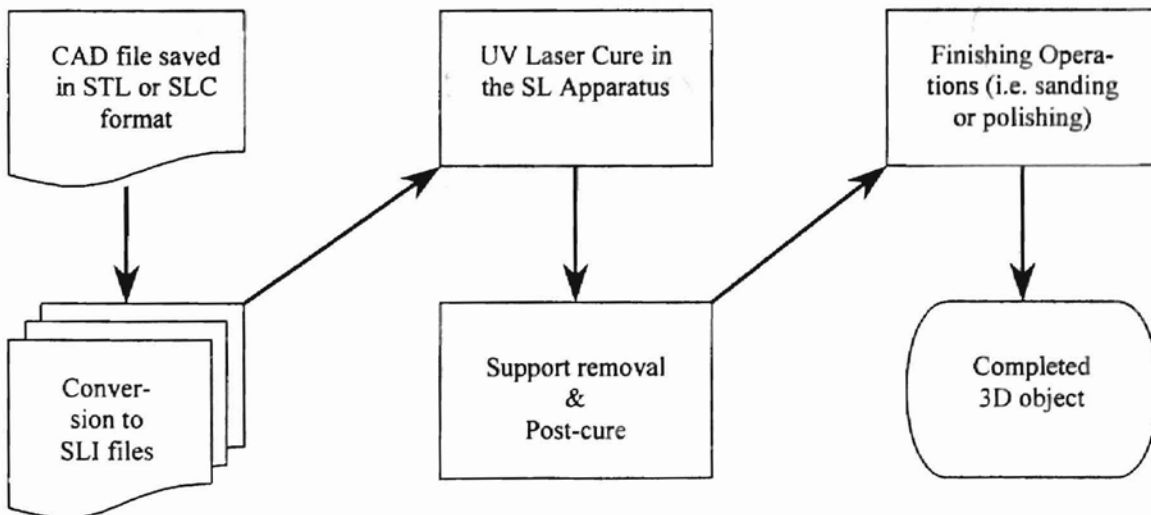
Figure 2.1 General steps for building a model in SLA

The individual processes that comprise the entire SL build process and some different build styles that have been developed for use on the SLA will now be considered.

2.1.3.1 Software Considerations

Initially, the object must be designed in a CAD environment. It may then be saved as an STL or SLC file. Several CAD software packages such as Pro/Engineer® or SolidEdge® have STL and/or SLC translators.

The STL format is more commonly used in SLA machines, as STL translators are more common than SLC translators. An STL file is a surface triangulation mesh of the solid part, and it may be saved in either binary or ASCII formats. Each triangle in the mesh is identified by its three vertices and an outward normal vector. Figure 2.2a shows the format of triangle identification within an ASCII STL file.

```
solid ASCII
  facet normal I J K
   outer loop
      vertex  X₁ Y₁ Z₁
      vertex  X₂ Y₂ Z₂
      vertex  X₃ Y₃ Z₃
   endloop
   endfacet
      :
      :
endsolid
```

(a)   (b)
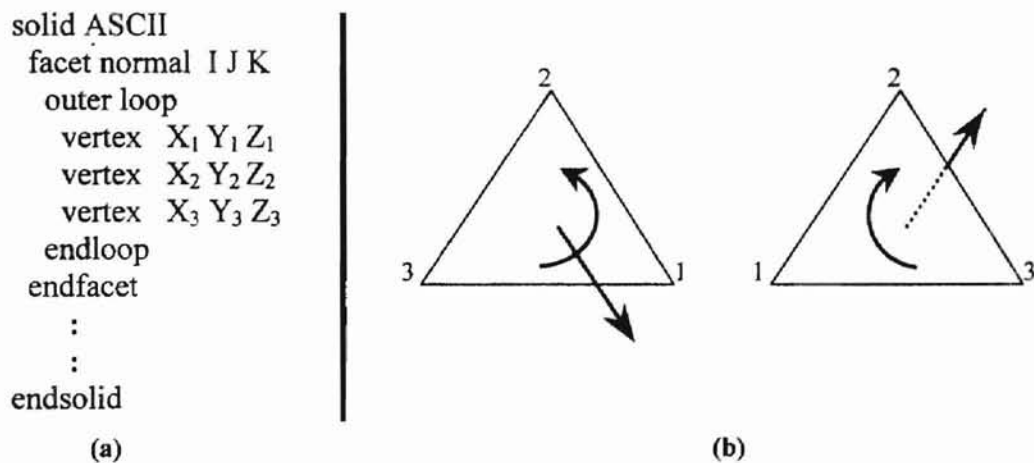
Figure 2.2 (a) Triangle identification within STL document. (b) Triangle orientation

I, J, and K are all floating-point integers and vectors **X**, **Y**, and **Z** are comprised of all floating-point integers. [Jacobs, 1992]

Two requirements must be met in order to ensure proper processing of an STL file. First, triangle ordering identifies interior or exterior surfacing. This is done using the right-hand rule, illustrated in Figure 2.2b. The second is that every triangle $_{must}$ share exactly 2 common vertices with each adjacent triangle. Under no circumstance may any triangle vertex intersect with the side of an adjacent triangle. [Jacobs, 1996]

The SLC format is not so popular as the STL format, due to the scarcity of CAD packages with SLC translators. Unlike the STL file, SLC files are considered a 2½-D (2-D drawing with a Z thickness) contour representation of a model's boundaries within each layer. The contour data within an SLC file contains the number of XY vertex locations for that contour, the number of gaps, and the list of floating point vertex points.

Once the STL or SLC file is generated, it must be converted into a group of slice (SLI) files through CSlice processing. SLI files are successive cross-sections of a model. After the slice program has finished, a program runs that merges all the SLI files into a lump project. Next, a prepare program is run and subsequently, the build program runs, which drives the mechanisms in the SLA machine and builds the model. [Jacobs, 1992]

2.1.3.2   The Laser Cure Process

Before a model is laser-cured, model scale, layer thickness, internal hatch, and build orientation must be considered. SLA software is capable of scaling model dimensions up or down from the CAD dimensions. For example, a CAD model with dimensions of 5' x 5' x 5' may be scaled down to 1" x 1" x 1" within the SLA software. [Dickman, 2001] Also, layer thickness should be specified before the build begins. Depending on the use of the model, one may choose a larger or smaller thickness, but for

parts that require exceptional accuracy, a layer thickness less than 0.005" is used. [Jacobs, 1992]

Recall that parts undergoing laser cure are subject to curl. Hatch patterns were introduced to alleviate this effect. Internal hatch specifies how the part will be solidified between borders. The Tri-Hatch pattern, for example, scanned lines parallel to the x-axis combined with lines at 60° and 120°. [Jacobs, 1996] Tri-Hatch was the most popular scanning pattern until the introduction of WEAVE™, which scans lines parallel to the x- and y-axes. The spacing in these hatch patterns is on the order of 0.01". [Dickman, 2001]

Finally, build orientation is considered before laser-curing a model. When a part is built during the laser cure process, it is built layer-by-layer from the bottom up. If minimal build time is desired, the model should be oriented such that it requires a minimum number of layers. For example, a cylinder with a diameter of 1" and a height of 5" may be built axially, horizontally, or at some other angle. If a build layer of 0.005" were selected, then it would require 1,000 layers for an axial build. Conversely, a horizontal build would require only 200 layers. [Dickman, 2001] Although the scanning time would essentially be the same, the horizontal build would be finished faster because it would not require as many recoats.

The actual build process begins with the elevator set just below the surface of the resin. Supports are designed to stabilize the part as it is built. Once the initial supports are built, the elevator drops enough to cover the solid polymer with another layer of liquid resin. A wiper moves across the surface, recoating the solid with a new layer of liquid resin. The laser draws each layer by first outlining the cross-section, and then filling it in, either with a hatch pattern or a quasi-hollow build pattern. If there are any cantile-

vered or other unsupported surfaces (i.e. ceilings), then additional supports are built for them because they tend to sag in their green state. This process continues until the top layer is completed and the model is completely submerged in the liquid resin. Next, it is raised out of the vat and drained. After draining, it is ready for post processing.

There are other build options available to the user. These include (but are not limited to): **/start, /stop, /zoff, /swapxy, /nodrain,** and **/nosweep.** [Jacobs, 1992] Each option allows for special build circumstances. For example, the **/zoff** option inactivates the recoater. This may be useful if one wished to observe the beam path without polymerizing any resin. The **/nodrain** option keeps the object submerged after it has been laser-cured. This may be useful if the part is too weak in its green state to support itself, and no one is available to post-process it. In this case, the liquid resin would support it, since the solid polymer is rarely greater than 6% denser than the liquid resin. [3D Systems, 2001]

2.1.3.3   Post-processing

Once a model has finished draining, it is ready for post-processing. Typical post-processing involves 4 steps: part removal, part cleaning, post-curing, and part finishing. [Jacobs, 1992]

Part removal involves moving the laser-cured part from the SLA machine to the cleaning area. Typically, the SLA platform is removed along with the part and carried to the cleaning area. There are issues to be considered during this process. First, proper removal ensures that no excess liquid resin is wasted but is properly drained. Also, special care is taken for parts that may be fragile in their green state.

Cleaning is the next stage. It is impossible to remove all the liquid resin by draining the part. Thus, it must be rinsed with proper solvents that safely remove excess liquid resin but will not harm the solid polymer. A variety of solvents including several kinds of alcohol, propylene carbonate, Di-Propylene Glycol Monomethyl Ether (DPM), and Tri-Propylene Glycol Monomethyl Ether (TPM) have been used. TPM commonly used because all the others tend to induce swelling on a part. [Jacobs, 1992] Once a part has been rinsed with TPM, it is rinsed with water. TPM dissolves in water and is removed by it. When the water rinse is complete, the part is air-dried using compressed air. Compressed air keeps water spots from forming on the part and forces water droplets through any tiny passageways.

When the cleaned part has been dried, it is ready to be post-cured. In this third phase, the part is placed into a UV oven, which is a chamber with a rotating base surrounded by UV lights and mirror walls. Time required to finish a post-cure is mostly dependent on the part's mass. Experiments on post-curing show that the post-cure time is proportional to the cube root of the part's mass. [Jacobs, 1992] This relationship, however, and should not be used as a sole guide to post-curing. Other factors such as surface area should also be considered. Extended post-curing does not harm the part. Therefore, parts are usually post-cured longer than the minimum time necessary. Generally, a part is post-cured for 1 to 1½ hours.

The final step is the finishing touches. Any supports are removed using a knife blade. The part may then be sanded to eliminate the effects of stair stepping, and it may be rinsed in water and air-dried once more. Depending on the ultimate purpose of the model, further finishing touches (i.e. painting or polishing) may be done to the part.

2.1.4   QuickCast™

Not all parts built in SLA need be solid. It is possible to produce quasi-hollow models in order to reduce weight, save resin, and make a model more conducive to its purpose. QuickCast™ (QC) was developed for this.

(a)

(b)

(c)
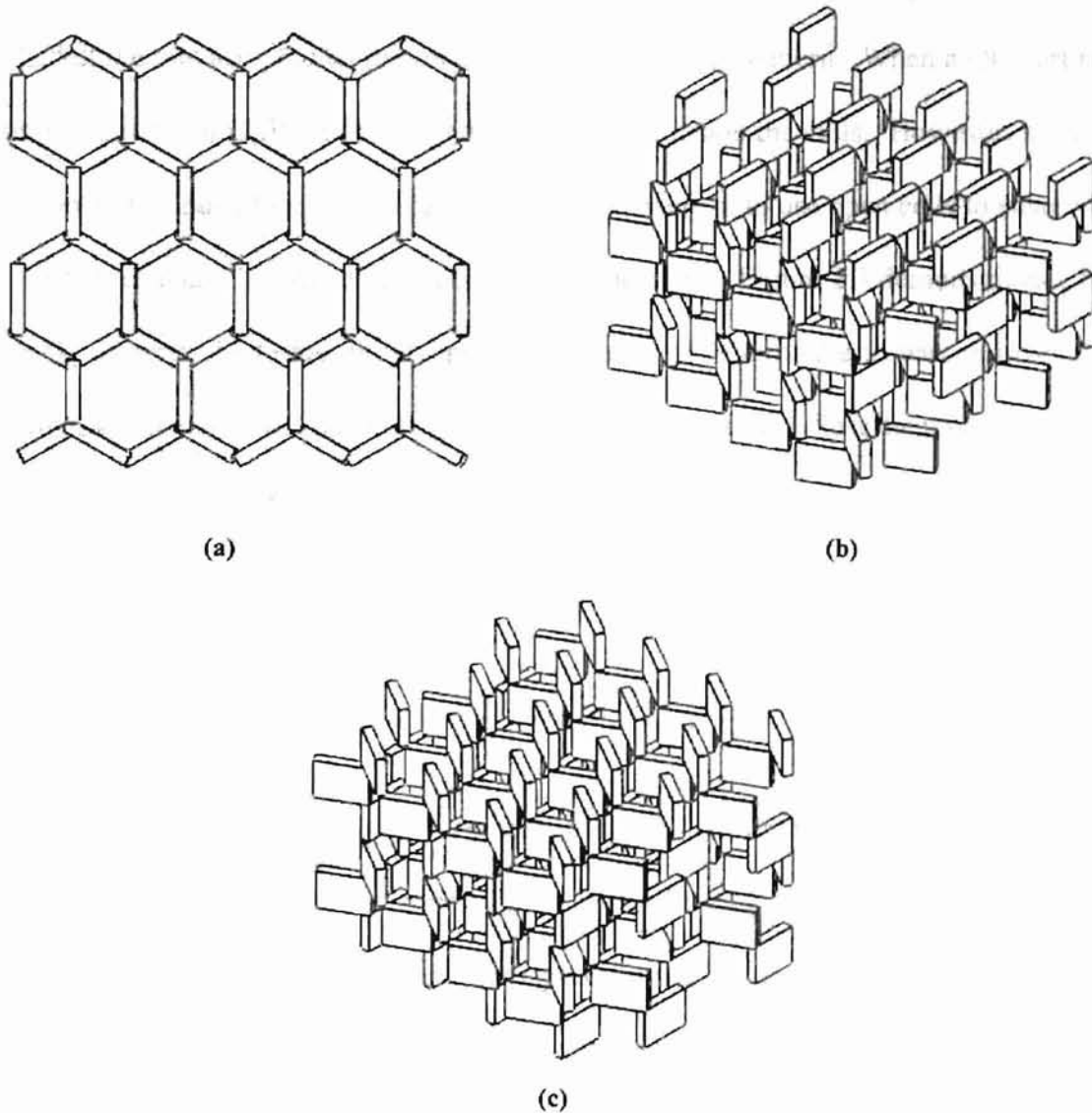
Figure 2.3 Hex QuickCast build. (a) Top View. (b) & (c) Orthogonal Views.

Introduced in 1993, the primary motivation for QC's development was its usefulness in shell investment casting. For many years, ceramic molds were created using wax.

A shell could be contoured around a wax mold, and the wax could be melted out. Although wax molds were effective in accuracy, it was learned that using SLA parts instead of wax could save time and money. QC parts could be burned out using a flash-firing method. [Jacobs, 1996] Since then, QC has become common among SL users.

A QC part is like a honeycomb structure. There are various QC patterns available, but the one used in this research effort had a hex-cell pattern. When a QC part rises out of the resin, it is filled with liquid resin, trapped inside the cells. However, since the resin must be drained from each cell, it is more convenient to use open cells to ensure that all of the resin can be drained from only a few locations. Figure 2.3 demonstrates a hex-cell QC pattern. Not only did QC provide a successful alternative to wax in investment casting, but it also could save weight, and thus valuable resin. Specifications on the QC build claim that a properly drained and post-cured QC model could reduce the weight of a model by as much as 80%. [Jacobs, 1996]

2.1.5 Applications of SLA

Although it is a relatively new technology, SL is already being applied in many different fields. SL has made strides within manufacturing and tooling sectors. SL has been applied to the automotive and aerospace industries, as well as the medical field. Past and current applications of SL reveal trends and potential of it.

2.1.5.1 Investment Casting

Investment casting, originally called the "lost wax" process, is often used to fabricate metal parts. For several millennia, wax parts had been used as dies for a variety of

applications. Several thousand years before Christ, Egyptians were implementing wax patterns to create jewelry. By 200 A.D., Indians in South America were using wax patterns to cast gold. Investment casting became popular in the U. S. in the early 1900s, and by World War II, it became a mechanism for producing high-tech parts, such as jet engine turbine blades. [Jacobs, 1996]

Investment castings can be either "solid mold" or "shell casting," depending on the method used to form the ceramic shell around the wax pattern. The solid mold casting process uses dispensable patterns arranged on a common gating system called a "tree." The tree is placed into a flask, and the ceramic slurry is poured around it. Once the slurry has dried, the wax is melted out, and the castings are removed from the tree.

Shell casting is similar to solid mold casting. The major difference arises in the creation of the ceramic shell. In shell casting, the tree is dipped into ceramic slurry and then allowed to dry. It dries much faster this way. In the end, a thin ceramic shell is all that remains.

Until SLA parts started being used, the wax patterns were costly and time-inefficient. However, they did provide detail, a desired characteristic. SLA parts proved that they could do the same job while saving time and money. There are methodological differences between casting with SLA and wax. Because SLA resins are cross-linked, they don't melt. An SLA part is removed from the ceramic mold via flash-firing. [Jacobs, 1996] This posed another problem. When heated, SLA parts tend to expand. This expansion creates stress on a ceramic shell and causes it to crack, thus rendering it useless. SLA parts could be used in solid mold casting without fear of damaging the mold. but they would not work in shell casting. Thus, QuickCast™ was introduced. The quasi-

hollow design of the QC would allow it to collapse in on itself during the flash-firing process, thus making it a viable alternative to wax for shell casting. However, studies have shown that QC parts would induce stress on a shell. [Hague and Dickens, 1995] When a QC part rises out of the liquid resin it must be drained of the liquid resin. Afterwards, the drainage holes must be sealed. Otherwise, the slurry could seep into them and create appendages on the final cast. However, when a sealed QC part is heated in the flash-fire process, it expands like a balloon before it collapses in on itself, thus inducing stress on the shell. To counter this effect, vent holes must be drilled into the part to relieve pressure due to gas expansion.

A variety of case studies have been performed on casting applications. One such study was performed on a subframe support structure that was to be used on the International Space Station. [Jacobs, 1996] Because size and weight were critical factors, QC became the casting material of choice. Mold patterns were created using QC, and aluminum alloy castings were made from these molds that successfully met their objectives.

Another study done specifically on molds for investment casting shows that using QC (as opposed to the traditional wax method) for cast pattern production will result in time savings of 60%. [Tsang and Bennett, 1995]

2.1.5.2   Aerospace

Not only is SLA useful in part development for aircraft and spacecraft components, but it has also proven useful for experimental analysis, particularly using wind-tunnel models and the like. Manufacturing a model with a simple airfoil cross-section, for example, might not be tedious, but as the airfoil gets more complex, so does its con-

struction. Figure 2.4 shows a simple NACA0012 airfoil and the more complex Selig1223 airfoil. [UIUC, 2001] Adding further complexities (i.e. twist, sweep, or dihedral) to a model complicates its construction.

Not all wind-tunnel tests can be successfully performed using RP models, especially SLA models. Bombardier Aerospace, Inc. performed an analysis of the feasibility of various RP methods for creating usable wind-tunnel models. [Chuk and Thomson, 1998] In their study, wind-tunnel tests fell into the following 3 categories: non-structurally loaded (< 25 ksi), lightly loaded (~50 ksi), and highly loaded (> 125 ksi).
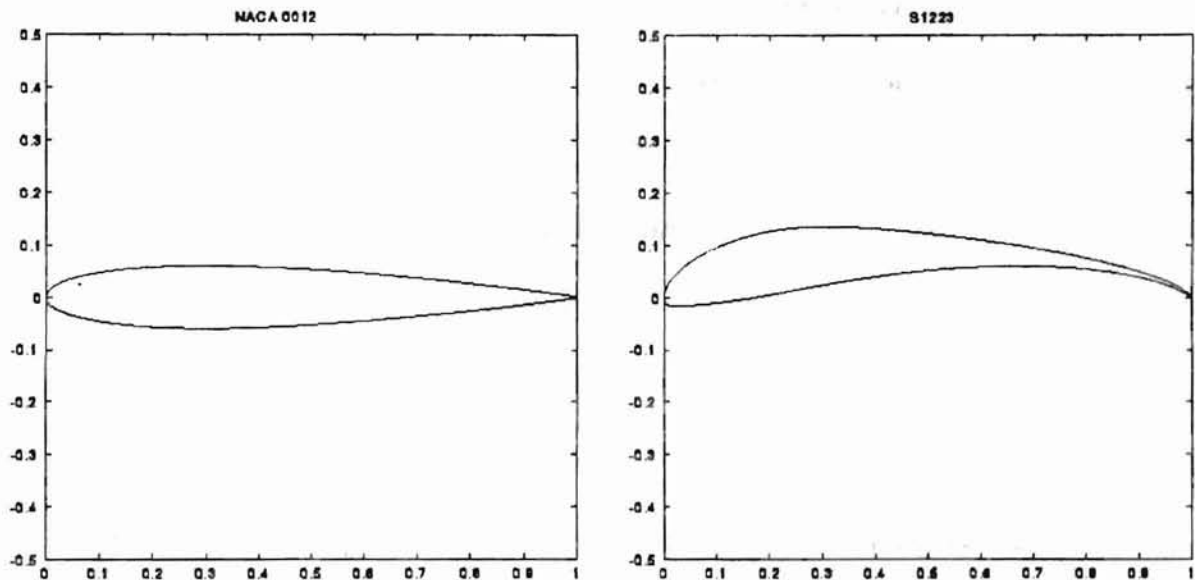
Figure 2.4 (a) NACA0012 Airfoil; (b) Selig1223 Airfoil

Although SLA was one of the few RP technologies that could pass the strict tolerance and surface finish requirements imposed by the researchers, it was only worthy to be used in the non-structurally loaded tests. Other methods such as NC machining and investment casting of RP models could produce parts that withstand the higher loads. Structural worthiness was not the only criterion used to determine which RP methods

were most feasible for wind-tunnel model creation. Other factors included time, cost, and ability to pass the tolerance and surface finish requirements.

SLA models have also been used for low-speed airfoil analysis. One such study performed at the University of Alabama in Huntsville compared wind-tunnel data from an SLA model to the same model built using traditional casting methods. In this study, the model had the shape of an NACA0012 airfoil (shown in Figure 2.4). Two models were built using an SLA-250. The surface of one had a distributed roughness due to resin overcure at the layer interfaces, and the surface of the other was sanded to produce a smooth finish. The model built using traditional casting methods had an aerodynamically smooth surface and the data derived from its test were used as control data in the experiment. All three airfoils were tested at a low Reynolds number (~150,000). Lift and drag were measured at angles of attack ranging from 0° to 16° in 2° increments. The data were plotted and compared to the predicted C_L vs. α curve with a slope of 2π. The results showed that the SLA models stalled at lower angles of attack, but the C_L vs α and C_D vs α curves for all three models were otherwise very similar. They concluded that SL was a promising method for producing wind tunnel models that could generate accurate experimental data. [Landrum, Beard, LaSarge, and von Sprecken, 1997]

SLA models can be built for early-stage conceptualization. Thus, engineers can build a model in SLA and determine if there is any interference or other anomaly within a part. An example of this is a model of a missile made entirely in SLA.

2.1.5.3   Miscellaneous Examples

Within the automotive industry, SLA is used to create master patterns for tooling and foundry applications, and design aid models. Chrysler, for example, has used SLA design aid models for proof of packaging, design verification, and marketing presentations. Engineers in France redesigned a starter for a Jeep Cherokee®. Though they did not have a physical model of the redesigned part, they could quickly build a replica of it in SLA and install it into the vehicle to see if the new design would work. [Jacobs, 1992]

Within the medical field, SLA is being used to design replacement joints and implants for the musculoskeletal system. Building such parts can be difficult due to the complex structure of anatomical parts, but SLA construction makes it easier. For example, DePuy, Inc did a case study involving a shoulder implant. [Jacobs, 1992] The development team was able to pore over a 3D model in the early conceptualization phase. These 3D models were useful in conveying ideas. Furthermore, they could scale the parts as necessary with relatively little trouble. Thus, using SLA, they were able to create freeform models much faster than they had before.

SLA is also being used to create life-size replicas of dinosaur skeletons on display at the Smithsonian Institute. Because dinosaur bones are subject to corrosion over the years from being on display, the Smithsonian has embarked on a venture to replace its actual dinosaur skeletons with SLA replicas. This will permit the preservation of the actual fossils. Recently, SharedReplicators, Inc. shipped a full-scale model of a Triceratops skull, made completely in the SLA-7000, to the Smithsonian Institute in Washington D.C. [SharedReplicators, 2001]

2.2 Composites

The study of composites is not limited to just the search for newer, stronger, and lighter materials, but also includes methods of composite preparation. This section discusses composite materials in a general sense, followed by a narrower review of carbon-fiber composites, especially those that have been used in this project. Then, there will be a review of some of the common curing techniques used today.

2.2.1 Materials

The study of composite materials began within the aerospace industry and was driven by the need to find strong, yet lightweight, materials. An advanced structural composite is applicable to aerospace construction and made by imbedding high strength, high modulus reinforcement fibers within a homogeneous resin matrix. Fibers carry the load; the matrix transfers the load from fiber to fiber.

(a) 0°

(b) 0° / 90°

(c) ±45°

(d) 0° / ±45° / 90°
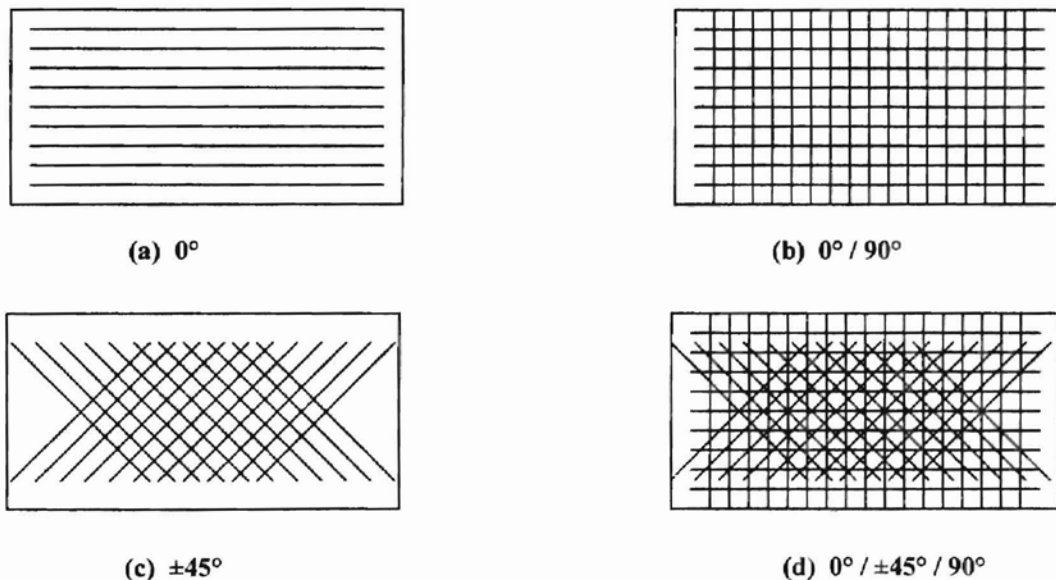
Figure 2.5 Composite ply tailoring [Vermillion, 2000]

The reinforcement fibers can be chopped "whiskers" randomly oriented within the resin matrix or they may be continuous strands that run in a given direction. Chopped whisker composites exhibit isotropic behavior, whereas fibrous composites exhibit anisotropic behavior. Anisotropic behavior is useful in designing a structure that needs more strength in one direction than in another. Composite fiber lay-up is not limited to unidirectional tape. It may be woven into a fabric, or multiple layers may be laid up with the fibers running in varying directions. Figure 2.5 demonstrates some of the directional possibilities of laying up fibers.

2.2.1.1   Fibers

Commonly used fiber materials include fiberglass, aramid fiber (Kevlar®), and carbon fiber. Fiberglass consists of long strands of glass fibers. Varieties of fiberglass include E-Glass (E for *electrical*), S-Glass (S for *strength*), and C-Glass (C for *corrosion*).

Aramid fibers are organic compounds consisting of carbon, oxygen, hydrogen, and nitrogen. They have low density and high tensile strength. Aramid fibers are used in applications that require added toughness or increased impact resistance. However, these fibers have low compressive strength and are hygroscopic and hydrophilic – two properties that are undesirable in aircraft design.

Carbon (or graphite) fibers are derived from one of three sources: rayon, petroleum pitch, or polyacrylonitrile (PAN). Carbon fibers made from rayon have a low modulus (≤ 50 GPa) and are primarily used with the rocket and missile industry. Carbon fibers made from pitch have a very high axial modulus (up to 896 GPa) and high axial

thermal and electrical conductivity. These fibers are ideally suited for spacecraft hardware and avionics. Carbon fibers made from PAN are developed through a complex polymerization and thermal carbonization process, and exhibit very high strength. In general, their compressive strength is greater than carbon fibers made from the previous two sources. Note that although the terms "carbon" and "graphite" are frequently used interchangeably, they are not technically the same. Carbon fibers are carbonized at 2400°F and have a 93% – 95% carbon content whereas graphite fibers are carbonized between 3450°F and 4500°F and have carbon content greater than 99%. [Vermillion, 2000]

2.2.1.2   Matrices

There are three major families of resin used in composites – ceramic, metal, and polymer. Ceramic matrices can be further divided into 4 groups – glass, conventional, cement, and carbon/carbon. Metal matrices are primarily alloys of aluminum, magnesium, and titanium. Polymer matrices can be divided into two classes – thermoplastic and thermosetting.

This project studies only composite laminates having the thermosetting resin matrix. Thermosetting resins consist of cross-linked polymers, and therefore do not melt once they have been cured. Typically, they have a glass transition temperature above which the cross-linked polymer becomes softer and below which it becomes brittle or "glass-like." There are 4 basic types of thermosetting resins – polyester, vinyl ester, phenolic, and epoxy. Polyester resins are produced from the reaction of dibasic acids with dihydric acids. Vinyl ester resins are made from epoxy ingredients and offer added toughness and resistance to corrosion. They are cured by adding a catalyst such as

methyl ethyl ketone peroxide (MEKP). Phenolic resins are produced from the condensation of alcohol with formaldehyde. Epoxy resins are the most common resins used in high-strength laminating. Epoxy resins offer corrosion resistance and high toughness.

2.2.1.3   Composite Fabrics

The composite laminate used in this research effort was a prepreg woven fabric. "Prepreg" is a term used to describe a composite fabric or tape that has been run through a resin bath prior to lay-up and is therefore "pre-impregnated" with resin. Not all laminates are prepreg. Some are dry and require the application of wet resin at the time of application to a surface. Also, composite fibers may be woven into several patterns. Some weave types include plain weave (1 over, 1 under), 5 harness satin (4 over, 1 under), and 2 x 2 twill. The fabric used for the research in this project was LTM-25, 2 x 2 twill pre-impregnated with epoxy resin.

Advanced Composites Group, Inc. (ACG) prepreg fabrics may come in one of three varieties – Low Temperature Moulding (LTM), Medium Temperature Moulding (MTM), and High Temperature Moulding (HTM). The category into which a laminate falls is related to the resin used to prepreg it. LTM resins cure between 30°C and 80°C, MTM resins cure between 85°C and 135°C, and HTM resins cure between 175°C and 235°C. [Advanced Composite Group, 2001]

The carbon fiber fabrics pre-impregnated with LTM resins are of particular interest to this project. Their ability to cure at lower temperatures makes them attractive to aerospace designers and manufacturers who do not have access to a high-temperature oven or autoclave. Furthermore, if carbon fiber twill were to be bonded to an SLA part

(as is the case in this project), the glass transition temperature of the SLA part, which is usually no greater than 80°C, would require special attention.

LTM-25 is one of many LTM fabrics available. Others include LTM-23, LTM-26, and LTM-48. Table 2.3 shows curing properties of several LTM fabrics.

Table 2.3 Cure characteristics of selected LTM fabrics [ACG, 2001]

	LTM25	LTM26EL	LTM45-1	LTM123
Max T_g (°C)	125	130	210	220
Typical Cure	65°C – 12 hrs	60°C – 9 hrs	80°C – 5 hrs	80°C – 16 hrs
Outlife at Room Temperature	5 – 6 days	6 – 7 days	6 – 7 days	2 days
Common Applications	Light Aircraft; UAVs	Light Aircraft; UAVs	Aircraft Proto- types; UAVs	High Stability Space Structures

Note that the typical cure listed in Table 2.3 for LTM fabrics is not a strict rule. More often, a Time vs. Temperature curve (where cure time is a function of cure temperature) is issued for each LTM fabric. Figure 2.6 shows the Time vs. Temperature curve issued by Advanced Composites Group, Inc. (ACG) for LTM25 fabric.

In Figure 2.6, the dotted lines represent an exponential curve fitted to the actual data given by ACG. The optimum cure time can be approximated using the following equation:

$$t = 352.39e^{-0.0223T}$$

Furthermore, the minimum cure time can be approximated using the following equation:

$$t = 127.91e^{-0.0195T}$$

Where,

$t \equiv$ time (hours)

$T \equiv$ temperature (°F)

28

These equations are not a rule, but should only be used if an actual chart from ACG is unavailable.

Cure Time for LTM 25 Resin
(Resin temp. NOT oven temp.)
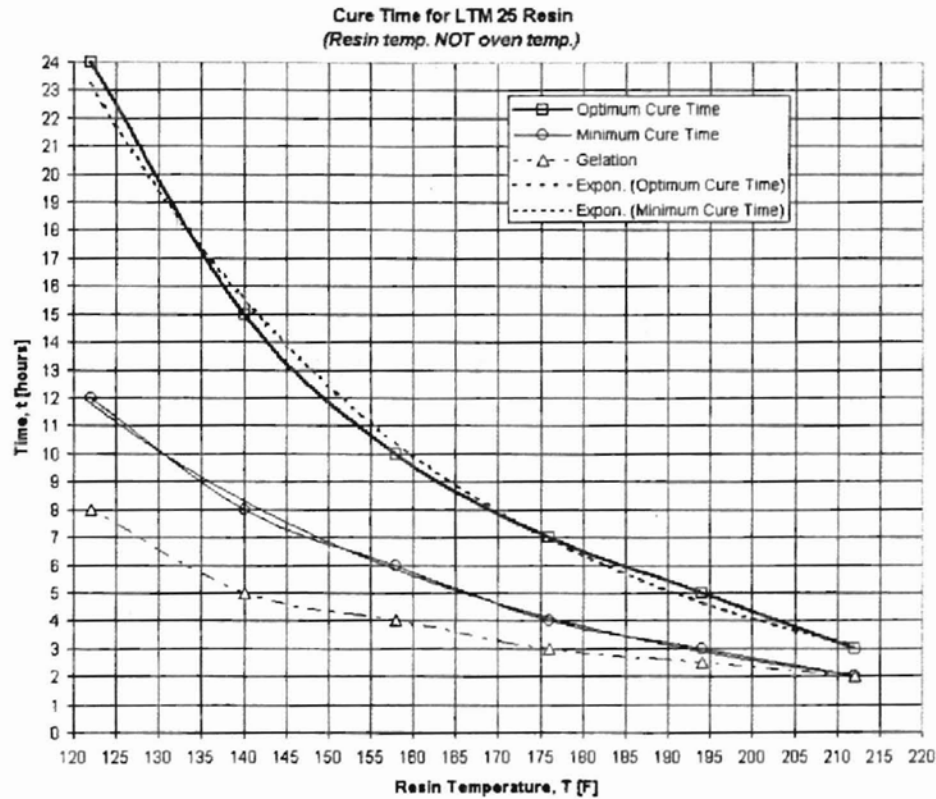
Figure 2.6 Cure time vs. cure temperature curve for LTM25 [ACG, 2001]

A recent study by NASA reveals characteristics of prepreg twill with LTM25 resin. Properties were explored under a variety of conditions. [Cruz, Shah, and Postyn, 1996] Table 2.4 lists some of the mechanical properties measured.

In Table 2.4, E is defined as the elastic modulus, and σ is defined as the ultimate strength. The superscript "t" refers to tensile properties; the superscript "c" refers to compressive properties. Also, the subscript "1" refers to the longitudinal direction; the

subscript "2" refers to the transverse direction. Other LTM25 carbon fiber twill proper-ties include density ($\rho = 0.0525$ lb/in^3) and nominal ply thickness ($t_{nom} = 0.00904$ in).

Table 2.4 Mechanical properties for LTM25 carbon fiber 2 x 2 twill [Cruz, Shah, and Postyn, 1996]

Property	CTD	RTD	ETW
E^t_1 (Msi)	7.57	7.06	6.48
E^c_1 (Msi)	7.46	7.20	8.37
E^t_2 (Msi)	7.58	7.52	6.11
E^c_2 (Msi)	7.84	7.54	7.22
σ^t_1 (ksi)	76.1	81.6	83.4
σ^c_1 (ksi)	113	93.1	55.1
σ^t_2 (ksi)	79.9·	88.8	85.0
σ^c_2 (ksi)	100	81.7	54.0

2.2.2 Sandwich Structures

Composite plies can strengthen a structure by a technique known as "sandwich-ing." A sandwich structure is a bonded structure in which some facing material (i.e. composite laminate) is separated by a core material, or substructure. The substructure is thicker and increases the structure's stiffness by spacing the facing materials apart. Fig-ure 2.7 shows the effect of increasing a substructure's thickness on the structure's stiff-ness, strength, and weight.

For any composite structure, the facing material would be either a composite fab-ric or tape. The substructure may be a variety of lightweight materials, including foam and honeycomb. A honeycomb substructure may be made of aluminum, fiberglass, graphite, or other material. Foam substructure materials include styrofoam, polystyrene, and PVC.

2t

t
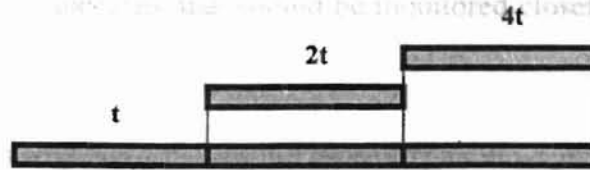
PROPERTY

Relative Stiffness	100	700	3700
Relative Strength	100	350	975
Relative Weight	100	103	106

Figure 2.7 Effect of thickness on a sandwich structure [Vermillion, 2000]

2.2.3   Curing Methods

Once lay-up of a composite lamina is complete, the part must be cured at a higher temperature. The main motivation for this higher-temperature cure is that it results in a more heat-resistant part. Carbon fiber cured at 250°F, for example, will usually be better able to withstand continuous temperatures in the 200–225°F range. [Vermillion, 2000]

The most common curing method is the autoclave or vacuum bag and oven. An autoclave allows temperature and pressure regulation. Aerospace firms use large autoclaves to cure large parts. When a composite is placed into an autoclave, it is cooked at a higher temperature and pressure. The high pressure is necessary to force the composite to adhere to the contours of a surface (otherwise, the composite will tend to peel). Furthermore, high pressure forces out excess resin, resulting in a lighter part. If an autoclave is unavailable, an ordinary oven supplemented with a vacuum bagging apparatus will suffice. In this situation, a composite is sealed in a bag and placed under a vacuum before being placed into the oven. Then, it remains under this vacuum for the duration of the cure. Note that when composites are cured in an oven or autoclave, it is not the oven

31

temperature, but the resin temperature that should be monitored closely to determine the degree of cure.

One such study done by Aerospatiale in France explored ways to cure composites using radiation. [Beziers and Denost, 1989] Radiation types used in the study include infrared, UV, gamma, X-rays, and electron beams. In each case, the composite was placed under a beam of radiation and cured. UV radiation is easy to apply, but it offers limited penetration into the laminate. X-rays offer sufficient penetration into the laminate but are limited by the low dosage requirements, thus increasing the time to cure. In almost all cases, radiation curing (particularly electron) demonstrated its ability to compete with autoclave curing, provided that one is willing to pay the cost of the equipment. Also note that resin chemistry must be suitable for radiation curing. Most of the resins performed in this research effort were acrylic resins.

Another method of composite curing under exploration involved resistive heating elements imbedded within layers of composite. [Joseph and Viney, 2000] Preliminary analyses showed that in an autoclave, the outer laminate layers were heating up faster than inner layers. In one study, layers of composite were stacked such that a heating plate was beneath them. The addition of resistive heating elements allows the layers to be cured literally from the inside out. Also, this particular study involved the placing of resistive carbon mats at various locations across the thickness of the section. [Zhu and Pitchumani, 2000] Regardless of the number of heating mats used, the results showed that the use of these internal resistive heating elements led to a reduced cure time and improved temperature homogeneity over the method of curing involving only the base plate.

The inclusion of imbedded resistive heating elements is not particularly a stand-alone curing process; it is more of a supplemental procedure. It may be used in conjunction with an autoclave, but could not achieve full cure all by itself.

CHAPTER 3

3. METHODOLOGY

From the start, *imbedded functionality* was the underlying theme of this research effort. The imbedded functions that were approved for further exploration included the following:

- Pressure Taps
- Heat Exchanger Tubing
- Thermocouple Grooves

The idea of curing composites to SLA parts was also included in the genre of imbedded functionality. By sandwiching an SLA substructure between layers of composite laminate, strength and stiffness of that part would very much increase. Thus, by adding a composite laminate, strength was being "imbedded" into the part.

This project involved design and experimentation. The design side revolved around the CAD development and design of SLA parts, including the imbedding of functions into a model. The experimental side revolved around the curing of LTM25 carbon fiber twill to SLA parts.

Preliminary studies were performed on the feasibility of applying SLA parts to practical problems. The preliminary studies evolved into the final project of developing a

multifunctional curing fixture in SLA that could cure composites without need for an autoclave. Figure 3.1 demonstrates the evolution of this research.
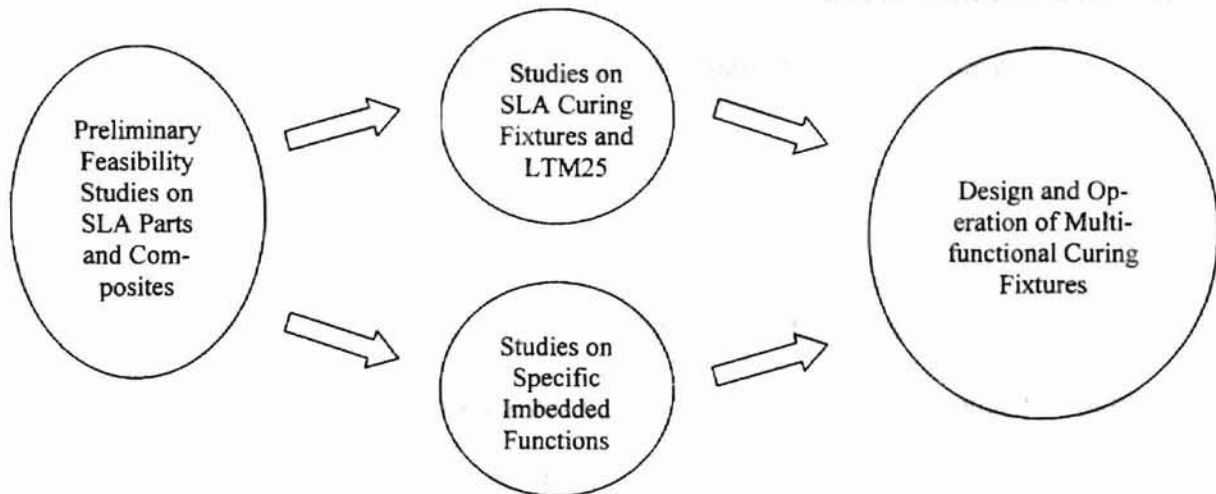
Figure 3.1 Evolution of research methodology

This chapter begins with the equipment and software used, then the feasibility studies, then the intermediate studies, concluding with the implementation the SLA multifunctional curing fixtures.

3.1   Software and Equipment

The 3D-design software package used throughout this project was SolidEdge® Version 8.0. All CAD designs were then sent to Freeform Composites, Inc. in Tulsa, OK, where they were built using the SLA-7000. Most of the parts were created using the SL7520 resin. The most recent models were made using the 700 ND resin. Furthermore, post-processing on all SLA parts was completed at Freeform Composites, Inc. by lab technicians before they were returned to Oklahoma State University for further analysis.

Other equipment utilized in this research effort include a Julabo® F12-MD recircula-tor (with its remote control software EZTemp), and a Fluke® data logger (with its data logging software HydraLogger). All tubing was clear vinyl, and all thermocouples used were T thermocouples (copper-constantan) having a diameter of 0.030 inches.

3.2   Feasibility Tests

To determine the limitations of design and building SLA parts, a small NACA0012 wing with imbedded tubing and pressure taps was designed. This would be useful in finding out the limitations of any imbedded tubing. To determine the feasibility of apply-ing composites to SLA materials, small half-cylindrical meshes were tested in an oven and vacuum bag.

3.2.1   NACA0012 Wing

A CAD drawing of the small wing is shown in Figure 3.2a. It has a span of 5" and a chord of 2". The imbedded tubing was designed such that the pressure taps would deliver a surface pressure distribution at mid-span. The taps were spaced using cosine spacing (with an initial angle $\theta_i = 30°$ from horizontal and thereafter a constant change in angle, $\Delta\theta = 15°$), having 9 taps on the upper surface and 9 on the lower. Figure 3.2b shows the cosine spacing technique as used for this wing. All tubing exits from the side through holes with a diameter of $1/16$ inch. All taps perforate the surface through holes with a diameter of $1/32$ inch. The ports that extend to the three upper and lower taps clos-

est to the trailing edge also include imbedded tubes that have a diameter of $^1/_{32}$ inches. This particular model was built using the QuickCast™ build style.

(a)

(b)
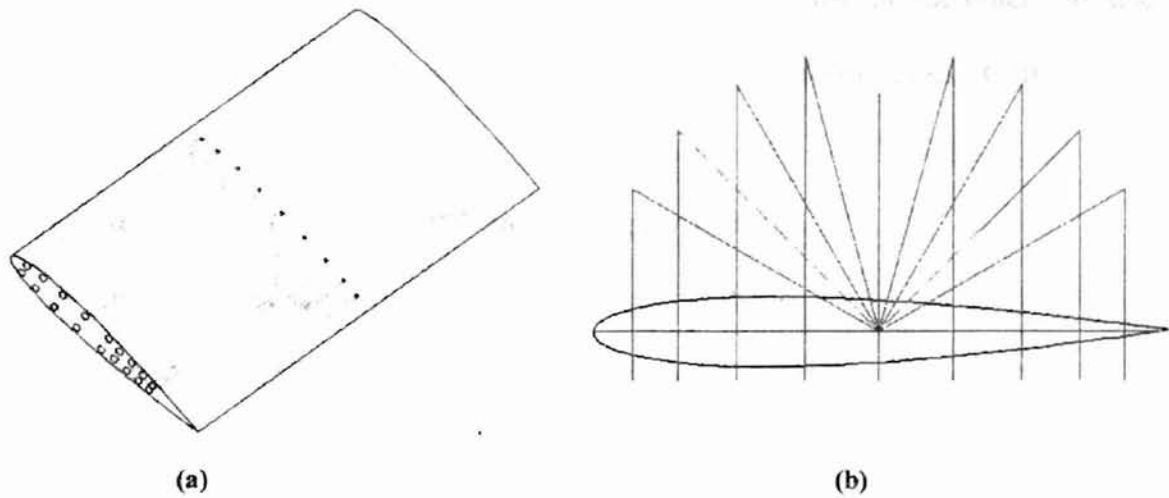
Figure 3.2 (a) NACA0012 wing with imbedded pressure taps (b) Cosine spacing of pressure taps

3.2.2   SLA Half-Cylindrical Meshes

This study was performed to demonstrate the viability of marrying carbon fiber laminate to SLA parts. The part used for this test is shown here in Figure 3.3a.

Wooden female
curing fixture

SLA part

Glass plate

Vacuum
bag

(a)

(b)
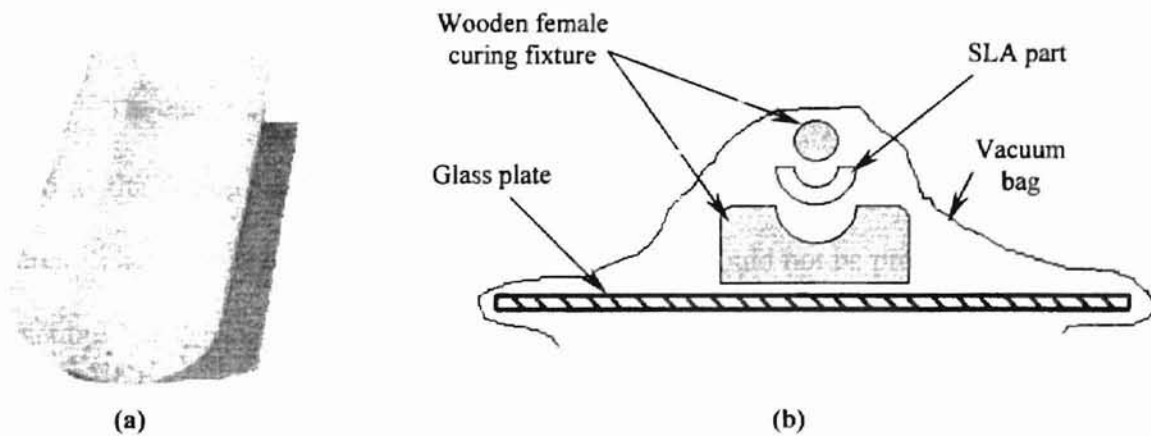
Figure 3.3 (a) SLA half-cylindrical mesh piece. (b) Cure process setup

This piece has an inner radius of $^{11}/_{16}$ inch, an outer radius of 1¼ inch, and an axial length of 2½ inches. Freeform Composites, Inc. provided this part. The curing fixture was built with tolerances that allowed one layer of LTM25 twill on the outer and inner surfaces (one layer of LTM25 twill is approximately 0.01 inches thick). Curing procedures were completed as follows:

1) One SLA part cured at 150°F and 25" Hg for 10 hours.

2) One SLA part cured at 150°F and 15" Hg for 10 hours.

3) Four SLA parts cured at 150°F and 15" Hg for 10 hours.

4) Three SLA parts cured at 140°F and 15" Hg for 10 hours.

5) Two SLA parts from (4) cured at 140°F and 23" Hg for additional 5½ hours.

3.3 Intermediate Designs and Testing

The intermediate studies include the design and usage of SLA female curing fixtures for curing composites, and the design and testing of parts with imbedded functionality.

3.3.1 SLA Curing Fixtures

The idea to use SLA parts, not only as a substructure in a composite sandwich but also as the curing fixture material, came from the desire to have "friendlier" curing fixtures. They would be friendly in the sense that they would not be prone to puncturing the vacuum bag (sharp corners on a curing fixture have such tendency), and they would reduce the effect of ridging (that is, the tendency of a curing fixture to squeeze excess resin into ridges at the place where the curing fixture halves meet). Two curing fixtures were

designed and tested in this segment of the project. The first was designed to complement a simple NACA0012 wing having a span of 18 inches and a chord of 4.25 inches. The curing fixture halves extend ½ inch beyond both tips of the wing. The curing fixture is designed with a tolerance of 0.03 inches (to allow approximately three layers of LTM25 to be applied to the wing). The curing fixture and wing halves are shown in Figure 3.4.
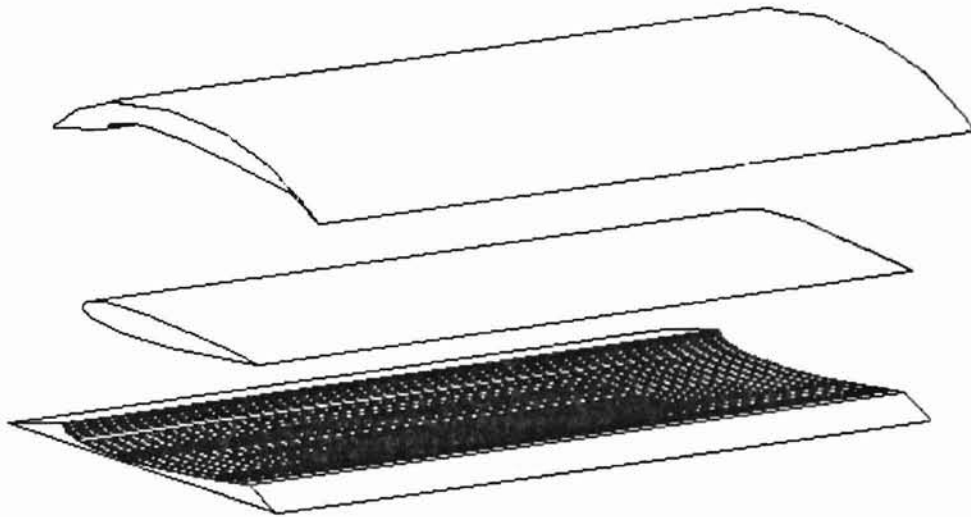
Figure 3.4 SLA NACA0012 wing with SLA curing fixture halves

Notice the curvature of the upper surface of the upper curing fixture. It was designed with the intent to reduce any tendency of the curing fixture to tear the vacuum bag during the curing process. The wing was built in QuickCast™, while the upper and lower curing fixture halves were built using the solid build method.

Two layers of LTM25 twill were applied to the QuickCast™ wing. The prepared wing was placed into the curing fixture, which was then placed into the vacuum bag. The part was cured in an oven at 140°F and 15" Hg for 12 hours.

The next curing fixture study was done using a more complex wing and curing fixture design. They are shown in Figure 3.5.

The wing has a span of 18 inches and a root chord of 4.25 inches. The following complexities were also designed into it: 0.5 taper, +3° geometric twist from root to tip, 3° dihedral, aerodynamic twist (Selig1223 airfoil at root, NACA0009 airfoil at tip). A cylinder having a diameter of approximately 0.625 inches was designed as a fuselage-like structure to house exit ports for imbedded pressure taps. Also, this wing was designed for possible use within a wind tunnel. An attachment appendage was design on the lower surface of the "fuselage" that would allow this model to be attached to the sting of a 6-DOF force balance.
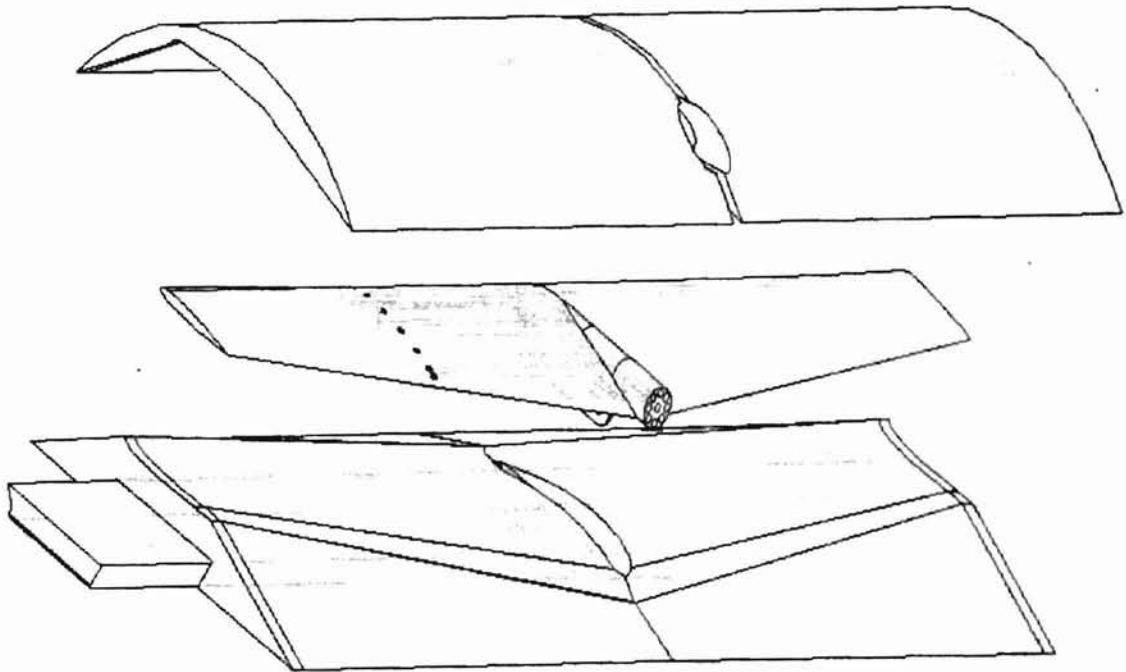
Figure 3.5 Complex SLA wing and curing fixture

The contours of the curing fixture were offset from the contours of the wing by 0.03 inches to allow application of 2 – 3 layers of LTM25. The curing fixture halves and auxiliary parts were built in the solid SLA build style. Both solid and QuickCast™ wings were built, but only the QC one was layered and cured.

The upper half of the curing fixture was divided into 2 sides. This was done to accommodate the fuselage-like cylinder. Dividing the upper curing fixture into 2 parts would allow the vacuum to apply pressure to composite layers around the cylinder. Also, two sliding auxiliary parts were incorporated into the lower half of the curing fixture (see Figure 3.5). Since the attachment appendage on the wing was also to be layered in composite, it was necessary to find a way to apply a side force to that part, thus allowing the LTM25 to adhere to the part as it cured. These auxiliary parts were designed to utilize the vacuum pressure to create a side force. This wing, too, was covered in 2 layers of LTM25 and cured at 140°F and 15" Hg for 12 hours.

3.3.2   Imbedded Functions

Three types of imbedded functionality were explored in this phase of the project – pressure taps, heat-exchanging (HX) tubing, and thermocouple grooves. The first was the imbedded pressure taps into wind tunnel models. Two models were designed to test this possibility. The first model was shown in Figure 3.2a, and the second is shown in Figure 3.6.
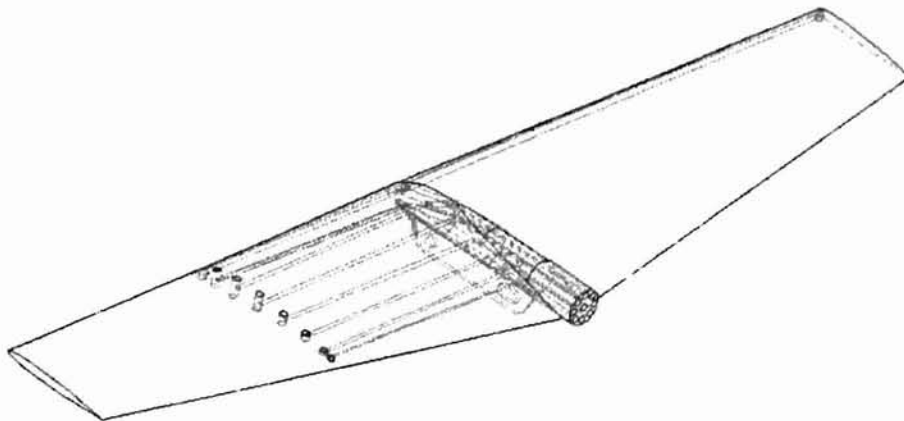
Figure 3.6 Complex wing with imbedded pressure taps.

The pressure taps imbedded into the complex wing were spaced using cosine spacing (with an initial angle $\theta_i = 20°$ from horizontal and thereafter a constant change in angle, $\Delta\theta = 20°$), having 8 taps on the upper surface and 8 on the lower. The taps are placed at halfway between the root and the tip of the port side. Each upper tap and its corresponding lower tap were connected to the same tube. Thus, one surface would need to be covered while measurements were being taken on the other. The tubes connecting the 6 taps closest to the leading edge to their exit tubes within the "fuselage" have a $1/16$-inch diameter. The tubes connecting the next tap to its exit tube within the "fuselage" has a $1/32$-inch diameter that tapers to $1/16$ inch by the time it reaches its exit port. The tube connecting the tap closest to the trailing edge to its respective exit tube within the fuselage has a diameter of $1/32$ inch. All exit tubes within the "fuselage" have a diameter of $1/8$ inch. The taps themselves have diameters of $1/8$ inch. For this SLA model, the excess resin was removed using compressed gas. The idea would be to layer the SLA model with composite and drill pinholes through the composite into the tap cavity.

The second imbedded functionality to be explored was heat-exchanger (HX) tubing. Three intermediate models were designed to investigate this capability. They are shown in Figures 3.7 through 3.9. Figure 3.7a shows a 4" x 4" x $3/8$" SLA substructure with HX tubes snaking through it. The HX tubes have a diameter of $1/8$ inch. Figure 3.7b shows that the HX tubing is $1/32$ inch from the upper surface and exits from a port that is $1/32$ inch from the lower surface.

Figure 3.8a shows a SLA disk with a radius of 2 inches and a thickness of $3/8$ inch. The placement of the HX tubing relative to the upper and lower surfaces is similar to the

placement of the HX tubing in the model shown in Figure 3.7. In this model, the tube spirals from the outer rim toward the center. Figure 3.8b shows the placement of the tubing relative to the surfaces of the model.

(a)　　　　　　　　　　　　　　　　　　　　(b)
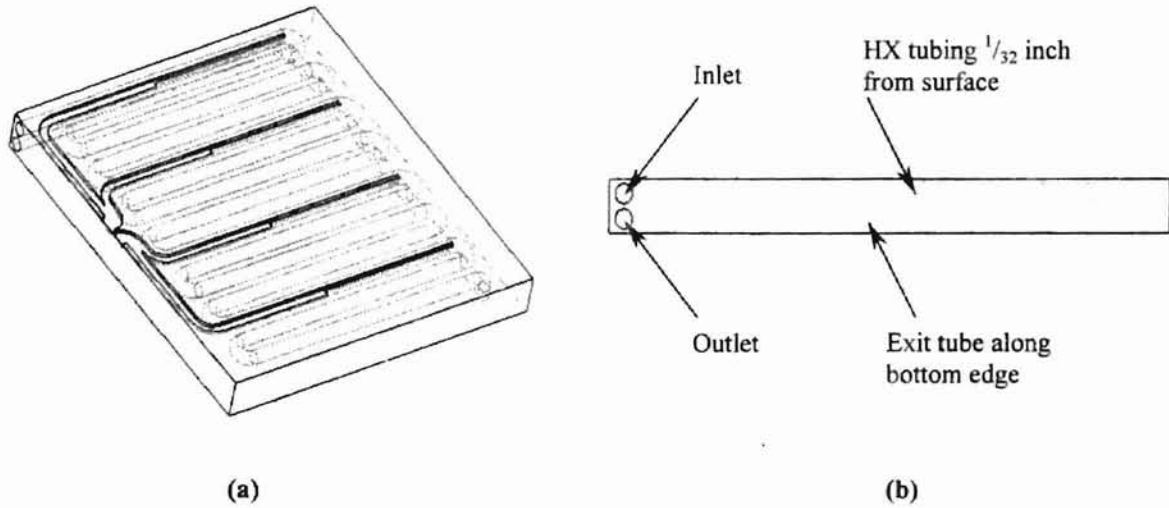
Figure 3.7 Square SLA HX model

(a)　　　　　　　　　　　　　　　　　　　　(b)
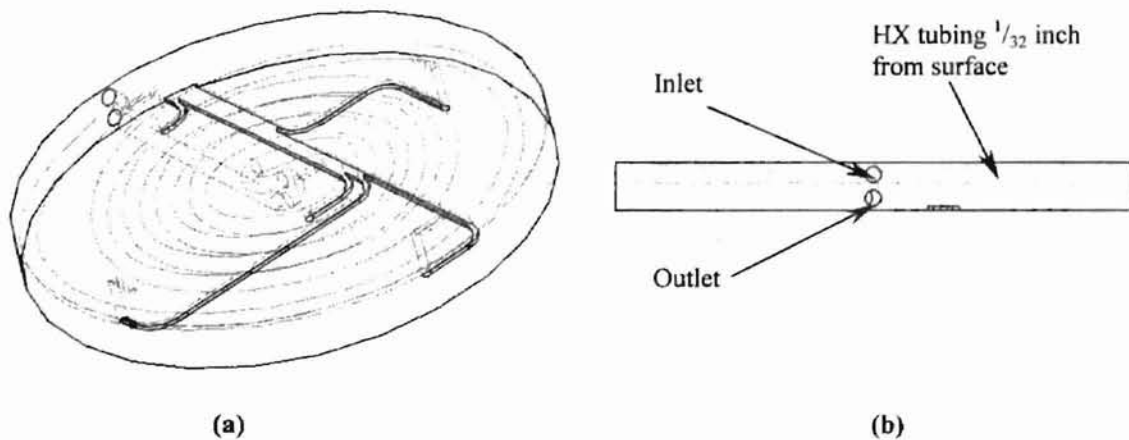
Figure 3.8 Circular SLA HX model

Figure 3.9 shows a half-cylindrical part with HX tubing snaking through it. The part has an outer diameter of 1¼ inches and an inner diameter of $^{11}/_{16}$ inches (same as the sample half-cylindrical mesh test parts supplied by Freeform Composites, Inc.) The axial

43

length of this part is 2 inches. Figure 3.9b shows that the tubing is placed such that it is $^1/_{32}$ inch from the outer surface of the part. The HX tubing all parts designed in this project has a diameter of $^1/_8$ inch. This part and the parts shown in Figures 3.7 and 3.8 were built using the QuickCast™ build method.

HX tubing $^1/_{32}$ inch from outer surface

Outlet

Inlet

(a)   (b)
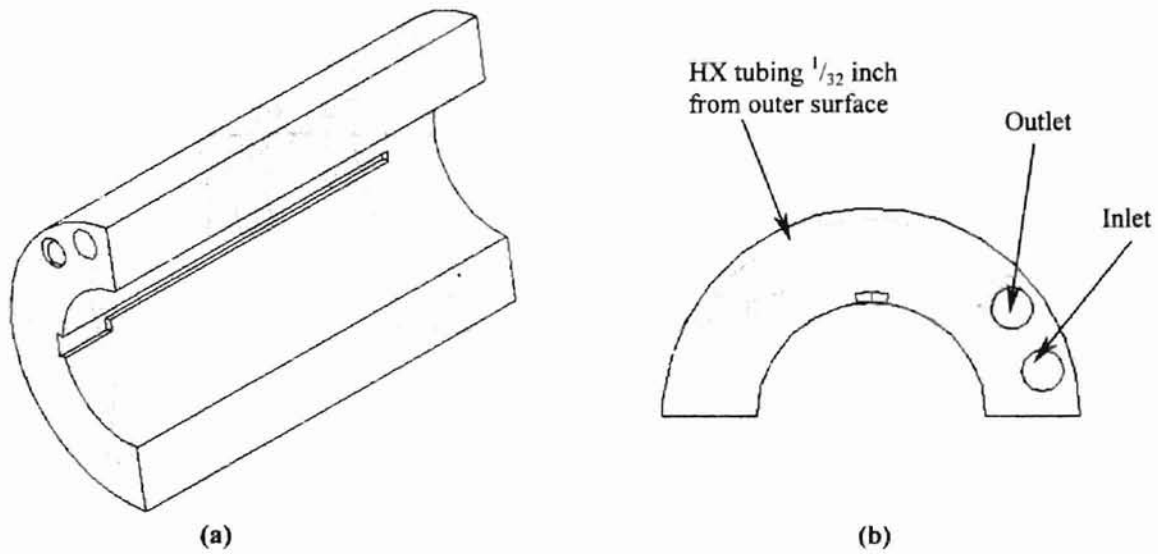
Figure 3.9 SLA Half-cylindrical HX part

The third imbedded function explored was the thermocouple surface grooves. They were designed with the expectation that the SLA part would be a substructure for a sandwich structure. Experimentally, the grooves are designed, the part is built, the thermocouples are laid into them, and the part is covered with composite laminate. The models shown in Figures 3.7 through 3.9 also have thermocouple grooves.

The grooves designed into all parts developed during this project had a depth of 0.03 inches and a width of 0.049 inches because the thermocouple wire used throughout this project had those measured dimensions. The model shown in Figure 3.7 permits 8 thermocouples, the model shown in Figure 3.8 permits 5 thermocouples, and the model shown in Figure 3.9 permits 2 thermocouples.

44

Experimentation was performed on the square HX model. Eight thermocouples were laid into the grooves on the SLA part. The part was sandwiched between 2 layers of LTM25 2 x 2 twill. It was cured at 140°F under a vacuum pressure of 15" Hg for 12 hours. Figure 3.10 shows the assembly of this part.

Composite Laminate

Thermocouples

SLA HX Substructure

Composite Laminate
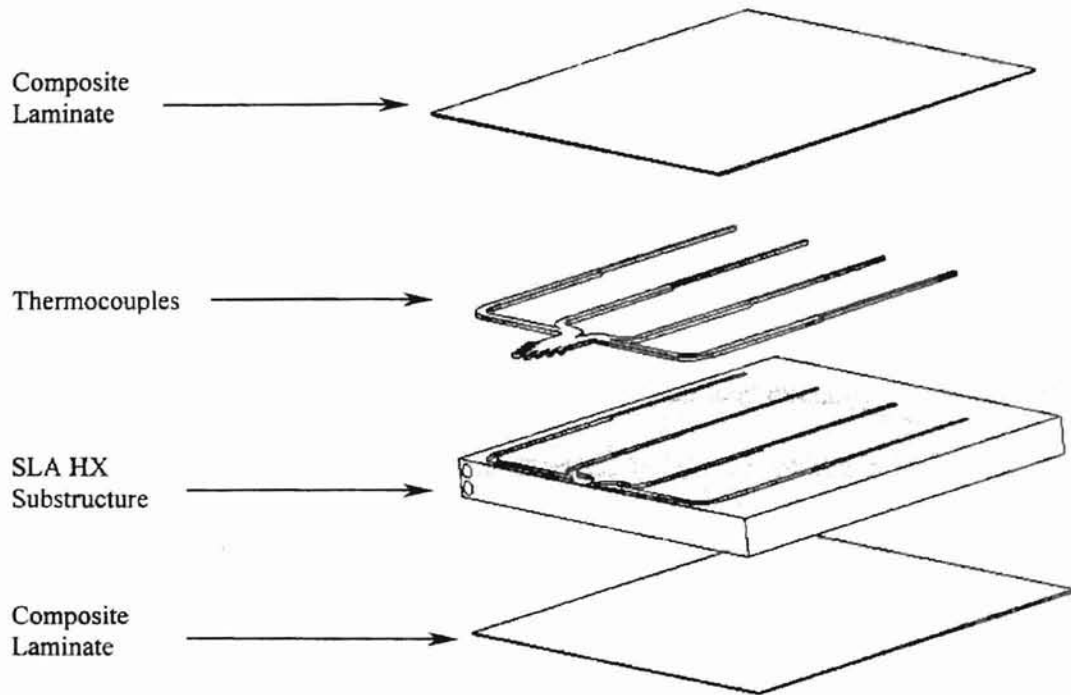
Figure 3.10 Assembly of SLA HX substructure, thermocouples, and composite

Testing was done through the following experiment. The assembled SLA sub-structure, thermocouples, and laminate were placed in an ice bath while water at approximately 140°F was pumped through the HX tubes. The objectives of this experiment were to determine the effectiveness of the heat-exchanging tubes and the ability of the imbedded thermocouples to read accurate temperatures. The experimental setup is shown in Figure 3.11.
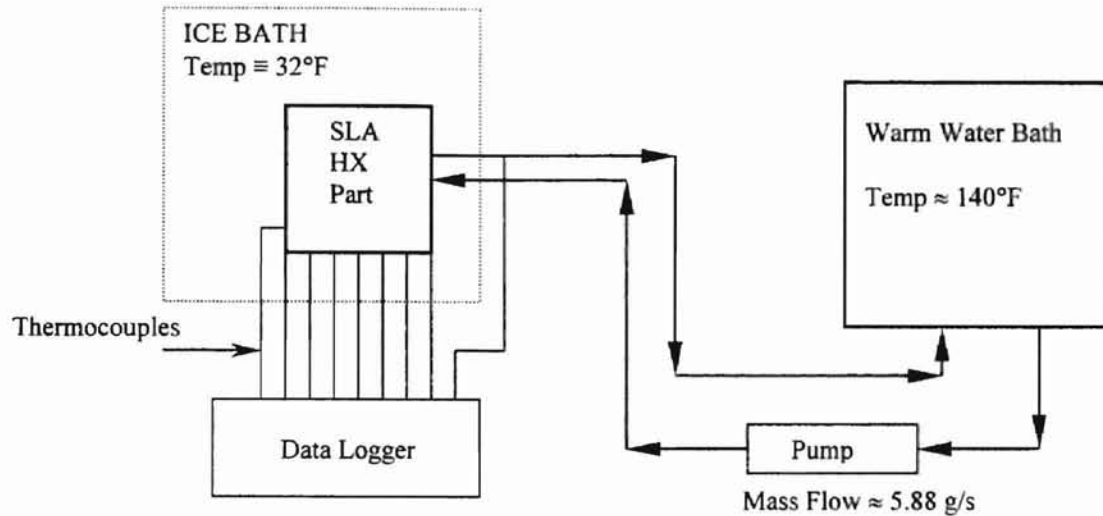
Figure 3.11 Experimental setup for square SLA HX

Warm water was pumped through the submerged heat exchanger at approximately 6 g/s. Data were collected in 2-second intervals from each of the 8 imbedded surface thermocouples and a ninth thermocouple within the flow at the HX exit until the temperature readings reached a steady-state condition. The thermocouples were ordered as shown in Figure 3.12.

In this experiment, the flow came into what was originally designed to be the exit port. Therefore, the 7th and 8th thermocouples were actually reading the temperatures of the flow closest to the inlet, and the 1st and 2nd thermocouples were reading the temperatures of the flow nearest to the exit. The 9th thermocouple was read after the 1st and 2nd thermocouples.

Lessons learned from the intermediate stage of this project were used to determine a final goal – the design and implementation of a working SLA multifunctional curing fixture that would cure composites without need for oven and vacuum bag.
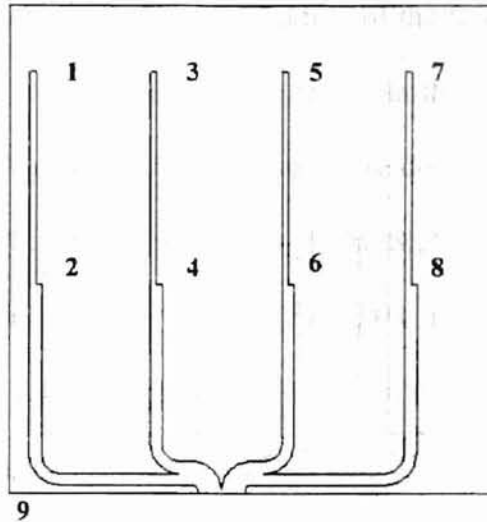
Figure 3.12 Thermocouple ordering on the square HX

3.4　Development of the SLA Multifunctional Composite-Curing Fixtures

The two areas involved in the development of SLA multifunctional composite-curing fixtures are design and experimentation. First, a multifunctional curing fixture was designed. Then, it was tested in order to prove that this concept is a viable one.

3.4.1　Design

The design phase began with selecting an SLA part upon which a composite laminate would be cured (male part). The female multifunctional curing fixture would be designed around this part. The part selected as the male part is the half-cylindrical part shown in Figure 3.9.

The female curing fixture designed to cure composites was designed as upper and a lower halves. During the design process, a multifunctional curing fixture model was designed and then refined after initial experiments were run on it. A sketch of the first

curing fixture is shown in Figure 3.13 and a picture of the first curing fixture is shown in Figure 3.14. The length of the curing fixture halves in the axial direction is 2¾ inches. The HX tubes within the upper and lower halves were designed $^1/_{32}$ inch from the curing surface to allow maximum heat transfer through the SLA resin. The tolerances on the cylindrical surfaces (curing surfaces) were offset 0.03 inches to allow 2 – 3 layers of LTM25 to be applied to the male part. The part would be put into place, and the two halves would be bolted together as shown in Figures 3.13 and 3.14.

The first HX curing fixture was a combination of QuickCast™ and solid SLA. The gray areas in Figure 3.13 denote the solid SLA portions of the curing fixture halves. The centers of the curing fixture halves were built in QuickCast™. The parts were built separately from SL 7520 resin and "glued" together in the post-processing phase.
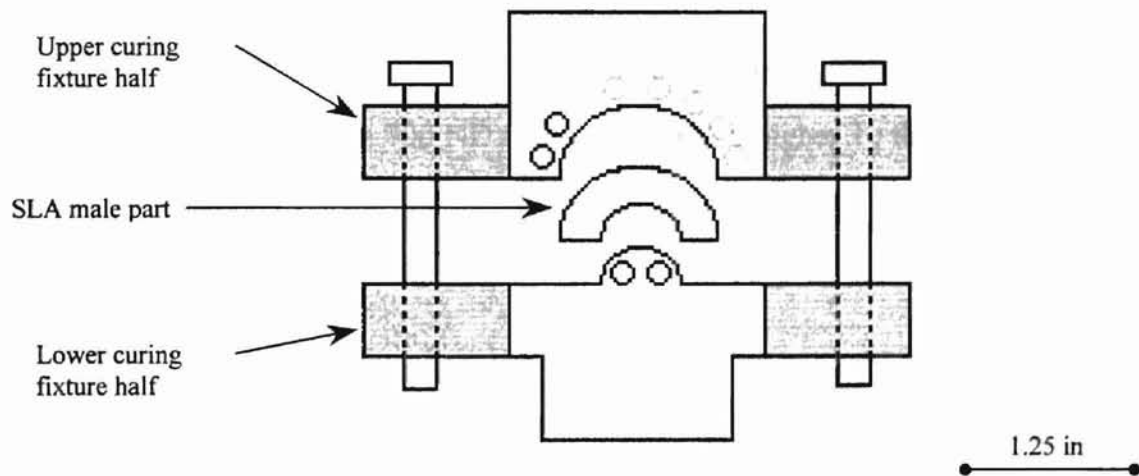
Figure 3.13 Sketch of first HX curing fixture design

In this curing fixture, there are no accommodations for thermocouples. When a part is properly layered with 2 – 3 layers of LTM25 and set into the curing fixture, the protrusion faces are designed to be 0.02 inches apart. Thus, tightening the bolts to make

the faces meet will introduce a force necessary to keep the laminate securely bonded to the male part.
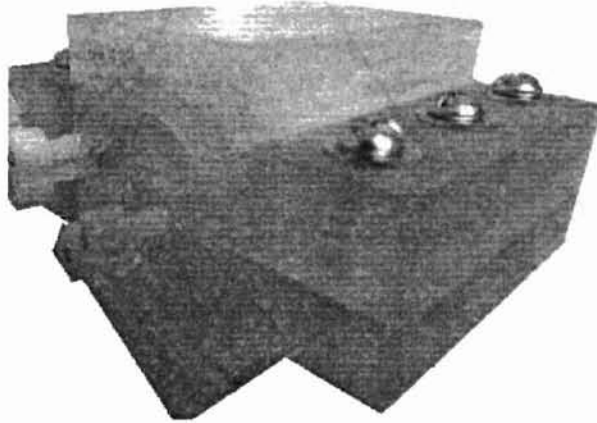
Figure 3.14 First multifunctional curing fixture assembled

The second multifunctional curing fixture was redesigned to include ports and grooves for thermocouples. The bodies of the upper and lower halves had fillets and rounded edges, thus giving them a sleeker look. Another major change is that the second curing fixture was built from 700 ND resin, which has a higher T_g than SL 7520 resin. The surface tolerances and the HX tubing did not changed with respect to the first multifunctional curing fixture.

After this multifunctional curing fixture was built entirely by the solid build method, thermocouples were inserted into the ports and grooves on the curing fixture halves. The grooves were filled in with epoxy and smoothed out. Otherwise, there would be small ridges on the surface of a cured part, indicating where LTM25 epoxy had been forced during the cure process. The curing fixture halves were then assembled and connected to the rest of a heat-exchanging system. Figure 3.15 shows the upper and lower halves of the second HX curing fixture design. Figure 3.16 shows the assembly of these curing fixture halves with a male part.

49

Thermocouple
grooves/ports
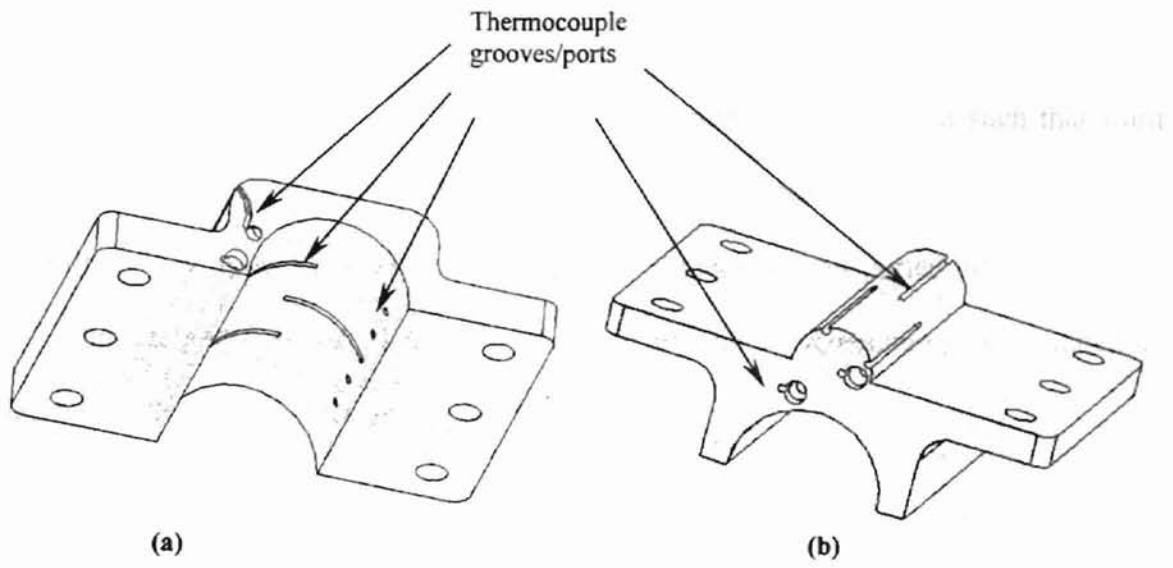
Figure 3.15 Second HX curing fixture design. (a) Upper half. (b) Lower half
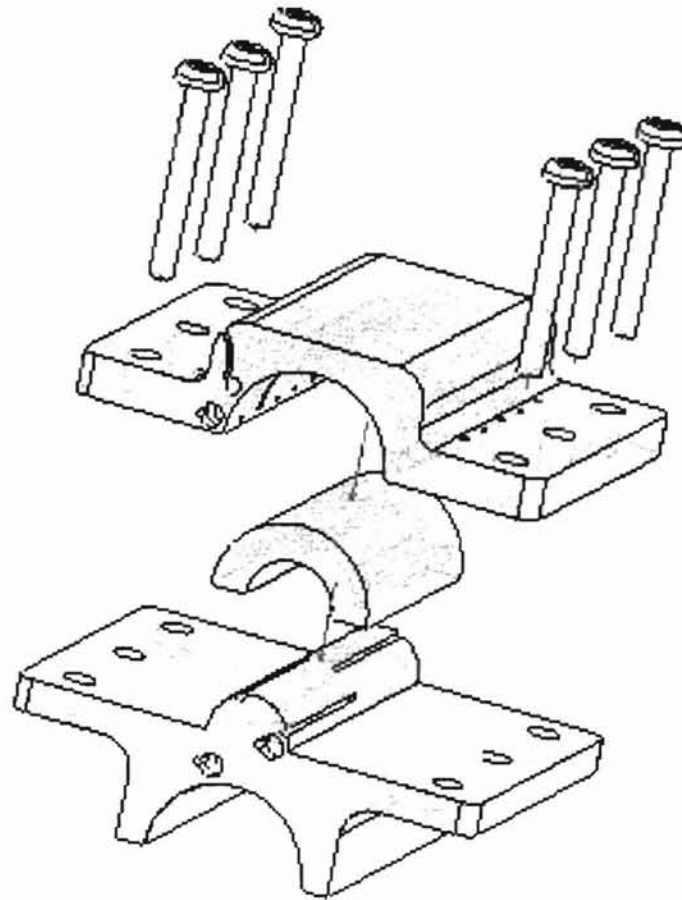
Figure 3.16 Assembly of the second curing fixture and male part

3.4.2   Testing

The multifunctional curing fixtures were connected to a system such that warm water could be pumped through them to supply the heat necessary for curing LTM25 carbon fiber. The system is shown in Figure 3.17. Water was transported through clear vinyl tubing to and from the SLA curing fixture halves, and temperature was regulated using the Julabo® F12-MD recirculator.
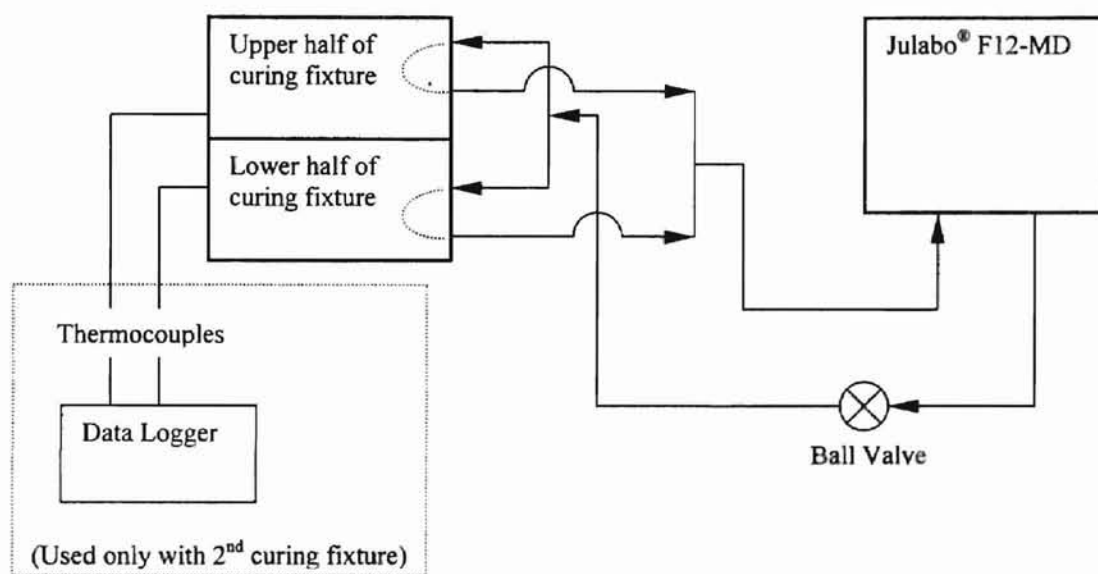
Figure 3.17 Experimental setup for multifunctional curing fixtures

Though the general system diagram applied to both multifunctional curing fixture designs, there were some changes made regarding experiments run with the first curing fixture and the second one. During experiments on the first curing fixture, there was no insulation on the vinyl tubing. Insulation was added to the tubing after experiments were completed on the first curing fixture. The Julabo® F12-MD recirculator was operated

manually during experiments on the first curing fixture and remotely (using EZ-Temp®

software) for tests performed using the second curing fixture.

For these experiments, the following constant parameters were used:

Mass Flow$|_{upper\ half} \approx 5.75$ g/s

Mass Flow$|_{lower\ half} \approx 9.0$ g/s

Valve fully open

These mass flow parameters were determined by experimentation and estimating

a density of water equal to approximately 0.98 g/cm^3.

3.4.2.1 First Multifunctional Curing Fixture

Testing on the first multifunctional curing fixture went as follows: 1) Surface

temperature tests for both unassembled and assembled configurations (to estimate the

surface temperatures during a cure process and what temperature losses might be ex-

pected through the tubing); 2) Curing composites using this part to determine if this

method of curing composites is successful.

Two tests were run to gather temperature data. The first test was an attempt to de-

termine temperature losses through the tubing. Recirculator temperature was set to 60°C.

A thermocouple was placed on the middle of the heating surfaces as shown in Figure

3.18.

Temperatures on both multifunctional curing fixture surfaces were recorded once

it reached a steady-state condition (approximately 5 minutes) for both unassembled and

assembled configurations.

The second test was conducted in order to determine which bath temperature

would result in a curing fixture surface temperature of 140°F (60°C). The curing fixture

halves were assembled and bath temperature was set to 60°C. After the surface temperatures reached a steady-state condition (approximately 5 minutes), the bath temperature was increased by increments of 1°C until the temperatures on the curing fixture surfaces measured approximately 60°C.

(a) Bottom view of upper half   (b) Top view of lower half
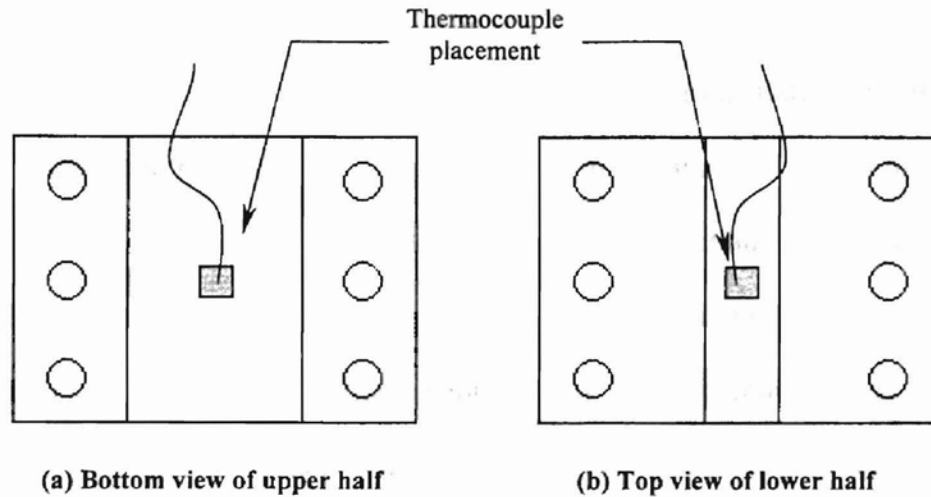
Figure 3.18 Thermocouple placement on heating surfaces of first curing fixture

Next, a part was cured using this multifunctional curing fixture. One layer of LTM25 and one layer of film adhesive were laid up on a part (shown in Figure 3.9). A thin plastic mold release was placed on the part to cover it and ensure that the part could be removed from the curing fixture after the curing process. The part was placed into the curing fixture (similar to Figure 3.16), and it was bolted tightly shut. The bath temperature was set to 66°C, and warm water was pumped through the curing fixture for approximately 12 hours. After the part was taken out, the edges were sanded to remove excess resin. Several parts were cured in this manner using this first multifunctional curing fixture.

3.4.2.2 Second Multifunctional Curing Fixture

Two general tests were performed: 1) Temperature tests on an empty curing fixture to estimate what bath temperature was required to maintain curing fixture surface temperatures of 140°F and 160°F; 2) Curing composites using this curing fixture while monitoring temperature via imbedded thermocouples.

Thermocouples were already imbedded into this curing fixture so no additional thermocouples were necessary. The upper half of the curing fixture was designed with the capability to house 11 thermocouples plus one at the inlet and one at the outlet – 13 total. The lower half of the curing fixture was designed to house 4 thermocouples plus one at the inlet and one at the outlet – 6 total. Only 8 thermocouples were used to take measurements because using any more would just add clutter to the experiment. Four were used at the inlets and outlets of both halves, two were imbedded in the surfaces of each half. Figure 3.19 demonstrates the locations and channel numbering scheme of the thermocouple used to record data (via the data logger).

(a) Upper half   (b) Lower half
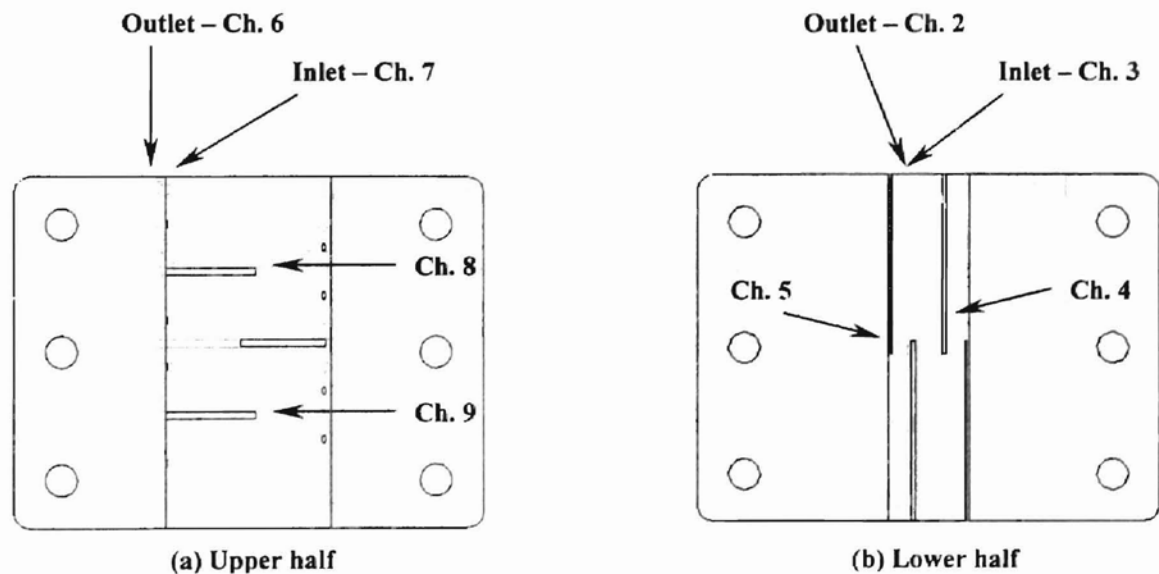
Figure 3.19 Thermocouple/data logger channel scheme

The setup for the temperature tests involved the assembled, but empty, curing fixture. Insulating tape (purchased from a local hardware store) was wrapped around the tubing connecting the outlet of the recirculator to the inlets of the curing fixture halves. No insulation was used on the tubing connecting the outlets of the curing fixture halves to the inlet of the recirculator. The temperature on the Julabo® recirculator was set to 60°C (140°F), 65.6°C (150°F), and 71.1°C (160°F). At each temperature, the system was allowed to reach steady-state (approximately 5 minutes), and temperatures were read from channels 4 and 8. This test was performed in order to determine the temperature losses from the recirculator to the curing fixture.

After data had been collected for the temperature loss tests, a test was run to determine which recirculator temperature setting would result in target temperatures of 60°C and 71.1°C within the curing fixture. The setup was the same as in the temperature loss test. Temperature was read only from channel 8. First, the temperature of the water bath was set to 60°C. After system temperature had reached steady-state (approximately 5 minutes), bath temperature was then increased by increments of 0.1°C. After each incremental increase, the system was allowed to stabilize (1 – 2 minutes). This incremental increase continued until the temperature read from channel 8 was approximately 60°C.

Next, the temperature of the water bath was set to 71.1°C. After steady-state conditions had been achieved (approximately 5 minutes), bath temperature was increased by increments of 0.1°C. After each incremental increase, the system was allowed to stabilize (1 – 2 minutes). This incremental increase continued until the temperature read from channel 8 was approximately 71.1°C.

The second general set of tests involved curing composites with this new curing fixture. Three parts were cured using this new curing fixture. Before curing each part, 5 coats of PMR liquid curing fixture release were applied to the curing surfaces of the curing fixture halves. One part was made from SL 7520 resin. It was covered with one layer of film adhesive and one layer of LTM25. The temperature of the Julabo® F12-MD was set such that the curing fixture temperature would be 60°C. Warm water was then pumped through the curing fixture for approximately 15 hours (according to the optimal curve on the LTM25 cure chart, Figure 2.6). The other two parts were made from 700 ND resin. One was covered with just one layer of LTM25. The other was covered with two layers of LTM25. To cure both parts, curing fixture temperature was set at 60°C for 2 hours and then ramped to and maintained at 71.1°C for 10 hours.

CHAPTER 4

4. RESULTS

This chapter sequentially discusses results from sections 3.2, 3.3, and 3.4.

4.1   Feasibility Studies

Preliminary geometries were selected to reflect either simple parts or common designs that have practical application. Crucial lessons learned from these studies would be applied to the intermediate studies and the multifunctional curing fixture designs.

4.1.1   NACA0012 Wing

The first test involved the design of a small wing with the intent to discover the limitations of the SLA-7000. Figure 4.1 compares the CAD drawing of the wing (see also Figure 3.2a) to the actual SLA model produced. Qualitatively, the physical shape of the SLA model was very much what was expected. The NACA0012 airfoil shape turned out as expected, and the trailing edge was sharp.

The imbedded pressure taps did not turn out as hoped. Some of the ports were clogged with resin that did not drain. Seemingly, the SLA-7000 had trouble replicating the $1/32$-inch diameter tubes near the trailing edge. They were all clogged. Some of the exit ports near the trailing edge were designed closer than 0.006 inches from the surface.

As a result, the surface didn't close around it, creating grooves rather than internal tubes. Most of the $^1/_{16}$-inch diameter tubes drained fairly well. Thus, it was determined that all internal tubing design henceforth would have a diameter no less than $^1/_{16}$ inch.
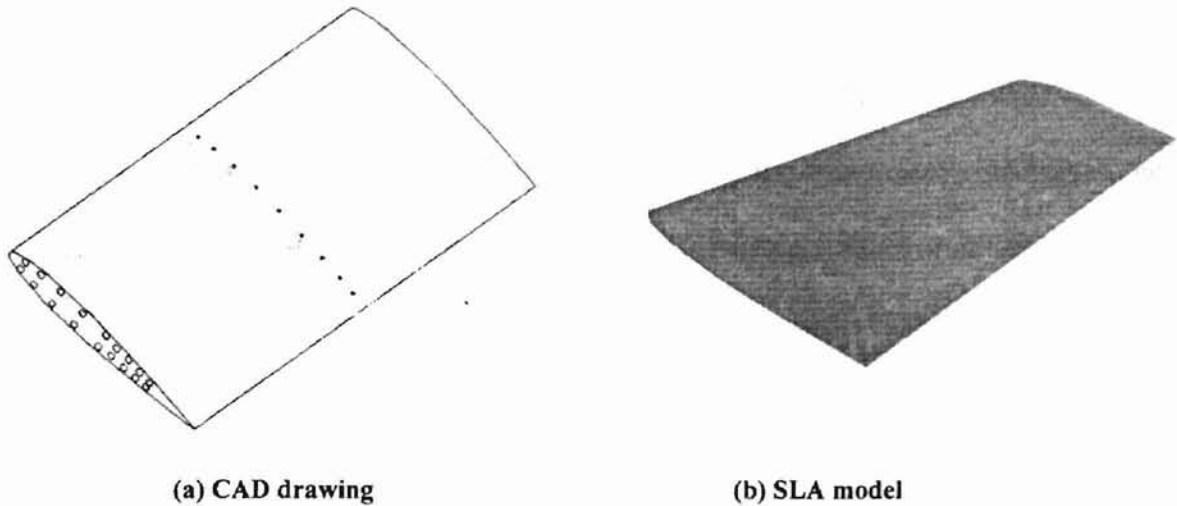
(a) CAD drawing   (b) SLA model

Figure 4.1 Comparison of NACA0012 wing CAD drawing to SLA model

4.1.2   SLA Half-Cylindrical Meshes

The results from the tests described in section 3.2.2 are as follows:

1)   The part crushed; it could not withstand the heat of the oven during the cure process. Since the oven has a temperature variability of approximately $\pm 5°F$ from the set temperature, a setting of 150°F may result in periods of time in which the oven is actually at a temperature of 155°F – above T_g of SL 7520 resin. Figures 4.2a and 4.2b show how this crushed part might look.

2)   This part turned out exactly as expected. The composite cured nicely and the SLA part did not crush. It is likely that the oven temperature

never exceeded the SLA part's T_g of 154°F during the cure. Figure 4.2c shows this part.

3) All four parts crushed. See the explanation for (1) and also Figures 4.2a and 4.2b. After seeing the results of this test, all future tests on SLA parts made from SL 7520 resin would be cured at 140°F.

4) The part did not crush, thus signifying that the glass transition temperature had not been exceeded during the cure process. However, the LTM25 fabric was still tacky as if it weren't fully cured. At this time, it was speculated that it hadn't been in the oven long enough.

5) Same as (4). Even after an additional 5 – 6 hours of cure and a higher vacuum pressure (23" Hg), the parts were still tacky and not fully cured. At this point, it was speculated that the LTM25 laminate that was being used had expired. Also, this test served to illustrate that pressure didn't have as big of an impact on crushing the part as originally thought and that temperature was the primary factor.

(a) Crushed SLA mesh   (b) Crushed SLA mesh   (c) Uncrushed SLA mesh
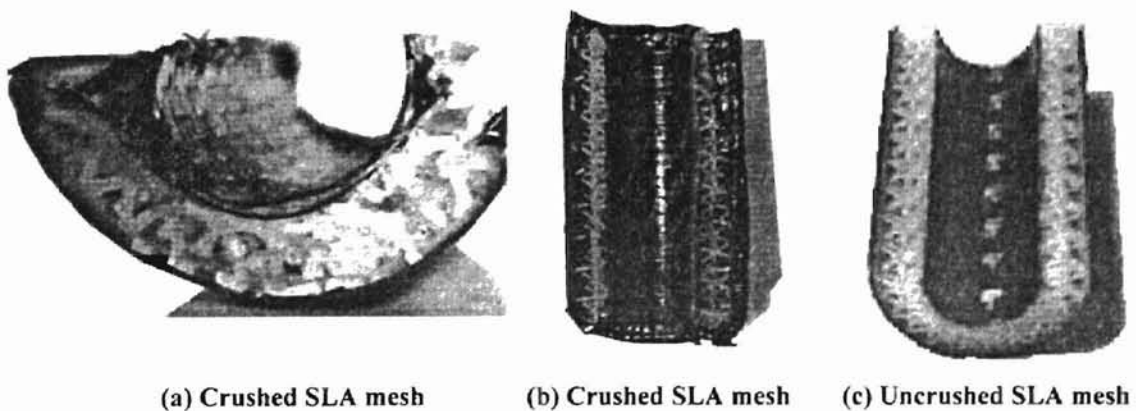
Figure 4.2 Qualitative results of tests in Section 3.2.2

4.2   Intermediate Studies

Lessons learned from the feasibility studies were implemented into the methodology of the intermediate studies.

4.2.1   SLA Curing Fixtures

The first wing to be built was the 18-inch long NACA0012 wing and its corresponding curing fixture halves. The CAD drawing of this wing is shown in Figure 3.4. The actual SLA wing and curing fixture are shown assembled here in Figures 4.3 and 4.4.
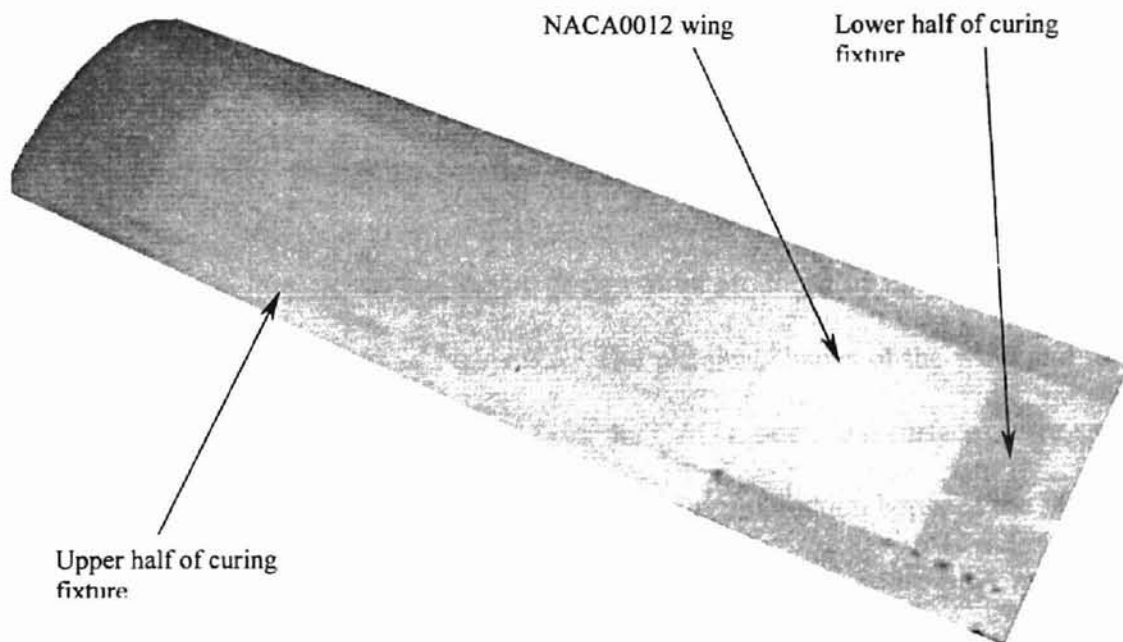
Figure 4.3 SLA NACA0012 wing and curing fixture

The SLA model of the wing turned out exactly as expected. Even the trailing edge turned out sharp and clean. The curing fixture halves also turned out as expected,

and they fit together. The process of using these curing fixtures to aide in curing LTM25 to the wing was a success. The curved design of the upper half of the curing fixture fit its purpose and the vacuum bag adhered to its contour, thus allowing a desirable pressure distribution on the composite throughout the cure. Afterwards, the surface of the wing turned out smooth and glassy.
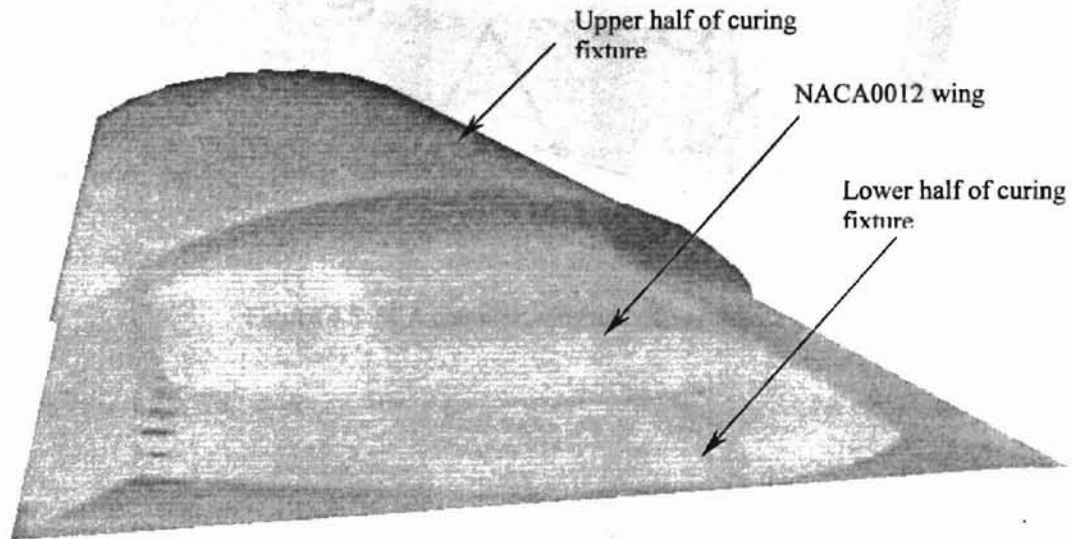
Figure 4.4 SLA NACA0012 wing and curing fixture

The next wing and curing fixture design to be produced by the SLA-7000 was the more complex design shown in Figure 3.5. The physical shapes of the wing and its curing fixture parts turned out as expected from the CAD model. All surfaces were smooth, and the trailing edge of the wing was sharp and clean. Interaction between the "fuselage" and the wing was also detailed. Figures 3.5, 3.6, and 3.7 show the SLA models built from this design.
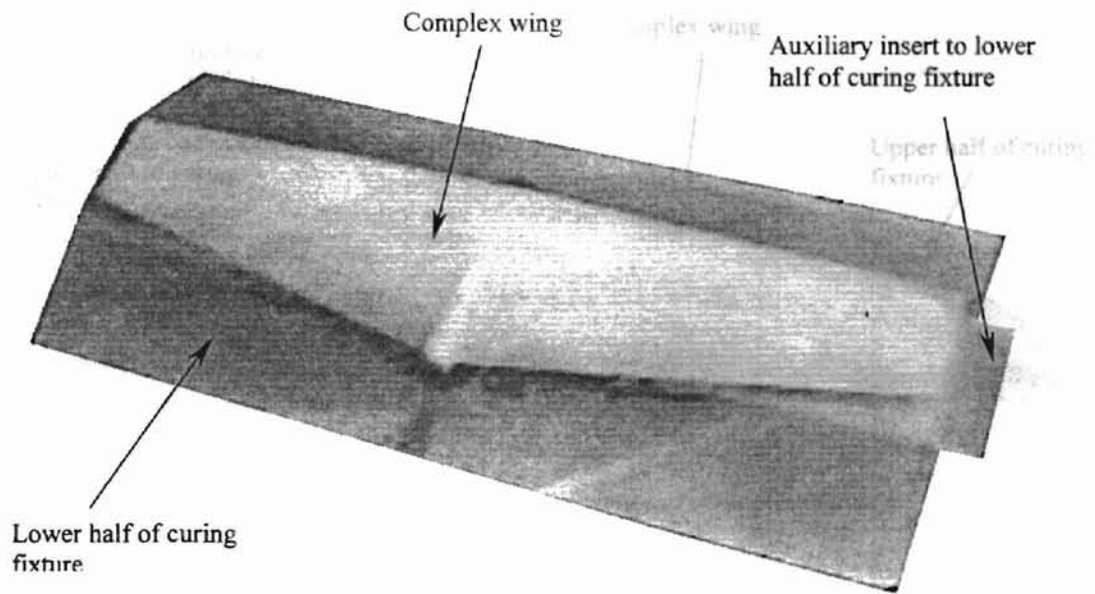
Figure 4.5 SLA complex wing and curing fixture parts
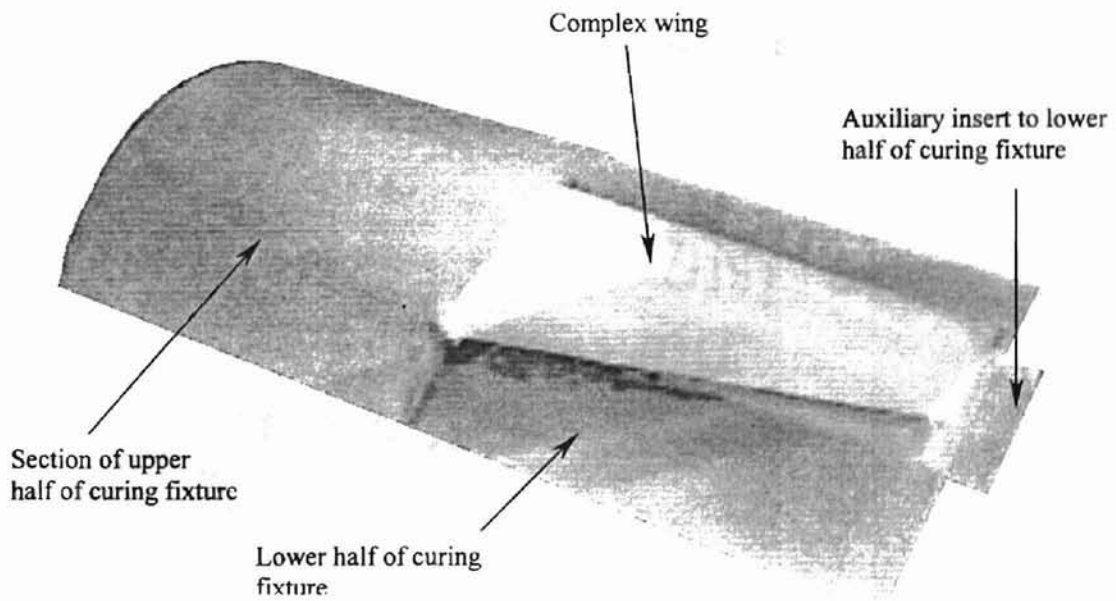
Figure 4.6 SLA complex wing and curing fixture parts
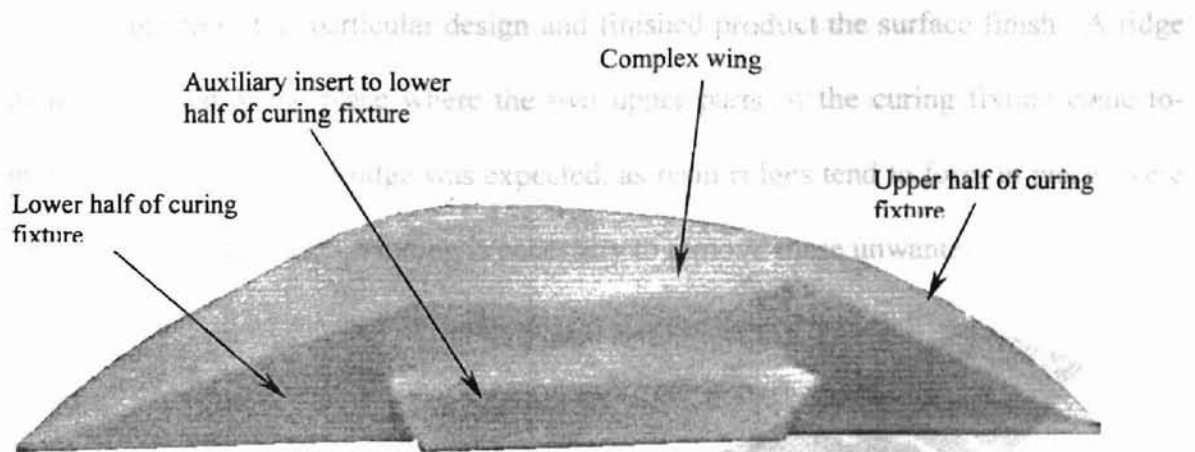
Figure 4.7 SLA complex wing and curing fixture parts

This curing fixture was also used to cure composites onto the complex wing, but it was more difficult to lay up with LTM25 carbon fiber. Places where there were sharp corners (particularly where the "fuselage" meets the wing) posed a problem for lab techs covering the wing with composite. Despite this minor technical difficulty, the rest of the wing turned out well. Figure 4.8 shows the upside-down covered wing and its mounting bracket. Figure 4.9 shows the covered wing with tufts on the tip of the port wing.
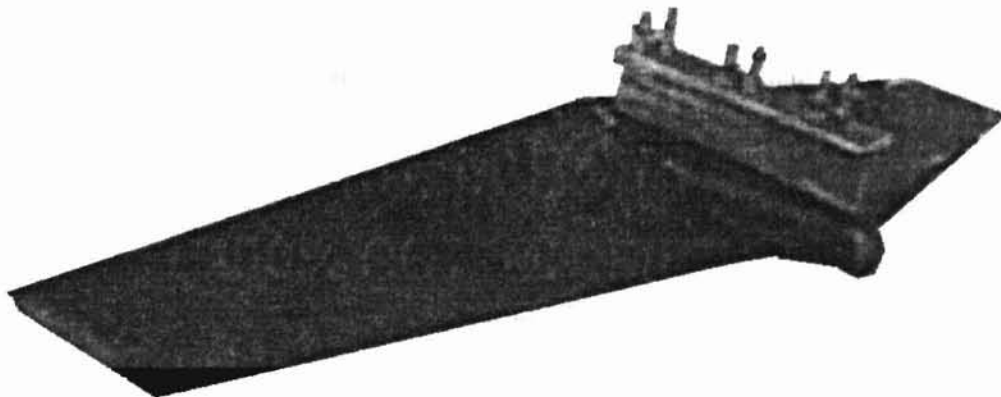
Figure 4.8 Covered complex wing with mounting bracket

Note from this particular design and finished product the surface finish. A ridge of resin formed at the place where the two upper parts of the curing fixture came together. However, such a ridge was expected, as resin ridges tend to form in places were curing fixture parts meet. Sanding is necessary to remove these unwanted ridges.
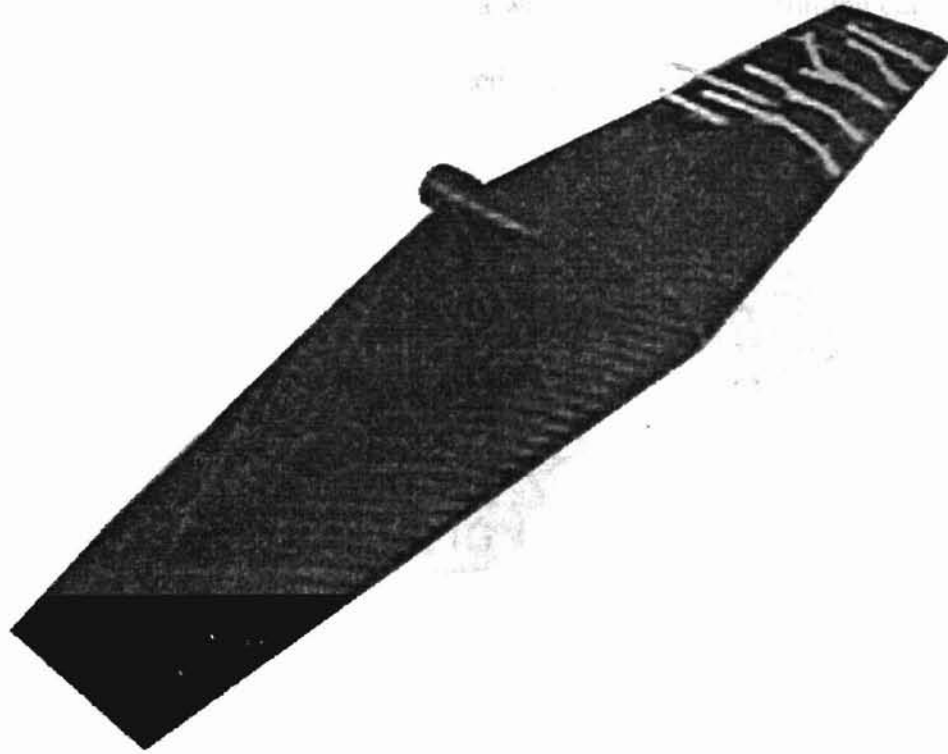
Figure 4.9 Covered complex wing with tufting

4.2.2 Imbedded Functionality

The pressure tap results for the small NACA0012 wing are elucidated in Section 4.1.1. Similar results were obtained from the pressure taps designed into the complex wing. Figure 4.10 shows the SLA model of the complex wing (prior to covering with composite).

More success was achieved by using compressed gas to blow out excess resin from the imbedded taps, but it was still unsuccessful at removing resin from the tubes having a diameter less than $^1/_{16}$ inches. The tap closest to the trailing edge could not be cleaned out. At this point, no further study of imbedded pressure taps was explored. They certainly show potential at locations on a wing away from the trailing edge, but difficulties arise as the trailing edge is approached and the need for smaller diameter tubing becomes necessary.
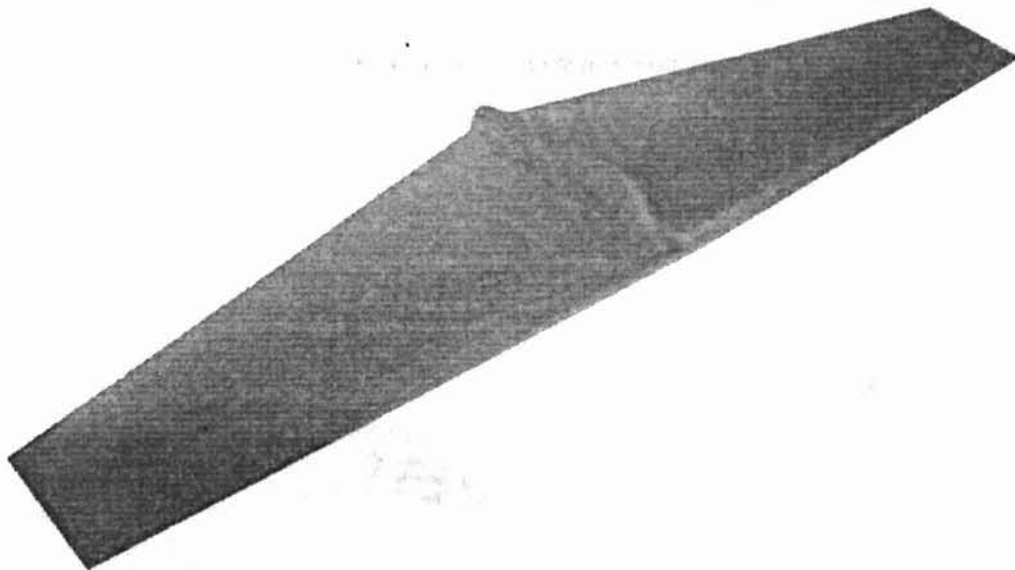
Figure 4.10 SLA complex wing

The imbedded heat exchanger tubes and thermocouple grooves showed promise. The parts shown in Figures 3.7 – 3.9 were built successfully in the SLA-7000. The SLA models of these three designs are shown in Figures 4.11 – 4.13.

(a) Upper face   (b) Perspective view
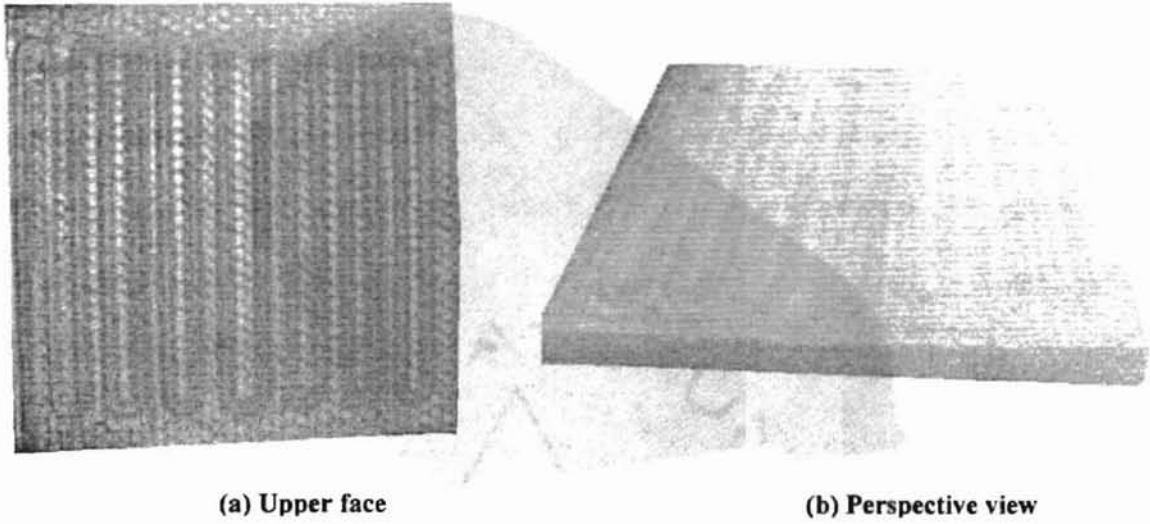
Figure 4.11 SLA square heat exchanger

(a) Upper face   (b) Lower face
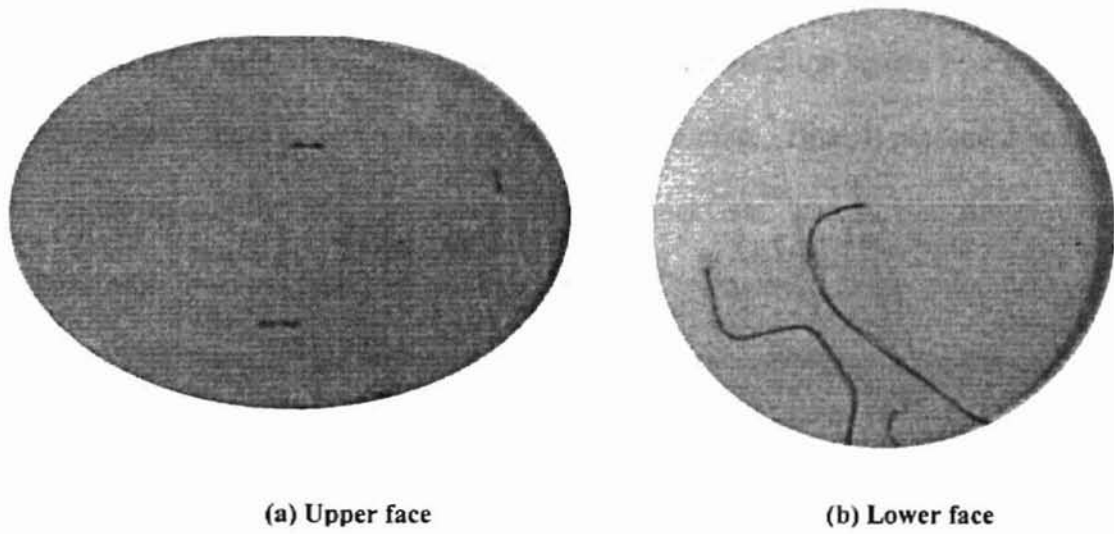
Figure 4.12 SLA disk heat exchanger
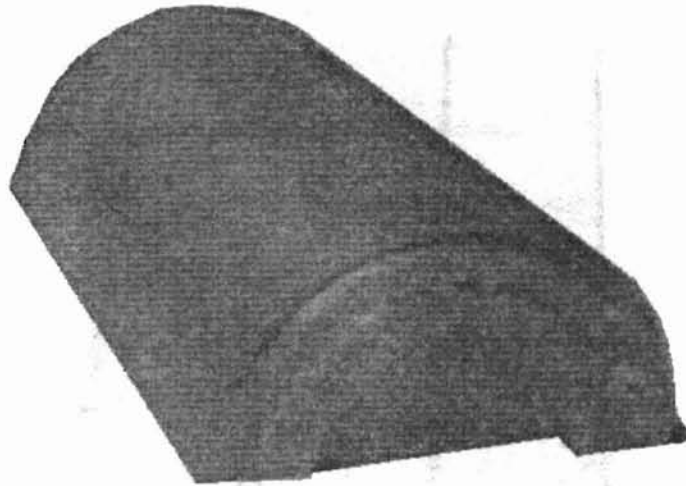
Figure 4.13 SLA half-cylindrical heat exchanger

The results regarding the build of these parts were mixed. Some of the parts turned out well – the tubing was intact and without flaw, but many of the disk-shaped heat exchangers ended up with flawed tubes imbedded within. In this case, flaws are holes in the tube walls. Yet, in the half-cylindrical parts and the square heat exchangers that were tested, there were no leaks in the internal tubing. Thus, it presented an uncertain scenario regarding imbedded tubes within a QuickCast™ part. Later, it was realized that tube wall thickness could be specified in the QC software, and the leaks were the result of not specifying a thick enough tube wall. That problem was quickly and easily rectified.

The thermocouple grooves turned out exactly as designed on each part, and the particular thermocouple wire used in these experiments fit into the grooves. Figure 4.14 shows the square heat exchanger with thermocouples all neatly in place prior to covering it with composite laminate.
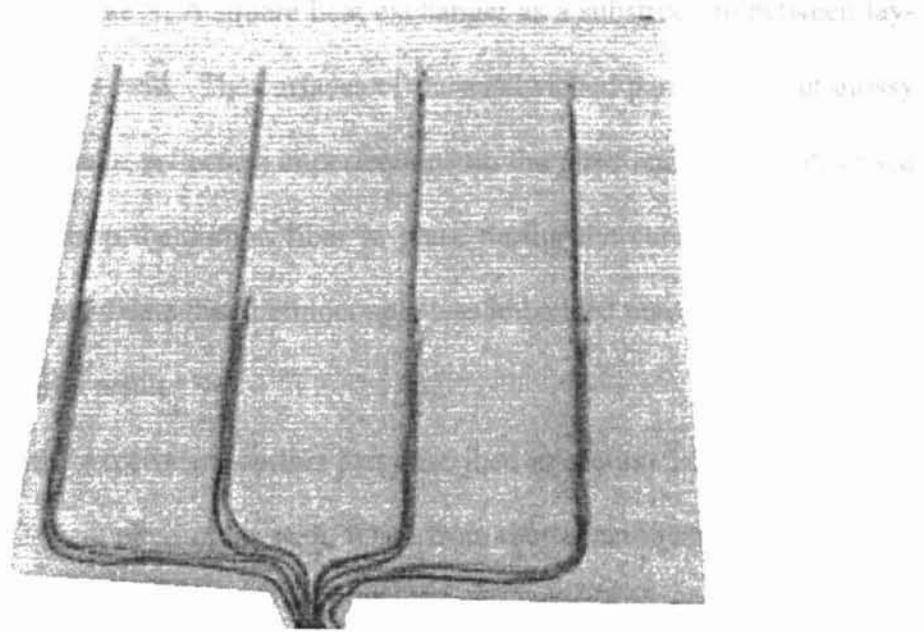
Figure 4.14. SLA square heat exchanger with thermocouples

Further tests performed on the SLA square heat exchanger demonstrated successful sandwiching of the SLA substructure, complete with imbedded thermocouples and HX tubing, and successful implementation of the imbedded thermocouples.
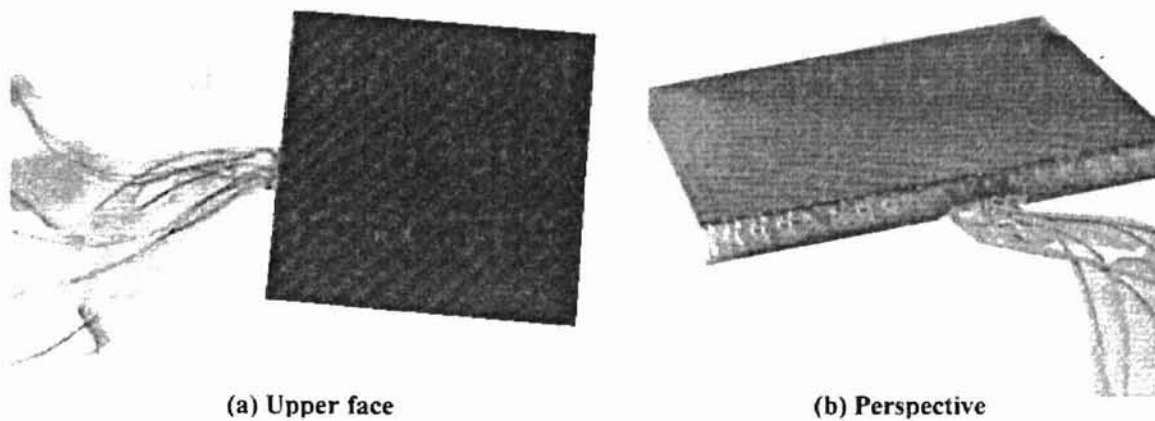
(a) Upper face   (b) Perspective

Figure 4.15 SLA square heat exchanger sandwiched between carbon fiber

Figure 4.15 shows the SLA square heat exchanger as a substructure between layers of LTM25 carbon fiber twill. The surfaces of the sandwiched part turned out glossy and smooth with a few nicks, reflecting imperfections on the glass and metal plates used as "curing fixtures" to keep the carbon fiber in place during the cure. There were no ridges, bumps, or dips to indicate that thermocouple was imbedded onto the surface of the part. This was the desired result.

The results of the experiment on this part described in section 3.3.2 and shown in Figures 3.11 and 3.12 were pleasing as well. Data from that experiment are represented here in Figure 4.16.

**Thermocouple and Outlet Temperatures
vs. Time**
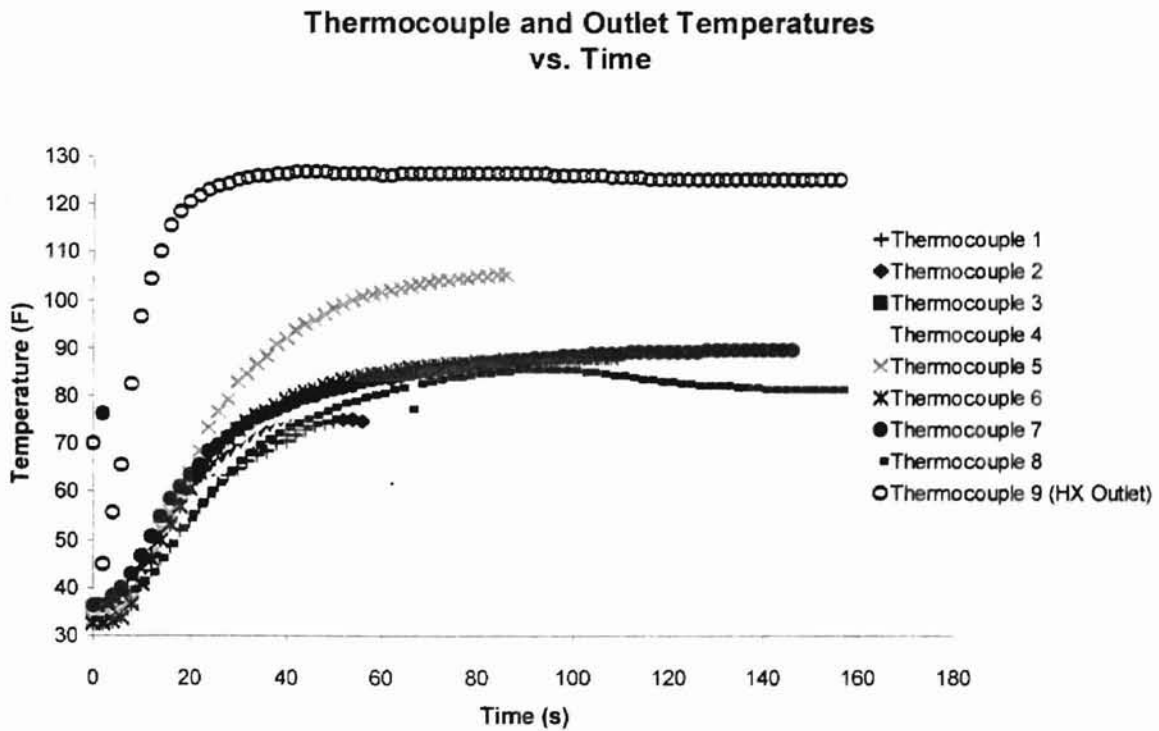
Figure 4.16 Temperature results from SLA square HX experiment

The data presented here follow the trend expected for this experiment. In this experiment, one would expect the surface temperature to start at the temperature of the ice

bath, and then approach some steady state temperature above that of the ice bath, but below that of the heated water bath after a period of time. The data show that the imbedded thermocouples are capable of reading good data and demonstrate that the SLA part is performing its function – regulating the surface temperature of the part. Thus, this technology could be used on the leading edge of a wing, for example, as a de-icing mechanism. In such a case, bleed air could be taken from the engine and run through imbedded tubes within the leading edge of a wing, thus de-icing them if necessary. This technology may also be implemented into a variety of cooling applications as well.

At the beginning of the experiment, the change in temperatures at thermocouples 6, 7, and 8 is steeper than the change in temperatures at thermocouples 1, 2, and 3. This can be expected; by the time the warm water has reached thermocouples 1 – 3, it has been slightly cooled by the ice bath. Thus, the change in temperature, ΔT, from the ice bath to the water flow at thermocouple 1, for example, is not as great as the ΔT from the ice bath to the water flow at thermocouple 7. The water flow at thermocouple 7 hasn't had as much time to be affected by the ice bath. The readings for thermocouple 5 are noticeably higher than the other thermocouples. Perhaps, thermocouple 5 may be closer to the internal flow than the others. Finally, note that the temperatures recorded at thermocouple 9 are much higher than those recorded by any other thermocouple. Recall that thermocouple 9 is actually within the flow. All other thermocouples are not within the flow, but are in a medium between the flow and the ice bath.

4.3   SLA Multifunctional Composite-Curing Fixtures

The crux of this project hinges on the implementation of imbedded functionality into an SLA curing fixture so that it will be able to cure a composite part without need for vacuum bag and oven. The particular geometry of this multifunctional curing fixture and its associated part is simple, but the success of this process demonstrates the proof of concept, which is the key issue regarding these results.

4.3.1   First Multifunctional Curing Fixture

The assembled first SLA multifunctional curing fixture is shown in Figure 3.14. It turned out well, complete with functional imbedded tubes. Figure 4.17 shows the first curing fixture connected to the recirculator. The results from the surface temperature tests described in Section 3.4.2.1 are as follows:

Unassembled Configuration (Bath Temperature = 60°C)

Upper Curing Fixture Steady-State Surface Temperature Reading: 39.2°C (102.6°F)

Lower Curing Fixture Steady-State Surface Temperature Reading: 42.3°C (108.1°F)

Assembled Configuration (Bath Temperature = 60°C)

Upper Curing Fixture Steady-State Surface Temperature Reading: 48.3°C (118.9°F)

Lower Curing Fixture Steady-State Surface Temperature Reading: 56.0°C (132.8°F)

Thermocouple

Julabo® F12-MD

Valve

Vinyl Tubing

Lower half of first
curing fixture

Upper half of first
curing fixture
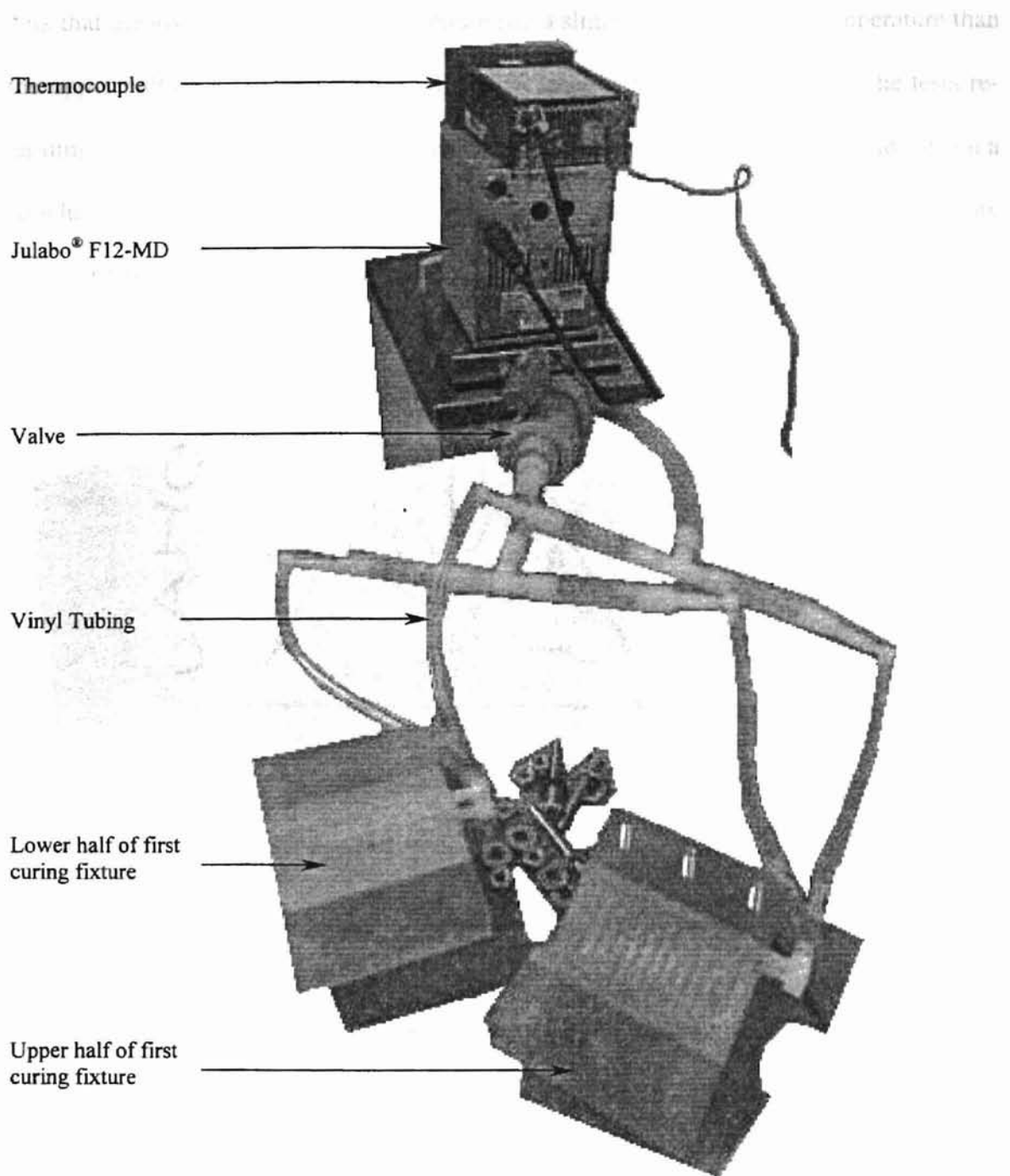
Figure 4.17 Halves of first multifunctional curing fixture connected to system

Note that for the assembled configuration, the surface temperature readings rose somewhat dramatically. Apparently, the ambient air temperature is much more affected by the heating of the lower and upper curing fixture halves. It also appears from these

data that the lower half of the curing fixture has a slightly higher surface temperature than the upper half of the curing fixture. The difference is more pronounced in the tests regarding the assembled configuration. But, the next test indicates that this first test is not a conclusive indication of temperature. Figure 4.18 shows the assembled curing fixture with a thermocouple inside the chamber.
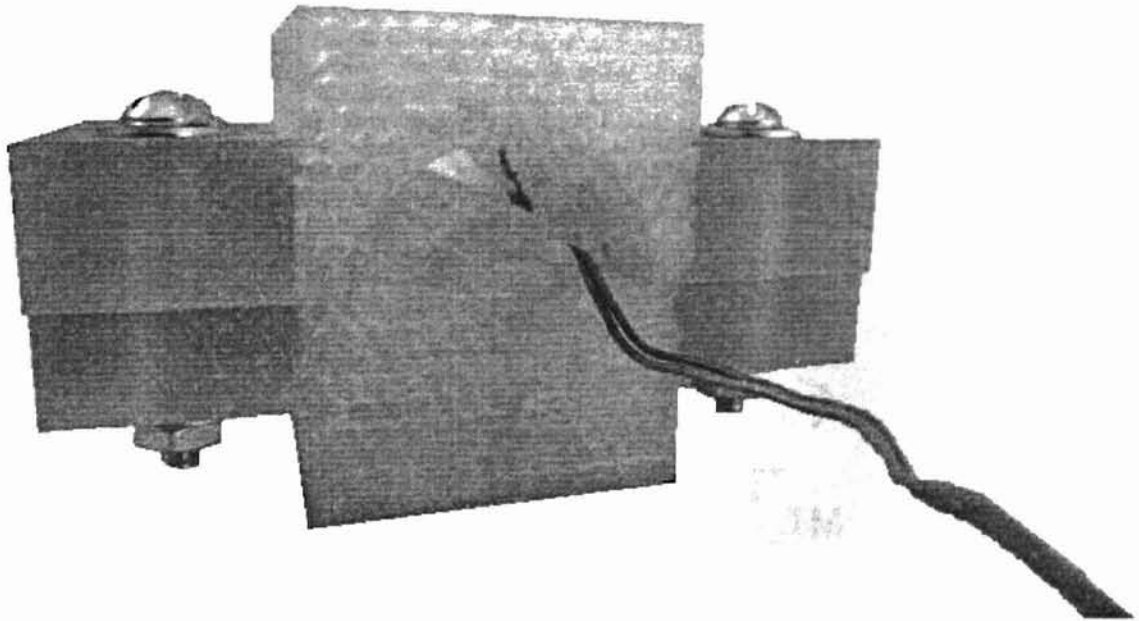
Figure 4.18 Assembled first curing fixture with thermocouple inside

The results of the next temperature test (finding what bath temperature will give a curing fixture surface temperatures of approximately 60°C) are as follows:

Lower Curing Fixture: $T_{bath} = 66.0°C$ (150.8°F) ➔ $T_{curing\ fixture} = 60.4°C$ (140.72°F)

Upper Curing Fixture: $T_{bath} = 66.0°C$ (150.8°F) ➔ $T_{curing\ fixture} = 60.6°C$ (141.08°F)

The data presented indicate that there is not much temperature difference on the surfaces of the upper and lower curing fixtures when they are assembled. Perhaps, the results of the first test were not entirely valid. This test was performed once more, and the results were identical.

The next test performed with the first curing fixture was that of curing a composite part. Figure 4.19 shows the first cured part as it came out of the curing fixture. Figure 4.20 shows the first cured part by itself.
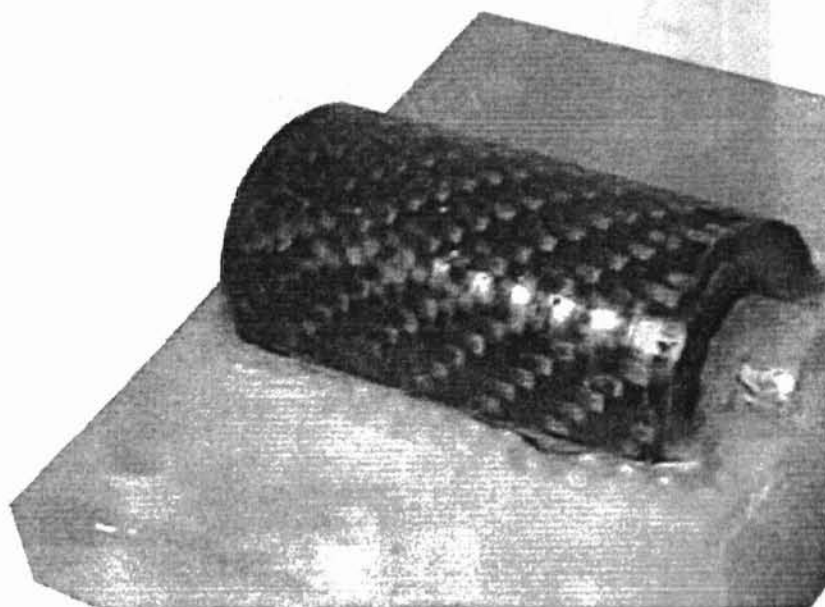
Figure 4.19 Cured part resting on lower half of first curing fixture
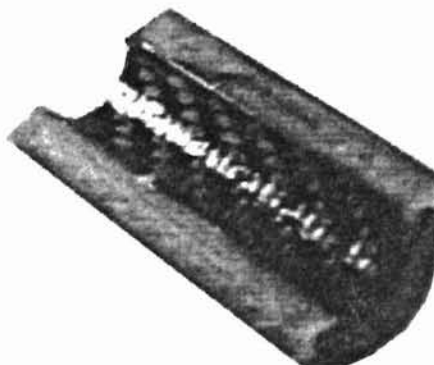
Figure 4.20 Cured part using first curing fixture

The results of this test were pleasing. The composite came out fully cured with smooth surfaces. The first test using the first curing fixture was a success. More parts were cured using the first curing fixture, and a leak was discovered in the HX tubing of the upper half of the curing fixture. Figure 4.21 shows the location of the leak on the first curing fixture.
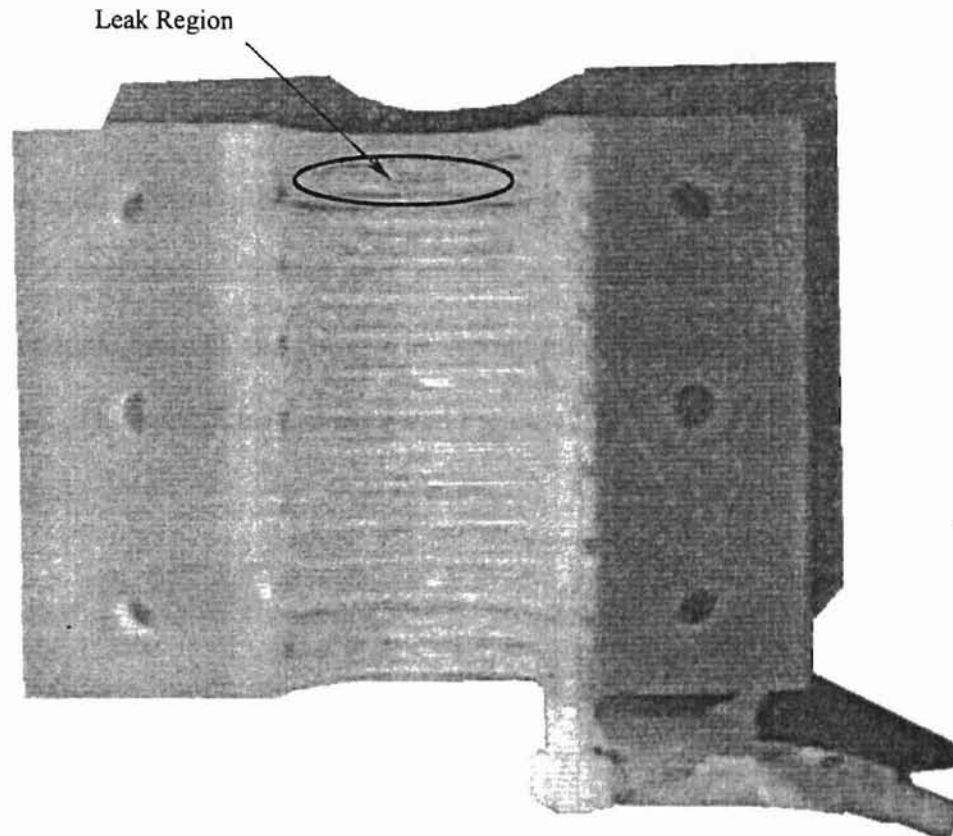
Figure 4.21 Leak location of the first curing fixture

The leak did not exist during the first curing process. Thus, the imbedded tubing acquired a hole after it had already been used. Discovery of this leak supported the results of the intermediate studies regarding imbedded functions. Some of the parts built had leaky tubes, as this part now did. The problem, however, was not design-related. Instead, it was a problem with imbedding tubes into QuickCast™ parts. The wall thick-

ness of tubes imbedded into a QuickCast™ structure was not set to be thick enough. After discovering this leak in the curing fixture, it was determined that the second multifunctional curing fixture would be built entirely solid to avoid this recurrence.

4.3.2   Second Multifunctional Curing Fixture

The second multifunctional curing fixture was built entirely solid to avoid the problems of leaking. Grooves and ports were added for thermocouples. The physical look of the curing fixture also became "sleeker" in effort to conserve resin. This model turned out as expected. Surfaces were smooth, and HX tubing was functional as well as the thermocouple grooves and ports. The second multifunctional curing fixture, complete with imbedded thermocouples, is shown in Figure 4.22.

(a) Upper half   (b) Lower half
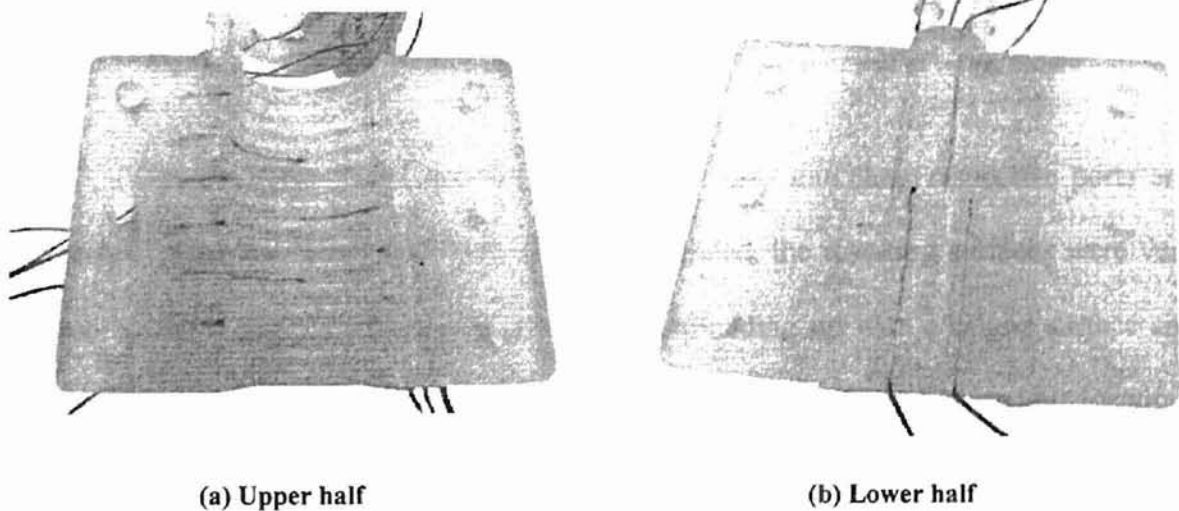
Figure 4.22 Second SLA multifunctional curing fixture with thermocouples

Figure 4.23 shows a close-up view of the thermocouples imbedded into the upper half of the curing fixture.
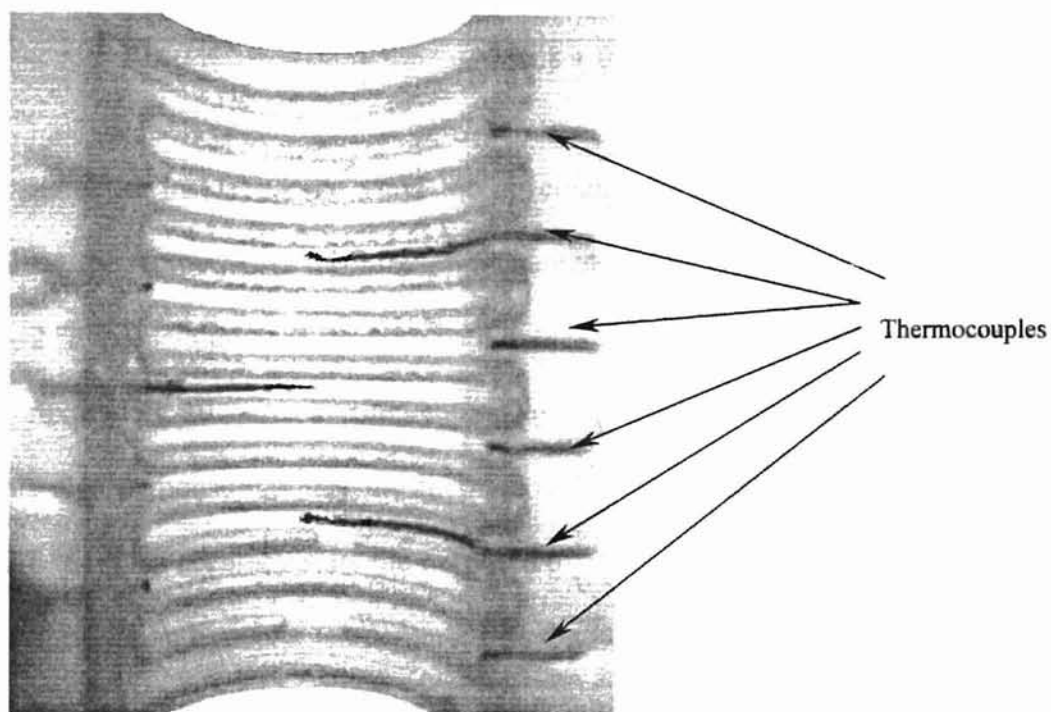
Figure 4.23 Imbedded thermocouples and HX tubing into upper half of curing fixture

Thermocouples were inserted with relative ease into their respective ports and grooves. After being covered with epoxy and sanded, the resulting surfaces were very smooth. Thus, parts could now be cured without ending up with a ridged surface and temperature data could be recorded directly from the curing fixture at various locations on the surface throughout the duration of the composite-curing process.

Surface temperature tests similar to those performed on the first multifunctional curing fixture were also performed. The results of the first test are shown in Table 4.1.

Table 4.1 Curing fixture surface temperatures at various bath temperatures

Bath Temperature (°F)	Ch. 4 Temperature (°F)	Ch. 8 Temperature (°F)
140	139.1 ± 0.7	138.1 ± 0.7
150	149.0 ± 0.7	147.9 ± 0.7
160	158.8 ± 0.7	157.8 ± 0.7

After insulating the vinyl tubing connecting the Julabo® to the curing fixture halves, the temperatures recorded from channels 4 and 8 show that there is approximately 1 – 2 °F temperature loss from the bath to the curing fixture. This is much better than the approximately 10 – 20 °F temperature loss incurred by the system without insulation. This also demonstrates that the thermocouples are reading data to an accuracy within ±0.7 °F. This accuracy suits the purposes of this project. Also, the upper curing fixture is experiencing a greater temperature loss than that of the lower curing fixture. The difference in surface temperatures of the upper curing fixture and the lower curing fixture is marginal at best. Finally, the new resin used to make the curing fixture (700 ND) is capable of withstanding temperatures of at least 160°F and possible higher temperatures.

The results of the second empty test performed on this curing fixture are as follows:

$T_{bath} = 60.8°C\ (141.4°F)$ ➜ $T_{Ch.\ 8} = 60°C\ (140°F)$

$T_{bath} = 72.4°C\ (162.3°F)$ ➜ $T_{Ch.\ 8} = 71.1°C\ (160°F)$

The temperatures in this test were taken only at channel 8 because channel 8 gave consistently lower readings than channel 4 in the previous test. Therefore, the assumption could be made that channel 4 temperatures would be slightly higher than 140°F and 160°F, but that would not really hurt the composite-curing process.

The first part to be cured using the second multifunctional curing fixture was a part made from SL 7520 resin. It was cured for 15 hours at a curing fixture temperature of 140°F. Figure 4.24 shows a comparison of the cured part to the original SLA part.
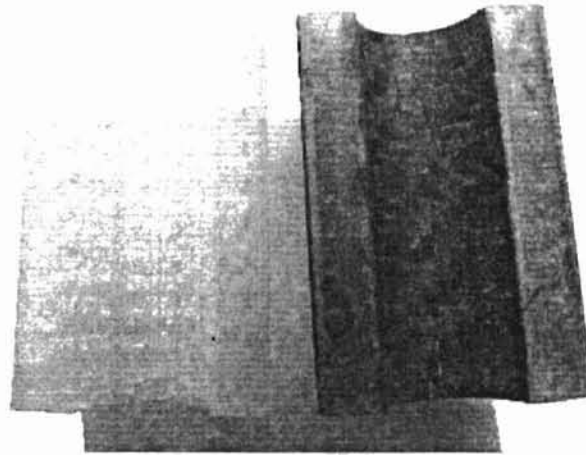
Figure 4.24 1 layer LTM25 composite and 1 layer film adhesive cured to SLA part

This part turned out as well as could be expected. The surface was not as shiny and smooth as previously cured parts. This could be because the curing surface of the multifunctional SLA fixtures was not polished and shiny. Otherwise, this multifunctional curing fixture performed on the level of an oven and vacuum bag. Figure 4.25 also shows this cured part.
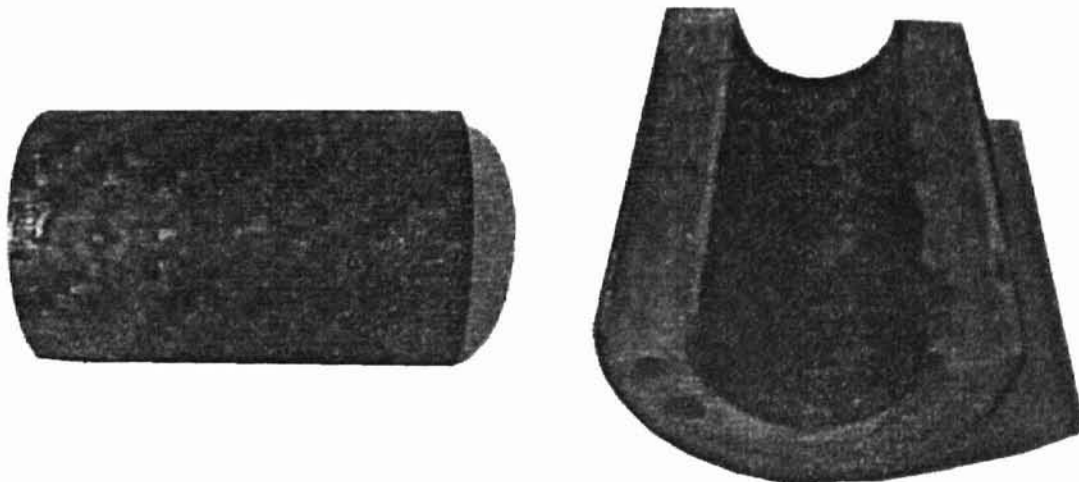
Figure 4.25 First part cured using the second curing fixture

No temperature data were taken during the curing process. This first test run was designed to see if the second curing fixture would work as well as the first curing fixture. Two other parts were cured, and their temperature results were recorded, thus demonstrating the functionality of the imbedded thermocouples.

The second part was cured with just one layer of LTM25 carbon fiber. It is shown in Figure 4.26.
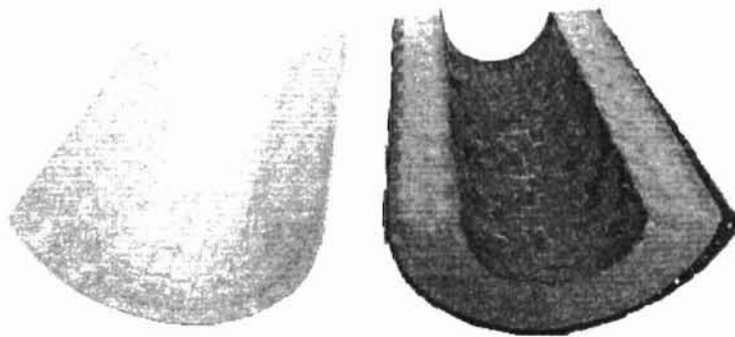
Figure 4.26 One layer of LTM25 composite cured to SLA part

Although the composite cured, it did not adhere completely to the SLA part. Notice from Figure 4.26 that it is peeling off of the outer surface. This is because there was only one layer of laminate used. Therefore, the tolerance of the curing fixture did not allow it to apply necessary pressure to the part throughout the cure. This test indicates the importance of tolerance design when developing parts.

Figure 4.27 shows the temperature of the surfaces throughout the cure process. This data demonstrates the functionality of the imbedded thermocouples. Also, it shows that the composite-curing process may now be monitored throughout its duration. This data follow the trend that was expected. Throughout this cure, the bath temperature was

slightly above the temperatures recorded by the surface thermocouples, thus reinforcing the results of the empty-chamber tests performed on this curing fixture. Temperature data gathered on the inlet and outlet thermocouples is shown in Figure 4.28

LTM25 Optimal Cure Surface Temps
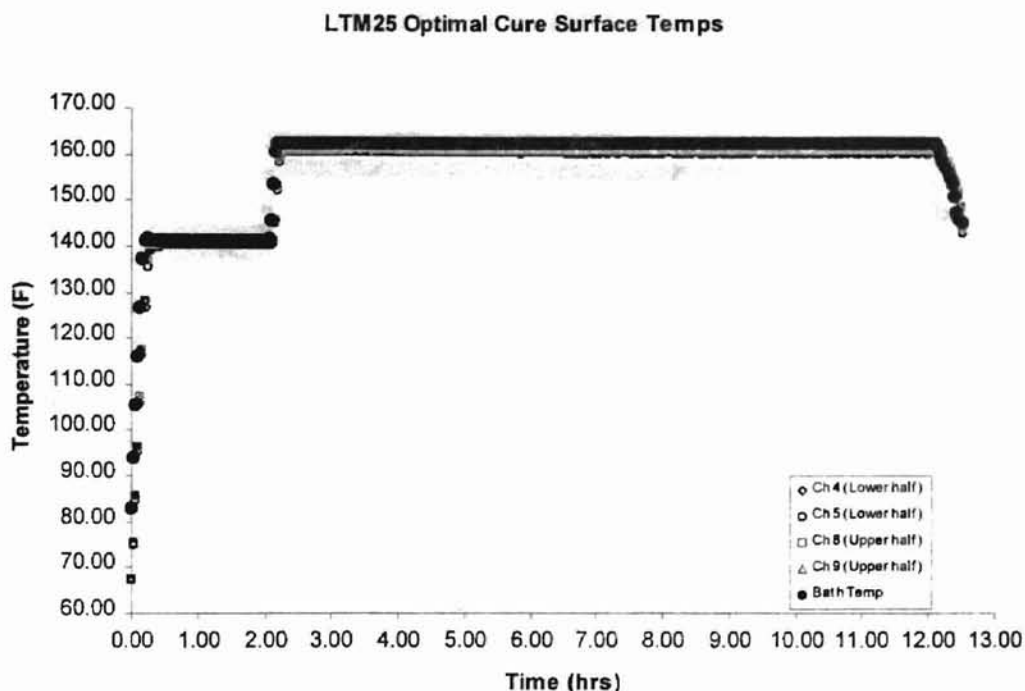
Figure 4.27 Temperature data from second cured part

Although this data demonstrate the feasibility of using imbedded thermocouples, it is not representative of the readings expected. Channel 6, for example, records temperature at the outlet of the upper curing fixture, and channel 7 records temperature at the inlet. In theory, channel 7 would record higher temperatures, given the heat loss through the curing fixture. However, Figure 4.28 shows that channel 6 consistently records higher temperatures. Furthermore, the temperatures (which should be internal flow temperatures) are recorded as being significantly lower than the bath temperature. Closer inspection of the thermocouples reveals improper insertion of them, as they have not only

been exposed to the internal flow, but to the atmosphere as well, thus affecting the recorded temperatures. This explains the unexpected results from the inlet/outlet thermocouples.

LTM25 Optimal Cure I/O Temps
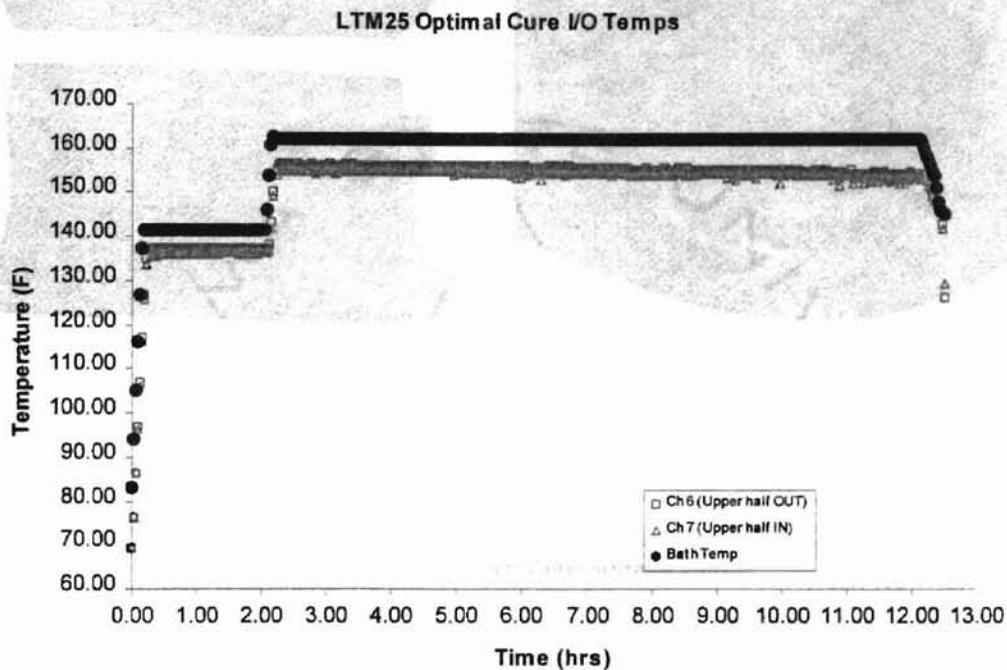
Figure 4.28 Inlet/Outlet temperature data on second cured part

A third part was cured using the same procedure as used for the previous part. It was cured using 2 layers of LTM25 carbon fiber. This time, the composite cured and adhered to the SLA part. As was the case for all composites cured using the second curing fixture, the surface finish was dull (most likely due to the unpolished surfaces of the curing fixtures). Figure 4.29 shows views of the third part.

Temperature data were recorded throughout the duration of this cure process. Figure 4.30 shows this data.
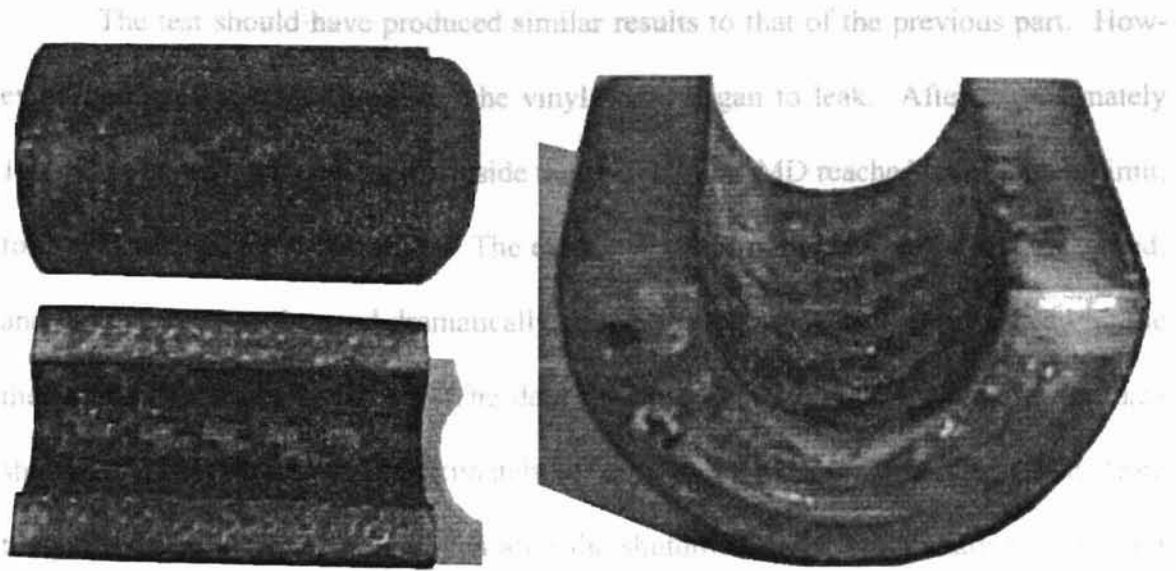
Figure 4.29 2 layers of LTM25 composite cured to SLA part

LTM25 Optimal Cure Surface Temps
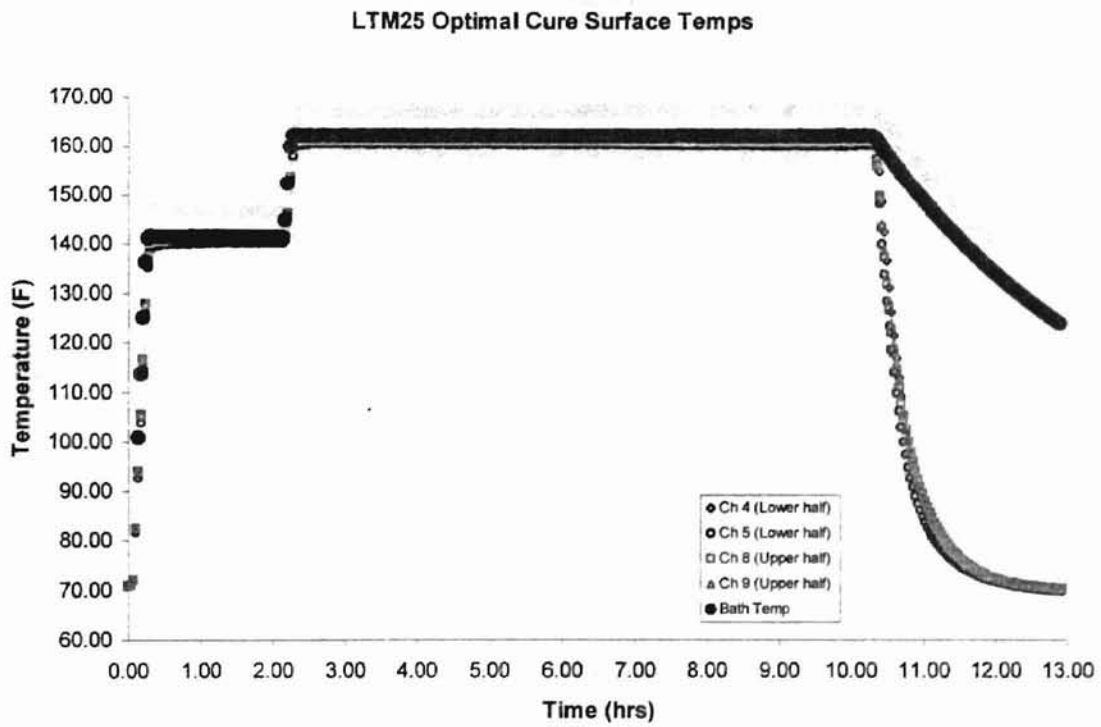
Figure 4.30 Surface temperature data from the third part

The test should have produced similar results to that of the previous part. However, during the curing procedure, the vinyl hoses began to leak. After approximately 10½ hours of curing, the reservoir inside the Julabo® F12-MD reached its minimum limit, forcing the machine to shut down. The circulation of water to the curing fixture ceased, and the temperature dropped dramatically, as seen in Figure 4.30. The data read by the thermocouples are still reliable. The data shown here are almost identical to the data shown in Figure 4.27 up to approximately the 10½-hour point, thus verifying results from the previous test. The data recorded after the shutdown of the recirculator is useful for demonstrating that the thermocouples can be used in diagnosing cure conditions. The shutdown did not affect the cure of the composite. The part itself turned out fully cured.

LTM25 Optimal Cure I/O Temps
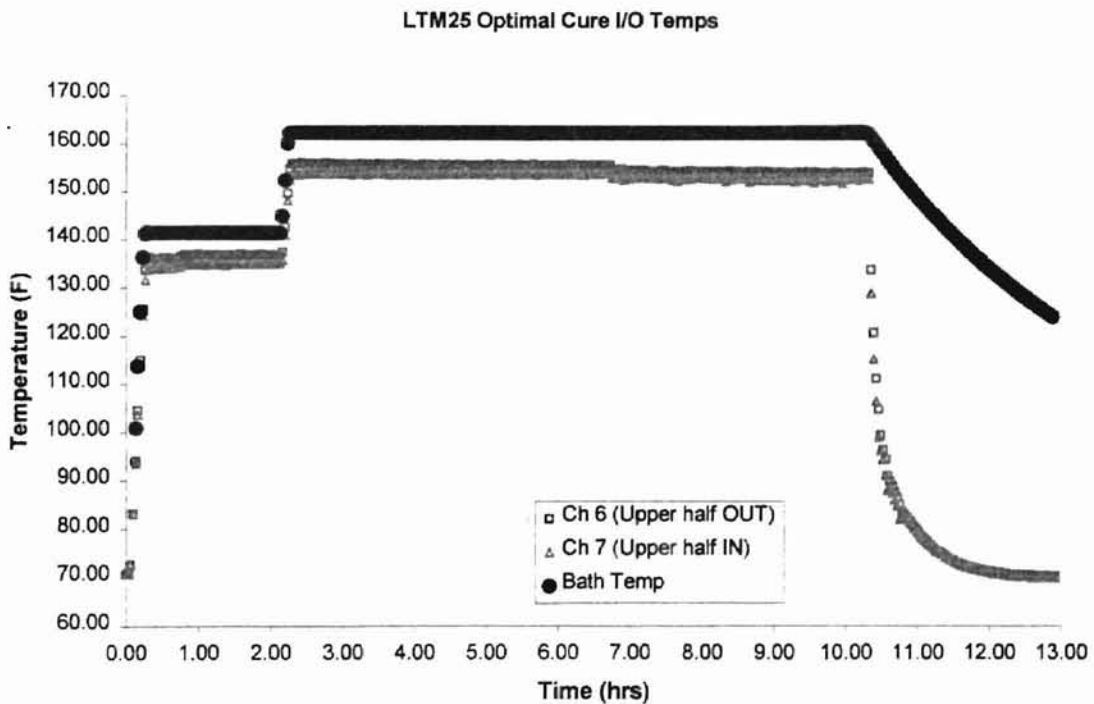
Figure 4.31 Inlet and outlet temperature data from the third part

The inlet and outlet temperatures, seen in Figure 4.31, were also recorded in this test. Generally, the data presented in Figure 4.31 verify that the data recorded for the second part was reliable. The inlet and outlet temperatures were still being read as significantly lower than the bath temperature, strengthening the notion that the inlet and outlet thermocouples may not have been properly imbedded. Figure 4.31 also demonstrates the time at which the water stopped circulating

CHAPTER 5

5. CONCLUSIONS AND RECOMMENDATIONS

5.1   Conclusions

The conclusions can be separated into three general areas, corresponding to the levels of the evolution of this project.

5.1.1   Feasibility Studies

The NACA0012 wing was designed to determine to what limits the SLA-7000 could imbed internal tubes, which would be a major functionality in designs developed during this project. Tubes having a diameter no less than $^1/_{16}$ inch could successfully be built into an SLA structure. Also, tubes cannot be built closer than 0.006 inches from a surface of a QuickCast™ part without breaking through the surface. Also, the curved sur-faced could be built smoothly, and sharp edges (i.e. airfoil trailing edges) could be built crisply.

The half-cylindrical SLA meshes demonstrated the physical susceptibility of the SLA resin to its glass transition temperature. After the cure temperature was adjusted, the parts were cured successfully, thus demonstrating that high temperatures will not af-fect the strength of the part if the temperatures are not near the glass transition tempera-

ture of the SLA resin. Also, reasonable pressure applied to a part during the cure has relatively little effect on the part. Finally, composite laminates will adhere to SLA parts without peeling off if the laminate had not expired before applying it.

5.1.2   Intermediate Studies

Regarding curing fixtures, it was known that tolerances would need to be designed into them in order to allow a fit that would provide adequate interference on the laminate, forcing it to conform to the surface contours of a part. Such tolerances need to allow the curing fixture parts to come together, thus minimizing the ridging of resin at those locations. The NACA0012 wing and curing fixture have demonstrated that SL can be used to produce viable parts and curing fixtures for them. Also, curing fixtures can be designed to allow a vacuum bag to conform around it without worries of ripping during the cure process. The complex wing tests have demonstrated that increasingly complicated parts and curing fixtures may be designed and built using SLA. Also, auxiliary curing fixture parts can utilize the vacuum pressure efficiently. Increasingly complex parts can be covered with carbon fiber relatively easily.

Regarding imbedded pressure ports in the complex wing, the implementation of compressed gas to remove excess resin from tubes was successful in tubes with diameters as small as $1/16$ inch. The failed attempts to build a clear tube with a diameter of $1/32$ inch validated the results of the NACA0012 wing with imbedded pressure ports.

The square heat exchanger demonstrated that imbedded HX tubing would provide a complex, snaking passage through a part. Without using SLA, such tubing may be difficult to insert into a part regardless of geometric complexity. The disk-shaped heat ex-

changer demonstrated the imbedding of a spiraling HX tube through it. The difficulties encountered in the imbedding of tubes into this heat exchanger brought to light possible leaks built into tubes imbedded into QuickCast™ structures. The half-cylindrical heat exchanger demonstrated that HX tubes could be imbedded into parts of increasingly complex geometry (in this case, the tubing was not coplanar).

The imbedding of thermocouples was successful. Tests performed on the square heat exchanger showed that thermocouples could be laid into surface grooves and covered with composite laminate. The finished part would be smooth and give no indication that thermocouples lay just beneath the surface. The thermocouples were valuable in pointing out that the HX tubing will transfer heat through the SLA boundaries and that the imbedded thermocouple will read accurate temperature data. The test performed on the square heat exchanger involving the ice bath and recirculating warm water demonstrated that this heat exchanging capability could be used in a variety of applications (i.e. de-icing mechanism on the leading edge of a wing). The second discovery showed that by imbedding thermocouples, temperature could be monitored accurately from within the part itself. No external attachments or thermocouples would be needed.

5.1.3   SLA Multifunctional Composite-Curing Fixtures

The first curing fixture proved that it is possible to cure a composite with nothing more than this heat-exchanging curing fixture. Information gathered from the first curing fixture led to the refined design of the second curing fixture. Leaks in the internal tubing indicated that imbedded tubing within a QuickCast™ structure might be problematic. This was largely fixed when the wall-thickness parameter was changed within the QC

88

software. To avoid potential problems, the second curing fixture was completely solid. It was designed with ports and grooves for thermocouples. The HX tubing was effective in transferring heat across the SLA boundary; the thermocouples were effective in reading and monitoring the temperature of the composite surface throughout the entire cure process. Currently, surface temperature might be estimated by reading the oven temperature or possibly by taping thermocouples to the surface at various locations. In such scenarios, a spider web of wires may be scattered across the part, creating headaches for lab technicians. This new curing fixture design, complete with thermocouples imbedded in an orderly fashion, not only did what could have only been estimated before, but also demonstrates a much more streamlined appearance.

5.2   Recommendations

Recommendations discussed here will apply to SLA substructures for composite sandwich structures, the three imbedded functions explored in this project, and the future of SLA composite-curing fixture technology.

5.2.1   SLA/Composite Sandwich Structures

This is currently a very limited technology. These structures are governed largely by the glass transition temperature of the SLA resin. The highest glass transition temperature of the most popular SLA resins currently on the market is approximately 80°C (176°F). [3DSystems, 2001] That severely limits the range of applications to which this technology can be applied. Currently, only LTM composite fabrics may be used in SLA

sandwich structures. MTM and HTM composites are cured above the glass transition temperature of these SLA resins. It is expected that more heat-resistant SLA resins will be developed over time. Until that happens, this technology is not useful for higher-temperature applications.

Another major concern is the strength of the SLA resin and the effect of aging on it. Current research is underway that looks at the effects of aging on SLA resin. Preliminary research on selected resins indicates that these resins lose approximately half of their strength in a 10-year time frame. [Akolkar, 2001] These results suggest that, at this time, this technology cannot be applied to moderate- or high-strength applications.

Finally, weight is another area of concern, especially if SLA sandwich structures are to be used in aerospace applications. SLA resin is denser than water, so it is necessary to build a substructure from as little resin as possible, while not sacrificing too much strength. QuickCast™ has shown potential in reducing part weight, but is still insufficient at this time for producing super-lightweight parts.

The main recommendation regarding SLA sandwich structures is to continue to develop the technology and let the resin development catch up to it. Design and build SLA sandwich structures that could be used in high temperature or high strength applications (if the material could handle it), and as better resins develop, continue with the applications. Also, to reduce weight, it may be beneficial to develop one's own substructure pattern rather than rely on 3DSystems to develop a pattern that will maintain a sufficiently high strength-to-weight ratio.

5.2.2   Imbedded Functionality

The major limitation for all cases is tube diameter, and it is entirely due to limitations of the SLA machine. Until the resolution of the machine and resins gets better, there is not much that can be done. So, tube diameters should be designed no smaller than $^1/_{16}$ inch. It is possible to experiment with tubes having diameters between $^1/_{16}$ inch and $^1/_{32}$ inch.

Another recommendation is to experiment with geometries much more complex than those examined in this project. An example of this would be to imbed HX tubing and thermocouples into the leading edge of a model wing. Also, it is suggested that other fluids, such as air, be pumped through the HX tubing to examine their effect on regulating temperature. An experiment could be developed using this model wing with imbedded HX tubes and thermocouples in its leading edge. Place it in a sub-zero environment and allow it to have ice form on it, thereby simulating ice buildup on a wing. Then, maintaining that arctic environment, circulate warm air through the tubes to simulate bleed air coming from the engine. The results of such an experiment would reflect the potential of imbedded multifunctionality into parts designed for aerospace applications.

Also, it is worthwhile to examine structural qualities such as strength as yet another imbedded functionality. Design of particular substructure patterns might be the start of a variety of imbedded structural components. These specially designed substructure patterns, for example, may be designed to carry more structural load in some areas than in others.

5.2.3   SLA Multifunctional Composite-Curing Fixtures

There should be an attempt to use this procedure on parts having a much more complex geometry. Perhaps, a curing fixture is designed to be used with the wing described in Section 5.2.2. Then, composites could be cured over it using an SLA multifunctional curing fixture.

Another recommendation concerns the tolerance issue. This is one of the most limiting features of the HX curing fixture as currently designed. Currently, the curing fixture would be redesigned each time that more or fewer than the specified number of layers of composite are applied to the part. This is very inefficient. Further research into curing fixture design would be required to solve this particular inadequacy.

Also, thermocouple placement at the inlets and outlets of a heat exchanger should be meticulously designed and monitored. From the results of this project, the slightest anomaly in inlet and outlet thermocouple placement will lead to unexpected temperature readings.

Finally, if the surface finish of a cured composite is of importance, then further research may be required into the surface finish of the curing fixture itself. Perhaps, a wet sanding technique may be explored in greater detail for parts requiring a glass-like finish.

BIBLIOGRAPHY

3D Systems, *www.3dsystems.com*, (2001)

Akolkar, S., "Material Property Characterization of Photo Epoxy Used in Freeform Composite Fabrication," *Masters Thesis*, Oklahoma State University, 2001.

Arena, A.S. Jr. (1999-2001). Associate Professor, Oklahoma State University. Personal Communications.

Beziers, D., and Denost, J., "Composite Curing: A New Process," AIAA Paper 89-2868, July 10-12, 1989.

Chen, C.C., and Sullivan, P.A., "Predicting the Total Build Time and Resultant Cure Depth of the 3D Stereolithography Process," *Rapid Prototyping Journal*, Volume 2, Number 4, 1996, pp. 27 – 40.

Chuk, R.N., and Thomson, V.J., "A Comparison of Rapid Prototyping Techniques Used for Wind Tunnel Model Fabrication," *Rapid Prototyping Journal*, Volume 4, Number 4, 1998, pp. 185 – 196.

Cruz, J.R., Shah, C.H., and Postyn, A.S., "Properties of Two Carbon Composite Materials Using LTM25 Epoxy Resin," NASA Technical Memorandum 110286, 1996.

Daily, C. L., "Rapid Prototyping with Stereolithography: A Designed Experiment to Test Shrinkage," *Masters Thesis*, University of Alabama – Huntsville, 1991.

Dickens, P.M., and Rahmati, S. "Stereolithography Process Improvement," *First National Conference on Rapid Prototyping and Tooling Research*, Buckinghamshire College, UK, November 6-7, 1995.

Dickman, J. (2000-2001). Vice President of Operations, SharedReplicators, Inc. Tulsa, OK. Personal Communications.

Dong, J., *Rapid Response Manufacturing: Contemporary Methodologies, Tools, and Technologies*, Chapman & Hall, 1998.

Fai, L.K., and Kai, C.C., *Rapid Prototyping: Principles and Applications in Manufacturing*, John Wiley & Sons (Asia) Pte Ltd, 1997.

Hague, R., and Dickens, P.M., "Stresses Created in Ceramic Shells Using Quickcast[TM] Models," *First National Conference on Rapid Prototyping and Tooling Research*, Buckinghamshire College, UK, November 6-7, 1995.

Handel, P., and Guerin, D., "Optimal Composite Curing System," *American Helicopter Society's 48th Annual Forum*, 1992, pp. 941 – 948.

Hull, C., Feygin, M., Baron, Y., Sanders, R., Sachs, E., Lightman, A., and Wohlers, T., "Rapid Prototyping: Current Technology and Future Potential," *Rapid Prototyping Journal*, Volume 1, Number 1, 1995, pp.11 – 19.

Hull, D., and Clyne, T.W., *An Introduction to Composite Materials* (2nd Ed.), Cambridge University Press, 1996.

Jacobs, P.F., *Rapid Prototyping & Manufacturing: Fundamentals of StereoLithography*, Society of Manufacturing Engineers, 1992.

Jacobs, P.F., *Stereolithography and Other RP&M Technologies*, ASME Press, 1996.

Johnston, N.J., Towell, T.W., Marchello, J.M., and Grenoble, R.W., "Automated Fabrication of High Performance Composites: An Overview of Research at the Langley Research Center," *International Conference on Composite Materials*, Gold Coast, Australia, July 14-18, 1997.

Jones, R.D., "Method for Making Freeform-Fabricated Core Composite Articles," *Application for Grant of U.S. Letters of Patent*, United States Patent and Trademark Office, Number SHI002-SRT, Aug. 15, 2000.

Joseph, C., and Viney, C., "Electrical Resistance Curing of Carbon-Fibre/Epoxy Composites," *Composites Science and Technology*, Number 60, 2000, pp. 315 – 319.

Kochan, A., "Rapid Prototyping Trends," *Rapid Prototyping Journal*, Volume 3, Number 4, 1997, pp. 150 – 152.

Landrum, D.B., Beard, R.M., LaSarge, P.A., and von Sprecken, N., "Evaluation of Stereolithography Rapid Prototyping for Low Speed Airfoil Design," AIAA Paper 97-0719, January 6-10, 1997.

Masood, S.H., and Lim, B.S., "Concurrent Intelligent Rapid Prototyping Environment," *Journal of Intelligent Manufacturing*, Volume 6, 1995, pp. 291 – 310.

Merriam-Webster's Collegiate Dictionary (10th Ed.), Merriam-Webster, Inc., Springfield, Massachusetts, 1993.

Pilato, L.A., and Michno, M.J., *Advanced Composite Materials*, Springer-Verlag Berlin Heidelberg, 1994.

Rahmati, S., and Dickens, P., "Stereolithography for Injection Mould Tooling," *Rapid Prototyping Journal*, Volume 3, Number 2, 1997, pp. 53 – 60.

Rapid Prototyping Chemicals, www.rpc.ch, (2001).

Raymer, D.P., *Aircraft Design: A Conceptual Approach*, AIAA, Inc., 1992.

Renap, K., and Kruth, J.P., "Recoating Issues in Stereolithography," *Rapid Prototyping Journal*, Volume 1, Number 3, 1995, pp. 4 – 16.

SharedReplicators, Inc. *www.sharedreplicators.com* (2001).

Spence, G.B., "Graphite Fiber Composite Materials," *Symposium on Graphite Fiber Composites*, ASME Winter Annual Meeting, Pennsylvania, November, 1967.

Springer, A., Cooper, K., and Roberts, F., "Application of Rapid Prototyping Models to Transonic Wind Tunnel Testing," AIAA Paper 97-0988, January 6-10, 1997.

The Advanced Composites Group, *www.advanced-composites.com*, (2001).

Tsang, H., and Bennett, G., "Rapid tooling – Direct Use of SLA Moulds for Investment Casting," *First National Conference on Rapid Prototyping and Tooling Research*, Buckinghamshire College, UK, November 6-7, 1995.

UIUC Airfoil Coordinate Database, *www.aero.aae.uiuc.edu/~m-selig/ads/coord_database.html*, (2001).

Ullett, J.S., Schultz, J.W., and Chartoff, R.P., "Novel Liquid Crystal Resins for Stereolithography – Processing Parameters and Mechanical Analysis," *Rapid Prototyping Journal*, Volume 6, Number 1, 2000, pp. 8-17.

Vermillion, B., *Composite Basics Seminar*, Oklahoma State University, February 12, 2000.

Wohlers, T., "Future Potential of Rapid Prototyping and Manufacturing Around the World," *Rapid Prototyping Journal*, Volume 1, Number 1, 1995, pp. 4 – 10.

Zhu, L., and Pitchumani, R., "Analysis of a Process for Curing Composites by the Use of Embedded Resistive Heating Elements," *Composite Science and Technology*, Number 60, 2000, pp. 2699 – 2712.

APPENDICES

Normalized NACA0012 Airfoil Coordinate Data
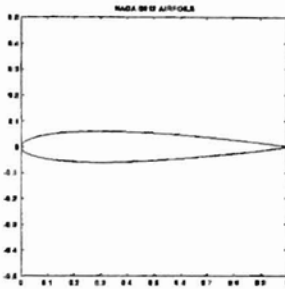
NACA 0012 AIRFOIL

X	Y
0.0000000	0.0000000
0.0005839	0.0042603
0.0023342	0.0084289
0.0052468	0.0125011
0.0093149	0.0164706
0.0145291	0.0203300
0.0208771	0.0240706
0.0283441	0.0276827
0.0369127	0.0311559
0.0465628	0.0344792
0.0572720	0.0376414
0.0690152	0.0406310
0.0817649	0.0434371
0.0954915	0.0460489
0.1101628	0.0484567
0.1257446	0.0506513
0.1422005	0.0526251
0.1594921	0.0543715
0.1775789	0.0558856
0.1964187	0.0571640
0.2159676	0.0582048
0.2361799	0.0590081
0.2570083	0.0595755
0.2784042	0.0599102
0.3003177	0.0600172
0.3226976	0.0599028
0.3454915	0.0595747

X	Y
0.3686463	0.0590419
0.3921079	0.0583145
0.4158215	0.0574033
0.4397317	0.0563200
0.4637826	0.0550769
0.4879181	0.0536866
0.5120819	0.0521620
0.5362174	0.0505161
0.5602683	0.0487619
0.5841786	0.0469124
0.6078921	0.0449802
0.6313537	0.0429778
0.6545085	0.0409174
0.6773025	0.0388109
0.6996823	0.0366700
0.7215958	0.0345058
0.7429917	0.0323294
0.7638202	0.0301515
0.7840324	0.0279828
0.8035813	0.0258337
0.8224211	0.0237142
0.8405079	0.0216347
0.8577995	0.0196051
0.8742554	0.0176353
0.8898372	0.0157351
0.9045085	0.0139143
0.9182351	0.0121823
0.9309849	0.0105485
0.9427280	0.0090217
0.9534372	0.0076108
0.9630873	0.0063238
0.9716559	0.0051685
0.9791229	0.0041519
0.9854709	0.0032804
0.9906850	0.0025595
0.9947532	0.0019938
0.9976658	0.0015870
0.9994161	0.0013419
1.0000000	0.0012600
0.0000000	0.0000000

X	Y
0.0005839	-.0042603
0.0023342	-.0084289
0.0052468	-.0125011
0.0093149	-.0164706
0.0145291	-.0203300
0.0208771	-.0240706
0.0283441	-.0276827
0.0369127	-.0311559
0.0465628	-.0344792
0.0572720	-.0376414
0.0690152	-.0406310
0.0817649	-.0434371
0.0954915	-.0460489
0.1101628	-.0484567
0.1257446	-.0506513
0.1422005	-.0526251
0.1594921	-.0543715
0.1775789	-.0558856
0.1964187	-.0571640
0.2159676	-.0582048
0.2361799	-.0590081
0.2570083	-.0595755
0.2784042	-.0599102
0.3003177	-.0600172
0.3226976	-.0599028
0.3454915	-.0595747
0.3686463	-.0590419
0.3921079	-.0583145
0.4158215	-.0574033
0.4397317	-.0563200
0.4637826	-.0550769
0.4879181	-.0536866
0.5120819	-.0521620
0.5362174	-.0505161
0.5602683	-.0487619
0.5841786	-.0469124
0.6078921	-.0449802
0.6313537	-.0429778
0.6545085	-.0409174
0.6773025	-.0388109
0.6996823	-.0366700

0.7215958	-.0345058	0.8742554	-.0176353	0.9716559	-.0051685
0.7429917	-.0323294	0.8898372	-.0157351	0.9791229	-.0041519
0.7638202	-.0301515	0.9045085	-.0139143	0.9854709	-.0032804
0.7840324	-.0279828	0.9182351	-.0121823	0.9906850	-.0025595
0.8035813	-.0258337	0.9309849	-.0105485	0.9947532	-.0019938
0.8224211	-.0237142	0.9427280	-.0090217	0.9976658	-.0015870
0.8405079	-.0216347	0.9534372	-.0076108	0.9994161	-.0013419
0.8577995	-.0196051	0.9630873	-.0063238	1.0000000	-.0012600

APPENDIX A-2

Normalized NACA0009 Airfoil Coordinate Data
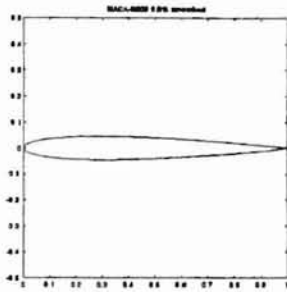
NACA0009 (9.0% smoothed)

X	Y
1.00000	0.0
0.99572	0.00057
0.98296	0.00218
0.96194	0.00463
0.93301	0.00770
0.89668	0.01127
0.85355	0.01522
0.80438	0.01945
0.75000	0.02384
0.69134	0.02823
0.62941	0.03247
0.56526	0.03638
0.50000	0.03978
0.43474	0.04248
0.37059	0.04431
0.33928	0.04484
0.30866	0.04509
0.27886	0.04504
0.25000	0.04466
0.22221	0.04397
0.19562	0.04295
0.17033	0.04161
0.14645	0.03994
0.12408	0.03795
0.10332	0.03564
0.08427	0.03305
0.06699	0.03023
0.05156	0.02720
0.03806	0.02395
0.02653	0.02039
0.01704	0.01646
0.00961	0.01214
0.00428	0.00767
0.00107	0.00349
0.0	0.0
0.00107	-0.00349
0.00428	-0.00767
0.00961	-0.01214
0.01704	-0.01646
0.02653	-0.02039
0.03806	-0.02395
0.05156	-0.02720
0.06699	-0.03023
0.08427	-0.03305
0.10332	-0.03564
0.12408	-0.03795
0.14645	-0.03994
0.17033	-0.04161
0.19562	-0.04295
0.22221	-0.04397
0.25000	-0.04466
0.27886	-0.04504
0.30866	-0.04509
0.33928	-0.04484
0.37059	-0.04431
0.43474	-0.04248
0.50000	-0.03978
0.56526	-0.03638
0.62941	-0.03247
0.69134	-0.02823
0.75000	-0.02384
0.80438	-0.01945
0.85355	-0.01522
0.89668	-0.01127
0.93301	-0.00770
0.96194	-0.00463
0.98296	-0.00218
0.99572	-0.00057
1.00000	0.0

APPENDIX A-3

Normalized Selig1223 Airfoil Coordinate Data

Selig1223 AIRFOIL

X	Y	X	Y	X	Y
		0.34777	0.13447	0.59428	0.05820
		0.31488	0.13526	0.64176	0.05976
		0.28347	0.13505	0.68832	0.05994
		0.25370	0.13346	0.73344	0.05872
		0.22541	0.13037	0.77660	0.05612
		0.19846	0.12594	0.81729	0.05219
		0.17286	0.12026	0.85500	0.04706
		0.14863	0.11355	0.88928	0.04088
		0.12591	0.10598	0.91966	0.03387
		0.10482	0.09770	0.94573	0.02624
		0.08545	0.08879	0.96693	0.01822
		0.06789	0.07940	0.98255	0.01060
		0.05223	0.06965	0.99268	0.00468
		0.03855	0.05968	0.99825	0.00115
1.00000	0.00000	0.02694	0.04966	1.00000	0.00000
0.99838	0.00126	0.01755	0.03961		
0.99417	0.00494	0.01028	0.02954		
0.98825	0.01037	0.00495	0.01969		
0.98075	0.01646	0.00155	0.01033		
0.97111	0.02250	0.00005	0.00178		
0.95884	0.02853	0.00044	-0.00561		
0.94389	0.03476	0.00264	-0.01120		
0.92639	0.04116	0.00789	-0.01427		
0.90641	0.04768	0.01718	-0.01550		
0.88406	0.05427	0.03006	-0.01584		
0.85947	0.06089	0.04627	-0.01532		
0.83277	0.06749	0.06561	-0.01404		
0.80412	0.07402	0.08787	-0.01202		
0.77369	0.08044	0.11282	-0.00925		
0.74166	0.08671	0.14020	-0.00563		
0.70823	0.09277	0.17006	-0.00075		
0.67360	0.09859	0.20278	0.00535		
0.63798	0.10412	0.23840	0.01213		
0.60158	0.10935	0.27673	0.01928		
0.56465	0.11425	0.31750	0.02652		
0.52744	0.11881	0.36044	0.03358		
0.49025	0.12303	0.40519	0.04021		
0.45340	0.12683	0.45139	0.04618		
0.41721	0.13011	0.49860	0.05129		
0.38193	0.13271	0.54639	0.05534		

APPENDIX B-1

Square SLA Heat Exchanger Temperature Data

Time in seconds (s); Temperature in °F

Time	Temp 1	Temp 2	Temp 3	Temp 4	Temp 5	Temp 6	Temp 7	Temp 8	Temp 9
0	36.61	36.20	34.45	37.72	33.29	32.55	36.34	37.03	70.17
2	36.52	36.20	34.59	37.72	33.29	32.64	76.36	37.03	44.87
4	36.84	36.61	35.92	38.09	33.94	32.83	38.13	37.40	55.71
6	38.41	37.81	38.22	38.50	35.28	33.71	39.88	38.82	65.66
8	40.11	40.15	41.44	40.43	37.63	36.75	42.94	39.69	82.50
10	41.48	43.77	46.41	41.89	41.57	40.79	46.41	40.98	96.46
12	43.72	47.09	50.22	45.23	46.77	45.73	50.81	43.17	104.46
14	46.05	51.08	54.60	48.91	52.35	49.63	54.92	46.14	109.98
16	48.59	54.02	58.38	52.44	55.59	53.34	58.56	48.82	115.70
18	51.76	57.26	61.07	55.10	59.81	56.76	61.15	52.12	118.40
20	54.15	59.63	63.48	58.15	63.92	60.57	63.52	55.37	120.30
22	56.94	62.23	65.52	60.30	68.63	63.97	65.57	57.80	121.78
24	58.92	63.97	67.83	62.76	73.19	66.90	68.28	59.99	122.83
26	61.56	65.57	70.18	64.95	76.58	68.46	69.87	62.00	123.72
28	63.57	67.30	71.51	66.50	79.25	70.80	71.33	64.32	124.35
30	64.63	68.50	72.70	68.19	82.75	72.79	72.92	66.37	124.98
32	66.50	69.39	74.02	69.43	84.71	74.55	74.07	67.83	125.35
34	67.61	71.02	75.04	70.89	86.72	75.83	75.35	69.52	125.66
36	68.41	72.04	75.92	71.82	88.41	76.88	76.23	71.02	125.87
38	70.23	72.79	76.84	72.97	90.62	78.11	77.19	72.22	126.24
40	70.67	73.50	77.59	73.80	91.96	79.17	77.94	73.36	126.34
42	71.60	74.24	78.42	74.77	93.52	80.13	78.81	74.24	126.55
44	72.83	74.82	79.25	75.48	94.85	80.83	79.38	75.08	126.55
46	73.76	75.43	79.91	76.27	95.89	81.40	80.13	76.05	126.55
48	74.16	75.74	80.57	76.88	96.79	81.97	80.65	76.75	126.55
50	74.47	75.39	80.92	77.46	98.12	82.58	81.27	77.59	126.24
52		75.17	81.18	78.11	99.11	83.14	81.75	78.33	126.24
54		74.95	81.22	78.77	99.80	83.54	82.18	78.95	126.19
56		74.64	81.27	79.21	100.48	84.02	82.71	79.47	126.14
58			81.31	79.74	100.91	84.41	83.14	80.13	126.08
60			81.35	80.17	101.55	84.67	83.54	80.61	126.03
62			81.44	80.52	102.02	85.06	83.89	81.14	126.03
64			81.57	81.05	102.49	85.37	84.19	81.57	126.08
66			81.75	81.35	102.84	85.67	84.50	77.24	126.14
68			81.83	81.57	103.18	85.93	84.76	82.53	126.19
70				81.97	103.56	86.15	85.11	82.84	126.24
72				82.40	103.82	86.37	85.37	83.28	126.19
74				82.75	104.07	86.50	85.58	83.58	126.24

76	82.97	104.29	86.67	85.80	83.84	126.19
78	83.28	104.50	86.76	86.19	84.19	126.24
80	83.45	104.76	86.85	86.41	84.50	126.24
82	83.58	104.93	87.02	86.63	84.67	126.19
84	83.80	105.10	87.19	86.85	84.89	126.19
86	83.97	105.27	87.28	87.06	85.11	126.19
88	84.15		87.37	87.28	85.28	126.19
90	84.28		87.45	87.45	85.41	126.19
92	84.45		87.54	87.71	85.50	126.14
94	84.54		87.63	87.84	85.54	126.14
96	84.63		87.71	88.02	85.54	126.03
98	84.71		87.76	88.19	85.54	126.03
100	84.84		87.80	88.32	85.37	125.98
102	84.89		87.84	88.45	85.06	125.88
104	84.93		87.89	88.54	84.80	125.82
106	85.02		87.89	88.67	84.58	125.72
108			87.89	88.76	84.32	125.61
110				88.84	83.97	125.46
112				88.93	83.67	125.40
114				88.97	83.45	125.30
116				89.02	83.19	125.25
118				89.06	82.97	125.19
120				89.10	82.80	125.04
122				89.19	82.62	124.98
124				89.23	82.45	124.93
126				89.28	82.23	124.93
128				89.32	82.10	124.93
130				89.41	82.01	124.93
132				89.41	81.88	124.93
134				89.41	81.79	124.93
136				89.45	81.66	124.88
138				89.49	81.57	124.88
140				89.49	81.35	124.88
142				89.54	81.27	124.88
144				89.49	81.27	124.88
146				89.54	81.27	124.88
148					81.22	124.88
150					81.22	124.88
152					81.22	124.88
154					81.22	124.88
156					81.22	124.88

APPENDIX C-1

Temperature Data from 2nd Test Using 2nd Multifunctional Curing Fixture

Time in hours (hr); Temperature in °F

Time	Ch 2	Ch 3	Ch 4	Ch 5	Ch 6	Ch 7	Ch 8	Ch 9	Bath Temp
0.00	69.19	69.45	67.40	67.70	69.05	69.52	67.59	67.51	83.03
0.03	76.03	75.67	75.19	74.98	76.32	76.50	75.27	75.30	94.10
0.07	85.67	84.63	85.53	84.88	86.35	86.49	85.67	85.60	105.33
0.10	95.12	93.84	96.11	95.26	96.68	96.32	96.22	96.32	116.19
0.13	104.06	102.69	106.90	105.85	106.93	106.23	107.11	107.07	126.91
0.17	113.42	111.64	117.51	116.37	117.13	116.26	117.61	117.61	137.10
0.20	122.38	120.07	127.91	126.54	126.81	125.82	128.08	127.94	141.30
0.23	131.00	128.47	137.12	135.63	134.91	133.55	137.09	137.05	141.57
0.27	132.88	130.70	140.41	139.09	137.06	135.53	140.31	140.21	141.48
0.30	131.60	129.97	140.83	139.72	137.25	135.58	140.80	140.60	141.46
0.33	132.93	130.82	140.90	139.82	137.45	135.85	140.80	140.66	141.44
0.37	131.74	130.10	140.87	139.89	137.32	135.69	140.73	140.60	141.44
0.40	131.80	130.36	140.85	140.01	137.40	135.78	140.75	140.62	141.44
0.43	132.34	130.53	140.85	140.07	137.37	135.91	140.85	140.61	141.46
0.47	133.10	131.57	140.90	140.25	137.48	136.05	140.90	140.66	141.44
0.50	132.56	131.64	140.90	140.22	137.35	136.02	140.87	140.66	141.44
0.53	133.58	132.05	140.83	140.19	137.45	136.16	140.87	140.70	141.44
0.57	132.26	131.06	140.87	140.30	137.39	135.86	140.87	140.63	141.44
0.60	131.56	130.02	140.89	140.31	137.44	135.94	140.82	140.72	141.44
0.63	132.19	131.17	140.91	140.30	137.46	136.03	140.91	140.77	141.44
0.67	133.51	131.98	140.80	140.36	137.42	136.10	140.80	140.67	141.44
0.70	133.17	131.60	140.90	140.39	137.41	136.19	140.90	140.69	141.44
0.73	133.32	131.75	140.88	140.40	137.46	136.27	140.88	140.67	141.44
0.77	133.11	131.65	140.91	140.41	137.43	136.14	140.91	140.68	141.44
0.80	132.63	131.10	140.91	140.37	137.42	136.14	140.94	140.74	141.44
0.83	133.07	132.21	140.90	140.36	137.31	136.26	140.90	140.69	141.44
0.87	133.79	132.23	140.91	140.34	137.33	136.34	140.88	140.78	141.44
0.90	132.90	131.27	140.84	140.43	137.35	136.13	140.90	140.70	141.44
0.93	132.06	130.39	140.88	140.37	137.30	136.11	140.92	140.71	141.44
0.97	133.10	131.64	140.90	140.39	137.35	136.29	140.93	140.80	141.44
1.00	133.61	132.18	140.90	140.39	137.42	136.16	140.87	140.73	141.44
1.03	132.85	132.04	140.89	140.38	137.30	136.05	140.89	140.76	141.44
1.07	131.81	130.62	140.87	140.46	137.35	135.96	140.87	140.77	141.44
1.10	133.02	131.86	140.78	140.44	137.30	136.14	140.92	140.81	141.44
1.13	132.97	131.57	140.83	140.39	137.38	136.13	140.90	140.73	141.44

1.17	133.75	132.46	140.83	140.46	137.38	136.16	140.87	140.73	141.44
1.20	133.54	132.24	140.82	140.45	137.34	136.25	140.92	140.72	141.44
1.23	132.41	130.87	140.82	140.48	137.37	136.11	140.92	140.75	141.44
1.26	132.96	132.21	140.82	140.45	137.31	136.09	140.86	140.79	141.44
1.30	133.68	131.91	140.89	140.46	137.44	136.26	140.93	140.69	141.44
1.33	131.90	130.50	140.79	140.48	137.51	136.12	140.92	140.82	141.44
1.36	133.46	131.73	140.85	140.48	137.47	136.45	140.95	140.72	141.44
1.40	132.24	130.68	140.83	140.49	137.34	136.26	140.93	140.72	141.44
1.43	133.52	132.23	140.95	140.47	137.43	136.24	140.88	140.81	141.44
1.46	133.29	132.31	140.92	140.45	137.40	136.29	140.89	140.79	141.44
1.50	133.51	131.84	140.90	140.46	137.38	136.30	140.90	140.73	141.44
1.53	133.74	132.07	140.85	140.45	137.47	136.32	140.85	140.72	141.44
1.56	132.94	131.30	140.90	140.46	137.49	136.27	140.84	140.77	141.44
1.60	133.54	131.90	140.79	140.45	137.48	136.39	140.83	140.76	141.44
1.63	133.29	131.55	140.91	140.41	137.43	136.31	140.91	140.78	141.44
1.66	132.46	131.13	140.77	140.40	137.39	136.10	140.91	140.71	141.44
1.70	133.07	131.43	140.83	140.46	137.42	136.26	140.80	140.70	141.44
1.73	132.07	130.74	140.92	140.48	137.37	136.18	140.95	140.82	141.44
1.76	131.51	130.32	140.88	140.37	137.36	136.04	140.81	140.71	141.44
1.80	133.14	131.34	140.84	140.47	137.42	136.34	140.91	140.80	141.44
1.83	133.25	132.10	140.85	140.41	137.43	136.18	140.91	140.81	141.44
1.86	133.28	131.71	140.91	140.40	137.36	136.31	140.84	140.74	141.44
1.90	132.06	130.56	140.91	140.47	137.33	136.14	140.84	140.74	141.44
1.93	133.00	131.16	140.90	140.50	137.32	136.13	140.87	140.73	141.44
1.96	133.04	131.64	140.87	140.47	137.42	136.20	140.91	140.81	141.44
2.00	133.80	132.10	140.85	140.48	137.47	136.18	140.92	140.82	141.44
2.03	133.64	132.14	140.85	140.48	137.34	136.28	140.92	140.75	141.44
2.06	133.79	131.85	140.84	140.41	137.53	136.51	140.95	140.78	141.53
2.10	133.75	132.46	140.94	140.43	137.42	136.40	140.87	140.77	145.85
2.13	134.07	132.64	141.25	140.78	138.11	137.02	141.38	141.22	153.75
2.16	138.21	136.27	145.70	145.09	143.10	141.92	145.90	145.80	160.77
2.20	145.32	143.50	153.26	152.32	150.32	149.18	153.42	153.36	162.41
2.23	149.34	148.27	159.51	158.44	155.35	153.82	159.44	159.34	162.39
2.26	150.29	148.89	161.18	160.25	156.37	155.00	161.04	160.91	162.34
2.30	147.84	148.81	161.43	160.54	156.52	154.99	161.30	161.14	162.32
2.33	143.41	148.85	161.40	160.54	156.53	155.16	161.40	161.14	162.34
2.36	148.64	149.41	161.42	160.69	156.31	155.02	161.36	161.26	162.32
2.40	147.62	149.30	161.42	160.69	156.37	154.74	161.38	161.25	162.32
2.43	146.29	147.80	161.46	160.69	156.38	154.72	161.46	161.19	162.30
2.46	147.11	149.69	161.47	160.78	156.46	155.03	161.34	161.17	162.32
2.50	146.47	149.55	161.47	160.81	156.43	154.86	161.47	161.20	162.32
2.53	145.49	149.08	161.43	160.84	156.42	154.93	161.43	161.23	162.32
2.56	144.00	147.93	161.48	160.79	156.51	155.08	161.48	161.25	162.32
2.60	144.77	149.13	161.45	160.82	156.34	154.95	161.35	161.29	162.32
2.63	144.39	149.66	161.48	160.88	156.33	154.87	161.38	161.28	162.34
2.66	143.46	149.74	161.42	160.79	156.35	154.98	161.42	161.26	162.32
2.70	142.63	149.28	161.40	160.90	156.29	154.89	161.40	161.30	162.30
2.73	142.67	149.62	161.37	160.81	156.36	155.07	161.44	161.21	162.32
2.76	140.69	147.18	161.45	160.78	156.50	155.01	161.45	161.28	162.32
2.80	143.14	149.93	161.41	160.88	156.33	155.00	161.38	161.28	162.32
2.83	142.60	149.82	161.50	160.81	156.19	154.56	161.37	161.30	162.32

2.86	142.31	149.47	161.39	160.86	156.38	155.05	161.45	161.22	162.32
2.90	141.01	148.21	161.46	160.80	156.39	154.92	161.46	161.30	162.32
2.93	141.81	149.77	161.39	160.89	156.38	154.81	161.39	161.26	162.32
2.96	141.33	149.70	161.42	160.89	156.34	154.74	161.45	161.22	162.32
3.00	141.09	149.59	161.47	160.91	156.30	154.90	161.47	161.27	162.30
3.03	140.90	149.34	161.49	160.93	156.42	155.05	161.46	161.33	162.32
3.06	139.69	148.64	161.46	160.80	156.62	155.16	161.40	161.30	162.32
3.10	149.39	149.35	161.44	160.84	156.23	154.86	161.47	161.27	162.32
3.13	149.61	148.77	161.46	160.90	156.42	155.02	161.43	161.23	162.32
3.16	149.59	149.59	161.44	160.88	156.20	154.30	161.38	161.31	162.32
3.20	149.70	149.26	161.38	160.82	156.17	154.94	161.38	161.28	162.32
3.23	149.70	149.70	161.42	160.89	156.18	154.95	161.45	161.25	162.32
3.26	150.42	149.88	161.40	160.84	156.29	154.89	161.50	161.30	162.32
3.30	150.13	148.89	161.38	160.88	156.47	155.17	161.38	161.28	162.32
3.33	150.30	149.53	161.48	160.89	156.24	154.71	161.45	161.22	162.32
3.36	150.44	149.77	161.42	160.82	156.31	154.84	161.38	161.22	162.32
3.40	150.03	148.52	161.34	160.85	156.43	155.10	161.41	161.18	162.32
3.43	150.60	149.46	161.45	160.88	156.14	154.87	161.38	161.31	162.32
3.46	150.86	149.29	161.44	160.85	156.23	154.83	161.37	161.21	162.32
3.50	150.89	150.02	161.40	160.87	156.30	155.03	161.40	161.27	162.32
3.53	150.64	149.84	161.45	160.89	156.14	154.71	161.45	161.25	162.32
3.56	150.21	149.87	161.46	160.89	156.05	154.85	161.42	161.22	162.34
3.60	150.25	149.55	161.43	160.87	156.19	154.86	161.36	161.20	162.32
3.63	150.46	149.56	161.48	160.91	156.30	154.97	161.48	161.24	162.30
3.66	150.65	149.51	161.46	160.87	156.12	154.99	161.36	161.23	162.34
3.70	150.58	149.41	161.39	160.80	156.28	155.08	161.46	161.29	162.32
3.73	150.43	149.63	161.41	160.88	156.07	155.04	161.44	161.28	162.32
3.76	150.55	150.18	161.42	160.90	155.98	154.92	161.42	161.29	162.32
3.80	149.49	148.12	161.44	160.85	156.20	154.80	161.34	161.21	162.32
3.83	143.81	149.82	161.40	160.77	155.96	154.76	161.40	161.17	162.34
3.86	140.85	149.76	161.44	160.81	155.96	154.67	161.37	161.24	162.32
3.90	149.68	149.58	161.43	160.80	156.02	154.85	161.36	161.26	162.32
3.93	149.54	148.57	161.42	160.86	156.14	154.98	161.42	161.25	162.32
3.96	140.79	149.63	161.41	160.88	156.04	155.01	161.38	161.18	162.32
4.00	149.69	149.45	161.43	160.84	156.19	155.09	161.37	161.27	162.32
4.03	149.85	149.34	161.46	160.87	155.89	154.72	161.46	161.30	162.34
4.06	149.44	149.07	161.39	160.89	155.98	154.71	161.45	161.22	162.32
4.10	149.26	149.53	161.38	160.88	156.04	154.84	161.44	161.18	162.32
4.13	149.44	149.28	161.39	160.90	156.08	155.05	161.39	161.29	162.34
4.16	149.63	149.80	161.41	160.88	156.17	155.04	161.41	161.21	162.32
4.19	149.13	149.69	161.48	160.81	155.94	154.84	161.44	161.28	162.30
4.23	149.89	149.79	161.37	160.81	155.99	154.79	161.43	161.27	162.32
4.26	150.48	150.18	161.46	160.83	155.96	154.62	161.40	161.26	162.32
4.29	150.18	149.57	161.39	160.79	156.11	155.12	161.46	161.19	162.32
4.33	150.00	149.93	161.48	160.82	155.97	154.77	161.48	161.28	162.32
4.36	149.14	148.30	161.42	160.86	156.25	154.91	161.39	161.16	162.32
4.39	150.14	149.74	161.42	160.83	156.08	155.02	161.36	161.19	162.32
4.43	149.43	149.80	161.38	160.78	155.84	154.61	161.45	161.25	162.32
4.46	150.26	149.90	161.38	160.78	155.80	154.77	161.41	161.18	162.30
4.49	149.75	149.61	161.49	160.90	155.95	154.79	161.36	161.20	162.34
4.53	150.47	149.57	161.38	160.79	156.01	154.81	161.42	161.20	162.32

4.56	150.14	149.64	161.42	160.82	155.88	154.75	161.49	161.29	162.30
4.59	150.21	149.84	161.43	160.86	156.08	154.89	161.39	161.29	162.32
4.63	149.86	149.39	161.44	160.85	156.07	155.17	161.41	161.18	162.34
4.66	149.75	150.48	161.40	160.80	155.82	154.59	161.43	161.26	162.34
4.69	149.95	149.21	161.40	160.80	155.99	154.62	161.46	161.26	162.30
4.73	149.72	149.25	161.44	160.88	155.90	154.70	161.44	161.21	162.34
4.76	149.85	149.18	161.37	160.87	155.96	154.96	161.37	161.27	162.32
4.79	149.97	149.53	161.48	160.88	155.81	154.91	161.45	161.25	162.32
4.83	150.06	149.22	161.44	160.85	156.23	155.13	161.41	161.28	162.32
4.86	150.52	150.18	161.43	160.73	156.02	154.72	161.46	161.26	162.32
4.89	148.75	150.29	161.43	160.84	155.79	154.69	161.40	161.23	162.34
4.93	150.37	149.60	161.35	160.79	155.97	154.84	161.38	161.22	162.34
4.96	150.00	149.43	161.38	160.72	155.84	153.91	161.38	161.22	162.32
4.99	150.19	150.02	161.44	160.74	155.93	154.70	161.37	161.10	162.32
5.03	140.72	149.43	161.32	160.65	155.78	154.38	161.28	161.15	162.32
5.06	140.84	148.74	161.33	160.73	156.02	154.76	161.33	161.17	162.32
5.09	140.61	148.75	161.27	160.71	155.67	154.53	161.37	161.08	162.32
5.13	139.41	148.63	161.32	160.72	155.84	154.21	161.25	161.12	162.32
5.16	139.85	148.50	161.29	160.73	156.15	154.79	161.26	161.06	162.32
5.19	140.90	148.71	161.36	160.70	156.22	154.95	161.29	161.13	162.32
5.23	139.78	148.33	161.38	160.69	156.01	154.64	161.28	161.15	162.32
5.26	140.58	149.22	161.37	160.64	156.16	154.53	161.31	161.11	162.32
5.29	140.79	148.59	161.31	160.62	156.24	154.87	161.28	161.12	162.32
5.33	140.90	149.24	161.39	160.63	156.12	154.88	161.32	161.06	162.32
5.36	140.18	148.53	161.35	160.62	156.11	154.74	161.32	161.02	162.30
5.39	140.25	148.42	161.31	160.65	155.70	154.21	161.31	161.01	162.32
5.43	140.73	148.94	161.39	160.66	155.95	154.65	161.36	161.13	162.32
5.46	139.77	148.59	161.31	160.55	155.93	154.60	161.27	161.04	162.32
5.49	140.62	149.63	161.38	160.62	155.97	154.47	161.25	161.11	162.32
5.53	139.93	149.11	161.37	160.64	155.89	154.63	161.30	161.00	162.32
5.56	140.52	149.40	161.35	160.59	155.91	154.34	161.22	161.02	162.32
5.59	140.71	148.78	161.27	160.64	156.00	154.66	161.31	161.04	162.32
5.63	140.27	148.78	161.34	160.54	155.90	154.20	161.30	161.01	162.32
5.66	140.79	149.03	161.29	160.56	155.88	154.45	161.32	161.02	162.32
5.69	140.96	148.49	161.38	160.59	156.01	154.67	161.31	161.05	162.32
5.73	140.31	148.52	161.35	160.65	156.10	154.54	161.31	161.11	162.32
5.76	140.30	149.35	161.36	160.70	155.99	154.62	161.30	161.03	162.32
5.79	140.85	148.62	161.31	160.65	155.90	154.57	161.24	161.01	162.32
5.83	140.92	148.69	161.31	160.59	155.67	154.04	161.28	160.98	162.32
5.86	141.30	148.50	161.29	160.50	156.01	154.68	161.32	161.09	162.32
5.89	141.25	149.35	161.30	160.54	155.99	154.63	161.24	161.11	162.30
5.93	139.95	148.13	161.39	160.63	155.68	153.65	161.36	161.13	162.34
5.96	140.90	149.14	161.29	160.59	155.75	154.31	161.32	160.99	162.32
5.99	140.22	148.56	161.25	160.56	155.48	153.54	161.22	161.09	162.32
6.03	140.19	149.11	161.29	160.53	155.89	154.32	161.26	161.03	162.32
6.06	141.20	148.20	161.32	160.56	156.02	154.68	161.32	161.09	162.32
6.09	139.51	147.96	161.22	160.59	155.48	153.78	161.22	161.09	162.32
6.13	141.20	148.46	161.32	160.59	155.91	154.55	161.25	161.02	162.32
6.16	141.40	148.79	161.35	160.59	155.87	154.51	161.25	161.08	162.32
6.19	140.63	148.84	161.36	160.63	155.88	154.48	161.32	161.09	162.30
6.23	142.22	148.34	161.29	160.53	155.95	154.62	161.29	161.10	162.32

6.26	140.22	147.96	161.22	160.52	155.74	154.18	161.29	161.02	162.34
6.29	140.34	148.75	161.27	160.54	155.23	152.90	161.27	161.07	162.32
6.33	141.55	148.98	161.27	160.54	155.92	154.39	161.30	161.03	162.32
6.36	141.45	148.18	161.37	160.57	155.73	154.23	161.30	161.10	162.32
6.39	141.18	148.31	161.26	160.57	155.86	154.16	161.30	161.00	162.30
6.43	141.55	148.64	161.36	160.53	156.02	154.49	161.23	161.06	162.32
6.46	141.49	148.31	161.27	160.54	156.03	154.50	161.24	161.01	162.30
6.49	140.90	148.57	161.33	160.53	155.78	154.42	161.29	161.06	162.32
6.52	142.40	147.98	161.24	160.58	156.00	154.66	161.27	161.01	162.32
6.56	141.70	148.72	161.25	160.48	155.97	154.44	161.18	161.05	162.32
6.59	140.42	148.23	161.25	160.49	155.71	154.14	161.28	161.02	162.30
6.62	141.53	148.66	161.32	160.59	155.88	154.48	161.25	161.12	162.32
6.66	141.79	149.08	161.30	160.54	155.73	154.03	161.20	160.97	162.32
6.69	141.60	148.46	161.32	160.46	155.98	154.51	161.19	161.05	162.32
6.72	141.32	148.68	161.34	160.51	156.00	154.50	161.21	161.04	162.32
6.76	140.99	148.39	161.21	160.48	155.84	154.40	161.18	161.05	162.28
6.79	141.62	148.55	161.24	160.55	155.73	154.43	161.27	161.08	162.32
6.82	141.63	148.25	161.24	160.48	155.83	154.40	161.18	161.08	162.32
6.86	141.35	148.28	161.23	160.54	155.86	154.49	161.27	161.00	162.32
6.89	140.31	148.62	161.21	160.58	155.66	154.27	161.27	161.07	162.32
6.92	141.06	148.36	161.29	160.53	155.81	154.28	161.29	161.09	162.32
6.96	142.00	148.36	161.31	160.45	155.74	154.47	161.21	161.08	162.32
6.99	141.57	148.57	161.32	160.59	155.78	154.41	161.29	161.09	162.32
7.02	140.88	148.65	161.27	160.58	155.73	154.20	161.31	161.07	162.32
7.06	141.89	148.51	161.27	160.44	155.89	154.53	161.20	161.07	162.34
7.09	141.09	148.72	161.28	160.52	155.57	154.24	161.25	161.01	162.30
7.12	140.55	148.42	161.31	160.58	155.67	154.34	161.21	161.08	162.32
7.16	140.97	148.44	161.26	160.50	155.58	154.18	161.29	160.99	162.32
7.19	140.84	148.64	161.26	160.57	155.85	154.59	161.26	161.00	162.32
7.22	140.43	149.11	161.23	160.50	155.72	154.43	161.23	161.03	162.32
7.26	141.64	148.47	161.26	160.56	155.95	154.55	161.22	161.02	162.30
7.29	142.07	148.59	161.31	160.52	155.80	154.34	161.28	161.08	162.34
7.32	141.57	148.60	161.29	160.46	155.84	154.41	161.25	161.02	162.32
7.36	140.74	148.88	161.24	160.57	155.69	154.36	161.27	161.10	162.32
7.39	141.50	148.73	161.35	160.59	155.51	153.91	161.28	161.02	162.32
7.42	141.22	148.42	161.31	160.51	155.60	154.50	161.24	161.04	162.32
7.46	141.25	148.71	161.30	160.54	155.56	154.19	161.20	161.10	162.32
7.49	141.21	148.54	161.27	160.51	155.79	154.56	161.23	161.03	162.32
7.52	141.96	148.52	161.24	160.48	155.63	154.43	161.31	161.01	162.30
7.56	140.51	147.31	161.24	160.58	155.60	154.27	161.31	161.04	162.32
7.59	140.47	148.64	161.30	160.54	155.29	154.16	161.23	161.00	162.32
7.62	141.73	148.12	161.31	160.49	155.67	154.54	161.21	161.08	162.32
7.66	140.66	148.53	161.22	160.49	155.48	154.11	161.28	161.02	162.32
7.69	141.33	148.53	161.29	160.56	155.38	154.11	161.29	161.09	162.30
7.72	139.77	148.42	161.31	160.55	155.47	154.17	161.21	161.05	162.32
7.76	141.43	148.12	161.31	160.45	155.40	154.34	161.24	161.05	162.34
7.79	140.64	148.45	161.24	160.57	155.06	153.96	161.24	161.07	162.30
7.82	141.49	148.96	161.24	160.58	155.20	154.20	161.28	161.01	162.32
7.86	141.98	148.10	161.23	160.50	155.29	154.25	161.19	161.06	162.32
7.89	141.82	147.68	161.24	160.44	155.49	154.56	161.24	161.04	162.30
7.92	141.51	148.54	161.33	160.50	155.58	154.49	161.19	161.00	162.32

7.96	140.52	148.60	161.22	160.56	154.98	153.91	161.19	161.06	162.34
7.99	140.49	148.70	161.23	160.43	155.25	154.02	161.23	160.99	162.32
8.02	140.20	148.01	161.20	160.54	155.29	154.26	161.27	161.03	162.32
8.06	139.74	148.02	161.32	160.59	155.17	154.18	161.28	161.02	162.32
8.09	140.93	148.44	161.23	160.53	155.12	153.95	161.19	161.06	162.32
8.12	141.26	148.56	161.24	160.55	155.37	154.40	161.18	161.08	162.32
8.16	141.90	148.66	161.28	160.52	155.44	153.94	161.28	161.02	162.32
8.19	140.99	148.16	161.28	160.42	155.61	154.54	161.25	161.05	162.32
8.22	139.64	148.40	161.29	160.49	155.11	153.91	161.25	161.05	162.30
8.26	140.40	149.01	161.33	160.50	155.35	154.29	161.20	161.00	162.34
8.29	140.77	148.70	161.26	160.46	155.18	154.12	161.26	160.96	162.32
8.32	140.19	148.61	161.33	160.50	154.95	153.82	161.19	161.00	162.34
8.36	140.67	148.61	161.23	160.47	155.32	154.23	161.20	161.07	162.32
8.39	139.11	148.00	161.32	160.56	155.35	154.18	161.29	161.02	162.32
8.42	140.85	148.42	161.27	160.48	155.53	154.40	161.20	161.07	162.30
8.46	140.79	147.93	161.22	160.52	155.41	154.44	161.22	160.99	162.32
8.49	140.41	148.08	161.24	160.51	155.30	154.30	161.21	161.01	162.32
8.52	141.49	148.25	161.27	160.51	155.53	154.10	161.27	161.07	162.32
8.56	140.93	148.00	161.22	160.59	155.51	154.51	161.19	160.99	162.34
8.59	140.66	148.50	161.32	160.46	155.38	154.51	161.19	161.02	162.32
8.62	140.11	148.52	161.27	160.48	155.33	154.10	161.21	161.08	162.32
8.66	140.24	148.02	161.27	160.58	155.40	154.40	161.31	161.14	162.32
8.69	139.94	148.06	161.18	160.45	155.07	154.04	161.25	161.05	162.30
8.72	140.85	148.38	161.17	160.51	155.47	154.30	161.17	161.04	162.30
8.76	140.53	148.31	161.26	160.47	155.19	154.26	161.20	161.00	162.32
8.79	140.61	148.28	161.27	160.44	155.39	154.56	161.27	161.07	162.32
8.82	139.83	148.44	161.30	160.54	154.99	154.16	161.23	161.10	162.34
8.86	140.20	148.35	161.24	160.54	155.33	154.36	161.27	161.00	162.34
8.89	140.89	148.26	161.25	160.52	155.44	154.34	161.25	160.98	162.32
8.92	141.73	148.22	161.21	160.42	155.31	154.31	161.21	160.98	162.32
8.96	141.19	148.02	161.21	160.42	155.40	154.34	161.25	161.08	162.32
8.99	140.47	148.62	161.24	160.44	155.30	154.26	161.20	161.01	162.32
9.02	140.60	147.84	161.30	160.47	155.19	154.39	161.26	161.07	162.32
9.05	140.06	149.08	161.23	160.50	155.09	154.29	161.20	161.07	162.30
9.09	141.65	148.27	161.29	160.43	155.39	154.55	161.23	161.00	162.32
9.12	141.33	148.36	161.21	160.48	155.20	154.14	161.25	161.05	162.32
9.15	138.74	147.50	161.32	160.53	154.95	153.38	161.29	161.06	162.32
9.19	140.09	148.07	161.23	160.47	155.19	154.12	161.20	161.00	162.32
9.22	139.86	149.14	161.23	160.50	154.79	153.55	161.20	161.00	162.32
9.25	139.70	147.82	161.28	160.48	155.04	154.24	161.21	161.04	162.32
9.29	139.53	148.45	161.21	160.48	154.77	153.10	161.18	160.98	162.32
9.32	141.11	148.41	161.20	160.50	155.15	154.02	161.16	161.06	162.32
9.35	139.94	146.75	161.25	160.52	155.31	154.24	161.18	161.08	162.32
9.39	141.84	148.26	161.32	160.56	155.15	154.28	161.22	161.09	162.34
9.42	140.86	148.26	161.22	160.59	155.05	153.78	161.22	161.09	162.32
9.45	141.38	147.97	161.20	160.47	155.29	154.33	161.20	161.00	162.32
9.49	140.85	148.35	161.21	160.58	155.03	154.03	161.24	160.98	162.32
9.52	141.21	148.37	161.23	160.47	155.15	154.35	161.19	160.96	162.34
9.55	141.37	148.67	161.26	160.56	154.95	154.08	161.26	160.99	162.32
9.59	140.20	147.94	161.23	160.57	155.29	153.66	161.20	161.03	162.32
9.62	141.63	148.19	161.25	160.49	155.27	154.34	161.22	161.05	162.32

9.65	141.08	147.31	161.24	160.45	155.40	154.27	161.24	161.04	162.32
9.69	140.94	148.91	161.23	160.57	155.09	154.29	161.26	161.06	162.32
9.72	140.98	148.51	161.30	160.51	155.13	154.13	161.20	161.04	162.32
9.75	141.81	148.13	161.29	160.39	155.11	154.35	161.25	161.05	162.32
9.79	141.15	148.65	161.20	160.54	154.96	154.13	161.20	161.07	162.30
9.82	141.15	148.65	161.31	160.45	155.07	154.20	161.27	161.01	162.32
9.85	141.41	147.94	161.33	160.47	155.29	154.56	161.26	161.03	162.34
9.89	141.69	147.98	161.30	160.54	155.29	154.26	161.27	161.00	162.32
9.92	141.08	148.61	161.23	160.54	154.99	153.93	161.27	161.03	162.32
9.95	141.75	148.07	161.26	160.43	155.22	154.52	161.23	161.03	162.32
9.99	138.29	148.19	161.15	160.49	154.48	152.14	161.22	161.08	162.34
10.02	142.21	148.09	161.25	160.49	155.38	154.51	161.22	161.08	162.32
10.05	142.11	148.27	161.32	160.46	155.41	153.98	161.22	160.99	162.32
10.09	140.55	147.25	161.25	160.45	155.14	154.34	161.22	160.98	162.34
10.12	142.21	148.43	161.29	160.49	155.21	154.41	161.19	161.06	162.32
10.15	141.98	147.94	161.26	160.43	155.12	154.25	161.26	160.96	162.32
10.19	142.00	148.02	161.31	160.51	155.20	154.37	161.24	161.01	162.32
10.22	141.86	147.91	161.27	160.51	154.96	154.03	161.20	161.01	162.32
10.25	142.18	148.20	161.25	160.49	155.05	154.15	161.25	161.05	162.32
10.29	141.83	148.35	161.21	160.55	154.97	154.10	161.18	161.01	162.32
10.32	141.90	148.09	161.28	160.45	155.00	154.17	161.24	160.98	162.32
10.35	141.33	147.93	161.25	160.49	154.98	154.01	161.29	161.09	162.30
10.39	141.67	148.30	161.29	160.49	154.88	154.18	161.19	161.02	162.30
10.42	140.41	147.78	161.31	160.51	154.80	153.93	161.21	161.04	162.32
10.45	141.25	148.75	161.24	160.58	154.80	154.03	161.31	161.11	162.32
10.49	140.19	147.50	161.26	160.50	154.58	153.75	161.26	161.06	162.32
10.52	141.37	148.33	161.25	160.56	155.05	154.25	161.29	161.02	162.32
10.55	141.48	148.11	161.13	160.54	154.86	153.99	161.23	161.03	162.32
10.59	141.70	148.16	161.22	160.49	155.07	154.21	161.18	161.05	162.32
10.62	140.89	148.22	161.25	160.48	154.57	153.91	161.25	161.08	162.32
10.65	140.21	146.95	161.21	160.55	154.94	154.24	161.18	161.08	162.30
10.69	141.81	148.20	161.23	160.47	155.25	154.42	161.20	161.06	162.32
10.72	141.51	148.87	161.29	160.60	154.52	153.92	161.16	161.06	162.32
10.75	141.04	148.44	161.20	160.57	154.92	153.96	161.20	161.07	162.32
10.79	138.90	147.32	161.25	160.46	154.58	152.94	161.19	160.99	162.30
10.82	140.75	148.59	161.18	160.58	154.27	153.67	161.25	160.98	162.32
10.85	141.18	148.38	161.23	160.50	154.79	154.09	161.27	161.00	162.32
10.89	137.96	147.50	161.20	160.50	153.56	151.59	161.26	161.00	162.32
10.92	142.10	148.32	161.17	160.48	154.70	154.03	161.24	161.04	162.34
10.95	140.15	148.40	161.19	160.49	154.41	153.71	161.19	160.99	162.30
10.99	140.71	148.68	161.17	160.51	154.33	153.70	161.24	160.97	162.32
11.02	139.92	148.78	161.16	160.60	154.26	153.79	161.16	161.06	162.32
11.05	141.67	148.00	161.26	160.49	155.05	154.22	161.16	160.96	162.32
11.09	137.83	147.71	161.13	160.57	153.49	151.96	161.27	161.00	162.32
11.12	140.37	148.78	161.20	160.48	154.53	153.76	161.27	161.01	162.32
11.15	140.78	148.99	161.21	160.58	154.13	153.47	161.27	161.08	162.32
11.19	141.62	148.91	161.20	160.51	154.53	153.73	161.17	160.97	162.30
11.22	141.14	148.37	161.29	160.46	154.55	154.05	161.26	160.99	162.32
11.25	137.95	147.99	161.22	160.59	153.75	152.11	161.19	160.99	162.34
11.29	139.56	148.85	161.14	160.47	153.99	153.03	161.17	161.00	162.30
11.32	141.15	148.49	161.21	160.48	154.30	153.64	161.24	160.98	162.34

11.35	139.54	148.60	161.15	160.59	153.48	152.38	161.19	161.02	162.30
11.39	140.07	148.62	161.24	160.58	153.93	152.83	161.24	161.01	162.34
11.42	141.50	148.73	161.28	160.49	154.61	153.94	161.25	161.08	162.34
11.45	141.17	148.90	161.26	160.49	154.48	153.45	161.26	161.09	162.30
11.48	140.00	148.72	161.21	160.58	153.50	152.40	161.24	161.01	162.30
11.52	141.37	148.47	161.25	160.59	154.21	153.61	161.16	160.96	162.34
11.55	141.55	148.38	161.30	160.58	154.70	154.00	161.17	161.04	162.32
11.58	140.09	147.53	161.26	160.50	154.15	153.32	161.20	161.03	162.30
11.62	140.45	148.63	161.12	160.52	153.94	152.98	161.15	160.99	162.32
11.65	139.83	148.55	161.17	160.44	154.40	152.46	161.14	161.04	162.32
11.68	140.76	148.73	161.22	160.49	153.88	153.21	161.15	160.96	162.32
11.72	140.58	147.88	161.31	160.51	154.57	153.17	161.27	161.07	162.32
11.75	140.32	148.87	161.15	160.59	153.95	152.98	161.15	161.09	162.32
11.78	140.03	148.45	161.24	160.51	154.03	153.30	161.17	161.07	162.34
11.82	139.21	147.96	161.26	160.49	153.68	152.01	161.26	161.06	162.30
11.85	141.27	148.20	161.12	160.49	154.18	153.31	161.16	161.02	162.30
11.88	140.76	148.36	161.22	160.56	153.51	152.28	161.25	161.02	162.32
11.92	141.26	148.15	161.21	160.52	154.14	153.30	161.18	160.98	162.32
11.95	139.94	147.55	161.15	160.49	154.11	152.81	161.15	161.05	162.34
11.98	142.29	148.65	161.30	160.47	154.59	153.69	161.27	161.00	162.32
12.02	141.22	148.69	161.15	160.55	154.17	153.24	161.18	161.08	162.30
12.05	141.90	149.10	161.22	160.56	154.38	153.48	161.28	160.99	162.32
12.08	141.73	148.79	161.15	160.55	154.24	153.34	161.21	161.05	162.32
12.12	140.77	148.50	161.13	160.56	153.65	152.75	161.23	160.99	162.34
12.15	141.03	148.57	161.19	160.53	153.71	152.75	161.25	160.99	161.40
12.18	142.39	149.08	161.33	160.50	154.56	153.82	161.20	161.06	160.03
12.22	141.95	148.54	161.03	160.34	154.06	153.49	160.93	160.74	158.68
12.25	140.27	147.51	159.64	159.18	152.39	151.52	159.68	159.58	157.42
12.28	138.33	145.21	158.44	157.84	151.81	151.15	158.37	158.31	156.15
12.32	137.22	145.59	157.15	156.69	150.15	149.18	157.12	156.98	154.96
12.35	137.43	144.38	155.93	155.43	149.29	148.58	155.86	155.76	153.68
12.38	135.55	143.06	154.69	154.22	147.97	147.33	154.65	154.45	150.96
12.42	135.49	141.99	153.52	153.06	147.50	146.60	153.49	153.39	147.69
12.45	134.89	140.14	151.74	151.23	145.94	145.50	151.70	151.47	146.25
12.48	130.72	136.91	148.74	148.41	143.06	142.09	148.71	148.61	145.67
12.52	114.36	129.31	143.22	143.15	126.05	129.61	144.39	143.75	145.22

Temperature Data from 3rd Test Using 2nd Multifunctional Curing Fixture

Time in hours (hr); Temperature in °F

Time (hr)	Ch 2	Ch 3	Ch 4	Ch 5	Ch 6	Ch 7	Ch 8	Ch 9	Bath Temp
0.00	70.08	70.63	71.07	71.03	70.77	70.74	71.07	71.14	--
0.03	70.35	70.79	70.97	70.97	70.83	70.75	71.12	71.08	--
0.07	71.62	72.16	71.84	71.84	72.67	72.82	72.13	72.02	--
0.10	80.30	81.81	82.21	81.74	83.14	83.18	82.61	82.64	--
0.13	89.37	91.72	93.61	92.79	94.03	93.64	94.14	94.03	100.92
0.17	99.72	102.12	105.07	103.94	104.58	103.73	105.56	105.45	113.74
0.20	111.54	111.65	116.27	114.81	115.05	113.91	116.82	116.61	125.10
0.23	122.16	121.13	127.51	125.87	125.66	124.26	127.92	127.79	136.29
0.27	129.31	129.18	137.11	135.27	133.68	131.63	137.31	137.24	141.12
0.30	129.01	130.78	140.22	138.74	135.75	133.71	140.26	140.12	141.57
0.33	130.89	130.72	140.60	139.38	136.30	134.36	140.63	140.46	141.48
0.37	129.70	132.05	140.74	139.52	136.10	134.13	140.70	140.50	141.44
0.40	129.74	132.12	140.67	139.63	136.03	133.93	140.67	140.54	141.44
0.43	130.59	132.26	140.71	139.76	135.93	133.93	140.77	140.64	141.44
0.47	130.84	131.49	140.62	139.81	135.98	134.15	140.76	140.55	141.44
0.50	130.90	131.89	140.71	139.87	136.01	134.07	140.75	140.64	141.44
0.53	131.10	131.85	140.64	139.93	136.17	134.20	140.77	140.64	141.44
0.57	131.40	131.87	140.66	139.92	136.19	134.53	140.80	140.69	141.44
0.60	130.26	131.29	140.59	139.94	136.08	134.08	140.69	140.59	141.46
0.63	130.33	131.42	140.69	139.94	135.98	134.25	140.75	140.59	141.44
0.67	130.51	132.18	140.63	139.95	135.82	134.12	140.77	140.73	141.46
0.70	130.31	131.68	140.63	139.99	136.10	134.33	140.84	140.73	141.46
0.73	128.18	130.13	140.59	140.05	136.05	134.36	140.79	140.73	141.44
0.77	127.40	129.56	140.53	140.05	136.64	134.63	140.76	140.70	141.42
0.80	127.52	129.78	140.65	140.04	136.93	134.92	140.88	140.68	141.44
0.83	127.04	129.91	140.61	140.04	136.89	134.85	140.81	140.71	141.44
0.87	128.08	129.51	140.62	140.08	136.86	134.79	140.89	140.79	141.46
0.90	127.18	129.71	140.68	140.08	136.89	134.96	140.89	140.75	141.44
0.93	128.07	129.64	140.62	140.11	136.89	134.96	140.92	140.72	141.44
0.97	126.97	129.57	140.61	140.13	136.85	134.85	140.91	140.81	141.44
1.00	125.18	129.46	140.60	140.16	136.95	134.81	140.80	140.70	141.42
1.03	124.98	129.61	140.68	140.14	136.85	134.89	140.88	140.75	141.46
1.07	123.79	129.51	140.66	140.08	136.90	134.90	140.89	140.76	141.44
1.10	124.07	129.93	140.66	140.19	136.87	134.73	140.93	140.76	141.44
1.13	128.04	129.54	140.61	140.14	136.82	134.89	140.88	140.75	141.44

1.17	127.95	129.63	140.70	140.19	136.81	134.87	140.80	140.84	141.44
1.20	126.14	129.50	140.67	140.13	136.85	134.84	140.87	140.81	141.44
1.23	124.99	129.82	140.66	140.15	136.93	135.10	140.89	140.76	141.44
1.27	124.07	129.55	140.63	140.19	136.90	135.00	140.83	140.76	141.44
1.30	123.30	129.67	140.64	140.14	136.85	134.85	140.85	140.85	141.44
1.33	122.99	129.50	140.71	140.24	136.89	134.95	140.91	140.78	141.44
1.37	122.98	129.90	140.70	140.20	136.78	134.74	140.91	140.74	141.44
1.40	122.78	129.73	140.67	140.20	136.88	134.98	140.87	140.81	141.44
1.43	122.65	129.92	140.69	140.18	136.90	135.03	140.86	140.79	141.44
1.47	122.75	129.78	140.65	140.14	136.82	134.92	140.88	140.75	141.44
1.50	122.62	129.68	140.65	140.14	136.82	135.03	140.85	140.82	141.44
1.53	122.19	129.56	140.74	140.23	136.91	134.94	140.84	140.87	141.44
1.57	122.19	129.60	140.70	140.23	136.98	135.01	140.84	140.77	141.44
1.60	122.74	129.70	140.67	140.20	136.98	135.11	140.94	140.77	141.44
1.63	122.48	129.82	140.72	140.15	136.79	134.93	140.85	140.75	141.44
1.66	122.33	129.84	140.71	140.23	136.85	135.05	140.91	140.84	141.44
1.70	122.12	129.63	140.67	140.16	136.84	135.01	140.90	140.73	141.44
1.73	122.03	129.71	140.71	140.24	136.79	135.12	140.85	140.81	141.44
1.76	122.12	129.56	140.73	140.26	136.84	135.08	140.83	140.77	141.44
1.80	122.27	129.91	140.68	140.17	136.85	135.12	140.91	140.88	141.44
1.83	122.04	129.96	140.72	140.15	136.80	135.00	140.86	140.76	141.44
1.86	121.77	129.55	140.66	140.19	136.94	135.01	140.86	140.86	141.44
1.90	122.11	130.00	140.63	140.22	136.83	135.04	140.79	140.79	141.44
1.93	121.82	129.88	140.65	140.24	136.76	135.02	140.88	140.75	141.44
1.96	121.98	129.96	140.66	140.19	136.90	135.07	140.83	140.83	141.44
2.00	121.60	129.66	140.67	140.23	136.88	135.08	140.90	140.80	141.44
2.03	121.95	129.87	140.67	140.27	136.81	135.05	140.94	140.84	141.44
2.06	123.49	130.51	140.73	140.19	136.87	135.21	140.87	140.80	141.42
2.10	122.50	130.04	140.71	140.23	136.78	135.15	140.88	140.81	141.44
2.13	122.42	130.00	140.76	140.26	136.77	135.11	140.93	140.86	141.46
2.16	123.27	130.60	141.12	140.65	137.40	135.84	141.36	141.32	144.88
2.20	126.41	134.63	145.71	145.04	142.62	141.03	146.25	146.12	152.49
2.23	134.66	141.06	153.28	152.28	149.74	148.10	153.81	153.68	160.05
2.26	141.15	145.33	159.32	158.09	154.80	152.63	159.68	159.45	162.27
2.30	148.83	146.52	160.99	159.90	155.78	153.61	161.22	161.02	162.39
2.33	149.09	146.78	161.25	160.25	155.90	153.84	161.38	161.21	162.34
2.36	152.83	146.63	161.30	160.31	155.92	153.79	161.50	161.30	162.32
2.40	152.29	146.80	161.20	160.47	155.92	153.62	161.50	161.36	162.32
2.43	151.88	146.66	161.26	160.50	155.98	153.78	161.49	161.29	162.32
2.46	151.90	146.85	161.28	160.45	155.84	153.84	161.51	161.38	162.32
2.50	152.53	147.14	161.24	160.64	155.93	153.86	161.47	161.44	162.34
2.53	152.15	146.93	161.22	160.63	155.85	153.75	161.52	161.36	162.32
2.56	150.39	146.84	161.23	160.64	155.86	153.89	161.53	161.43	162.32
2.60	149.45	146.76	161.23	160.70	155.92	153.82	161.53	161.46	162.32
2.63	148.93	147.02	161.21	160.65	155.87	153.81	161.51	161.38	162.32
2.66	148.21	147.11	161.24	160.64	155.86	153.90	161.47	161.37	162.34
2.70	147.46	146.92	161.22	160.65	155.97	153.88	161.52	161.45	162.34
2.73	146.45	146.86	161.32	160.66	155.88	153.75	161.52	161.39	162.30
2.76	144.88	146.69	161.33	160.73	155.99	153.89	161.56	161.39	162.32
2.80	145.12	146.87	161.23	160.74	155.92	153.93	161.50	161.40	162.32
2.83	144.21	147.07	161.33	160.77	155.92	153.76	161.50	161.37	162.32

2.86	143.96	146.85	161.28	160.72	155.94	153.87	161.48	161.38	162.32
2.90	143.86	147.22	161.25	160.75	155.87	153.77	161.48	161.35	162.32
2.93	143.13	146.97	161.30	160.70	155.89	153.76	161.43	161.37	162.30
2.96	142.93	146.80	161.27	160.74	155.86	153.79	161.46	161.36	162.34
3.00	142.81	146.78	161.31	160.61	155.80	153.74	161.51	161.34	162.34
3.03	142.93	146.66	161.30	160.67	155.82	153.79	161.50	161.33	162.32
3.06	143.09	147.16	161.22	160.59	155.71	153.72	161.42	161.39	162.32
3.10	142.51	146.82	161.28	160.69	155.77	153.74	161.48	161.38	162.32
3.13	141.92	146.83	161.20	160.63	155.79	153.62	161.43	161.30	162.30
3.16	141.54	146.96	161.32	160.69	155.78	153.71	161.45	161.39	162.32
3.20	141.28	146.87	161.34	160.68	155.73	153.76	161.47	161.40	162.32
3.23	141.11	147.10	161.27	160.67	155.82	153.72	161.43	161.40	162.34
3.26	140.89	146.98	161.34	160.68	155.94	153.80	161.54	161.41	162.32
3.30	140.67	147.10	161.23	160.60	155.79	153.86	161.50	161.36	162.32
3.33	140.74	146.83	161.23	160.60	155.66	153.62	161.43	161.33	162.32
3.36	140.30	146.90	161.30	160.60	155.72	153.76	161.43	161.40	162.32
3.40	140.53	146.97	161.26	160.57	155.79	153.76	161.50	161.33	162.32
3.43	140.21	146.91	161.24	160.61	155.73	153.77	161.41	161.38	162.30
3.46	139.97	146.88	161.27	160.65	155.80	153.87	161.41	161.37	162.32
3.50	140.10	147.04	161.34	160.67	155.90	153.83	161.50	161.40	162.32
3.53	139.92	146.92	161.29	160.56	155.68	153.75	161.49	161.39	162.34
3.56	139.68	146.96	161.32	160.66	155.74	153.78	161.42	161.42	162.32
3.60	139.72	146.82	161.26	160.63	155.82	153.72	161.42	161.32	162.32
3.63	139.88	146.82	161.25	160.59	155.74	153.68	161.48	161.32	162.30
3.66	140.20	146.94	161.24	160.64	155.63	153.73	161.47	161.37	162.32
3.70	139.80	146.84	161.24	160.64	155.83	153.76	161.43	161.30	162.34
3.73	140.08	146.72	161.29	160.56	155.64	153.74	161.45	161.35	162.32
3.76	138.61	147.00	161.30	160.60	155.76	153.69	161.43	161.40	162.32
3.80	138.85	147.01	161.34	160.67	155.86	153.86	161.50	161.44	162.34
3.83	138.93	146.92	161.32	160.66	155.78	153.71	161.45	161.42	162.30
3.86	138.92	147.01	161.27	160.54	155.66	153.73	161.47	161.40	162.30
3.90	138.81	146.93	161.33	160.57	155.69	153.69	161.43	161.43	162.32
3.93	139.32	146.97	161.34	160.61	155.73	153.66	161.50	161.44	162.30
3.96	139.10	146.95	161.28	160.58	155.70	153.64	161.48	161.38	162.32
4.00	139.37	147.12	161.22	160.59	155.68	153.81	161.48	161.38	162.32
4.03	139.19	146.81	161.21	160.61	155.70	153.70	161.47	161.34	162.32
4.06	139.85	147.43	161.32	160.56	155.71	153.88	161.49	161.32	162.32
4.10	137.57	146.81	161.21	160.65	155.73	153.84	161.47	161.38	162.30
4.13	138.05	147.15	161.25	160.65	155.67	153.81	161.44	161.41	162.34
4.16	138.54	146.90	161.27	160.64	155.72	153.69	161.43	161.40	162.32
4.20	139.12	147.04	161.27	160.64	155.76	153.80	161.41	161.34	162.32
4.23	139.19	146.97	161.27	160.58	155.73	153.80	161.47	161.44	162.32
4.26	139.01	147.00	161.23	160.63	155.65	153.69	161.49	161.33	162.32
4.30	139.25	147.20	161.20	160.57	155.59	153.59	161.47	161.37	162.30
4.33	139.79	147.03	161.26	160.63	155.65	153.82	161.49	161.39	162.34
4.36	139.80	147.21	161.34	160.64	155.73	153.83	161.50	161.37	162.32
4.40	139.05	147.03	161.23	160.60	155.76	153.79	161.40	161.30	162.32
4.43	138.99	147.14	161.30	160.61	155.80	153.83	161.50	161.30	162.32
4.46	138.76	146.75	161.29	160.62	155.78	153.91	161.45	161.35	162.32
4.50	139.26	147.38	161.31	160.58	155.70	153.84	161.54	161.34	162.32
4.53	139.59	147.20	161.26	160.57	155.62	153.82	161.43	161.43	162.32

4.56	139.12	146.94	161.30	160.54	155.66	153.80	161.50	161.30	162.30
4.60	138.90	146.92	161.28	160.62	155.74	153.88	161.42	161.38	162.34
4.63	138.69	147.05	161.31	160.59	155.64	153.71	161.48	161.35	162.34
4.66	138.16	146.96	161.22	160.59	155.75	153.85	161.49	161.35	162.32
4.69	138.03	147.10	161.26	160.67	155.62	153.92	161.43	161.39	162.30
4.73	138.25	147.15	161.25	160.59	155.61	153.94	161.51	161.41	162.30
4.76	137.31	146.86	161.26	160.66	155.55	153.75	161.49	161.39	162.32
4.79	137.47	146.98	161.24	160.61	155.57	153.74	161.44	161.34	162.34
4.83	137.81	147.15	161.25	160.55	155.67	153.88	161.48	161.35	162.34
4.86	137.95	147.05	161.25	160.65	155.71	153.84	161.51	161.41	162.32
4.89	137.83	146.97	161.30	160.64	155.56	153.82	161.50	161.40	162.32
4.93	138.02	147.09	161.29	160.66	155.64	153.78	161.42	161.39	162.32
4.96	137.74	146.84	161.31	160.65	155.67	153.87	161.44	161.41	162.32
4.99	137.82	146.92	161.35	160.66	155.71	153.88	161.52	161.35	162.32
5.03	137.71	146.82	161.25	160.62	155.74	153.91	161.42	161.38	162.32
5.06	137.58	146.95	161.28	160.59	155.54	153.68	161.48	161.38	162.32
5.09	138.15	147.21	161.28	160.58	155.64	153.77	161.41	161.38	162.32
5.13	137.89	146.86	161.29	160.53	155.62	153.89	161.49	161.29	162.32
5.16	138.19	147.09	161.22	160.66	155.58	153.81	161.49	161.32	162.32
5.19	138.13	146.99	161.29	160.63	155.72	153.79	161.42	161.39	162.32
5.23	138.04	146.91	161.31	160.65	155.63	153.77	161.48	161.38	162.32
5.26	137.99	146.76	161.26	160.56	155.62	153.75	161.42	161.32	162.32
5.29	138.24	147.10	161.27	160.51	155.62	153.86	161.47	161.30	162.34
5.33	137.23	147.01	161.31	160.61	155.67	153.83	161.47	161.37	162.30
5.36	138.29	146.86	161.32	160.59	155.61	153.88	161.45	161.42	162.32
5.39	138.14	147.31	161.31	160.61	155.67	153.63	161.47	161.31	162.32
5.43	138.09	147.16	161.29	160.56	155.65	153.89	161.49	161.39	162.32
5.46	138.20	147.04	161.24	160.54	155.73	153.89	161.50	161.30	162.32
5.49	138.36	147.02	161.22	160.62	155.64	153.74	161.45	161.42	162.32
5.53	138.23	146.89	161.22	160.60	155.65	153.82	161.46	161.32	162.32
5.56	138.80	146.99	161.26	160.63	155.52	153.88	161.42	161.32	162.32
5.59	138.91	147.00	161.20	160.54	155.56	153.76	161.50	161.36	162.28
5.63	138.69	146.85	161.31	160.55	155.54	153.71	161.48	161.38	162.32
5.66	139.08	147.06	161.23	160.63	155.72	153.82	161.39	161.36	162.34
5.69	138.82	146.98	161.28	160.55	155.60	153.90	161.41	161.31	162.32
5.73	139.28	146.89	161.22	160.53	155.42	153.62	161.49	161.29	162.32
5.76	139.59	147.27	161.33	160.57	155.62	153.92	161.49	161.40	162.32
5.79	139.24	147.22	161.22	160.56	155.58	153.78	161.45	161.39	162.32
5.83	138.36	147.16	161.19	160.66	155.61	153.85	161.42	161.39	162.32
5.86	138.11	147.14	161.21	160.61	155.63	153.90	161.47	161.41	162.32
5.89	139.00	146.96	161.29	160.66	155.51	153.78	161.49	161.29	162.32
5.93	138.52	146.98	161.21	160.62	155.64	153.84	161.45	161.35	162.32
5.96	138.33	146.89	161.29	160.63	155.55	153.71	161.42	161.39	162.30
5.99	138.65	147.17	161.30	160.58	155.60	153.86	161.40	161.40	162.32
6.03	138.62	147.08	161.21	160.62	155.57	153.74	161.48	161.38	162.32
6.06	138.87	147.36	161.25	160.62	155.54	153.78	161.45	161.32	162.32
6.09	137.94	146.78	161.28	160.61	155.67	153.90	161.41	161.31	162.32
6.13	138.33	147.26	161.35	160.59	155.65	153.88	161.49	161.35	162.32
6.16	138.24	147.17	161.30	160.61	155.53	153.76	161.50	161.40	162.32
6.19	138.03	147.17	161.33	160.57	155.75	153.85	161.39	161.30	162.32
6.23	138.29	147.22	161.22	160.56	155.48	153.81	161.45	161.35	162.30

6.26	137.95	146.99	161.22	160.66	155.61	153.91	161.39	161.32	162.32
6.29	137.78	146.99	161.32	160.66	155.61	153.78	161.42	161.38	162.32
6.33	138.84	146.92	161.26	160.66	155.55	153.68	161.49	161.32	162.30
6.36	138.30	147.00	161.33	160.57	155.59	153.62	161.43	161.39	162.32
6.39	138.78	147.20	161.23	160.64	155.59	153.76	161.46	161.36	162.32
6.43	138.62	147.25	161.25	160.55	155.61	153.71	161.48	161.31	162.30
6.46	138.73	147.49	161.32	160.62	155.51	153.78	161.49	161.32	162.32
6.49	139.41	147.20	161.29	160.63	155.65	153.89	161.49	161.39	162.32
6.53	138.43	147.26	161.25	160.66	155.61	153.91	161.48	161.35	162.32
6.56	138.54	147.07	161.30	160.57	155.69	153.89	161.36	161.40	162.32
6.59	140.74	147.34	161.30	160.60	155.59	153.82	161.50	161.33	162.32
6.63	140.56	147.26	161.29	160.62	155.61	153.88	161.49	161.35	162.32
6.66	139.50	147.42	161.34	160.65	155.60	153.84	161.48	161.41	162.30
6.69	139.43	147.41	161.27	160.68	155.50	153.87	161.47	161.34	162.32
6.73	139.46	147.34	161.30	160.57	155.63	153.86	161.47	161.40	162.32
6.76	141.25	150.13	161.34	160.61	154.67	152.97	161.37	161.34	162.34
6.79	141.43	150.00	161.38	160.56	154.68	152.88	161.35	161.35	162.30
6.83	140.70	150.65	161.33	160.53	154.72	153.15	161.39	161.33	162.34
6.86	140.76	150.27	161.35	160.63	154.48	153.05	161.45	161.25	162.32
6.89	141.17	150.31	161.33	160.50	154.89	153.52	161.36	161.26	162.32
6.93	140.37	149.92	161.33	160.57	154.36	152.59	161.36	161.30	162.32
6.96	141.36	150.10	161.28	160.55	154.47	153.14	161.41	161.31	162.32
6.99	144.19	150.30	161.25	160.52	154.27	152.87	161.44	161.35	162.32
7.03	144.91	150.05	161.23	160.57	154.59	153.32	161.43	161.23	162.32
7.06	145.26	150.46	161.24	160.54	154.56	153.03	161.37	161.30	162.32
7.09	145.47	150.24	161.22	160.56	154.44	153.01	161.35	161.28	162.32
7.13	145.52	150.18	161.23	160.53	154.52	153.12	161.36	161.26	162.32
7.16	145.52	149.72	161.20	160.50	154.62	153.09	161.33	161.20	162.32
7.19	145.44	149.36	161.25	160.45	154.64	153.27	161.31	161.21	162.32
7.23	146.10	150.23	161.28	160.51	154.43	153.03	161.41	161.28	162.32
7.26	146.20	149.62	161.24	160.48	154.26	153.00	161.44	161.20	162.32
7.29	146.48	150.13	161.28	160.49	154.31	153.01	161.35	161.18	162.30
7.33	145.56	149.62	161.17	160.41	154.20	152.96	161.37	161.24	162.32
7.36	145.99	149.58	161.23	160.44	154.36	152.96	161.40	161.20	162.32
7.39	145.67	149.63	161.21	160.42	154.17	152.81	161.31	161.21	162.32
7.43	146.96	150.28	161.26	160.46	154.28	153.02	161.36	161.26	162.32
7.46	146.49	150.01	161.29	160.39	154.55	153.28	161.39	161.25	162.32
7.49	146.30	149.42	161.24	160.41	154.37	153.06	161.34	161.24	162.32
7.53	146.42	149.94	161.22	160.49	154.15	152.91	161.42	161.25	162.30
7.56	145.60	149.89	161.18	160.45	154.34	152.80	161.38	161.21	162.30
7.59	146.28	149.70	161.28	160.46	154.08	152.54	161.32	161.22	162.34
7.63	146.15	150.14	161.26	160.46	154.35	152.68	161.39	161.22	162.34
7.66	145.88	149.70	161.25	160.36	153.91	152.28	161.35	161.22	162.34
7.69	146.31	150.07	161.28	160.39	154.14	152.84	161.38	161.22	162.34
7.73	146.31	150.40	161.28	160.39	154.11	152.77	161.38	161.15	162.32
7.76	145.80	149.96	161.28	160.45	154.30	153.10	161.41	161.18	162.32
7.79	146.07	149.86	161.18	160.45	154.27	152.70	161.41	161.21	162.34
7.83	146.20	150.19	161.20	160.37	154.43	153.06	161.33	161.24	162.32
7.86	145.54	149.56	161.18	160.39	154.24	152.81	161.41	161.25	162.32
7.89	145.91	149.87	161.22	160.46	154.24	153.14	161.32	161.15	162.30
7.93	145.24	149.74	161.15	160.36	154.28	153.08	161.35	161.22	162.32

7.96	146.51	149.83	161.24	160.45	154.24	153.17	161.38	161.15	162.34
7.99	146.01	149.40	161.25	160.46	154.31	153.14	161.38	161.22	162.30
8.03	145.94	149.80	161.22	160.42	154.28	152.91	161.28	161.15	162.30
8.06	145.89	149.57	161.19	160.43	154.22	153.08	161.39	161.19	162.34
8.09	146.23	149.72	161.17	160.44	154.13	152.83	161.30	161.14	162.32
8.13	146.27	149.29	161.21	160.35	154.37	153.17	161.37	161.24	162.30
8.16	146.43	149.89	161.13	160.41	154.29	153.19	161.37	161.20	162.32
8.19	146.22	149.95	161.20	160.47	154.05	152.82	161.39	161.20	162.30
8.22	146.19	149.98	161.26	160.37	154.16	153.02	161.33	161.23	162.32
8.26	146.18	149.37	161.19	160.36	154.28	153.08	161.32	161.19	162.32
8.29	145.97	149.80	161.15	160.45	154.17	152.94	161.35	161.25	162.32
8.32	146.22	149.74	161.16	160.40	153.88	152.35	161.36	161.22	162.32
8.36	146.40	149.62	161.17	160.44	154.40	153.13	161.37	161.24	162.32
8.39	146.06	149.58	161.23	160.41	154.09	152.76	161.30	161.13	162.34
8.42	147.36	150.17	161.19	160.46	154.31	152.95	161.29	161.22	162.32
8.46	146.99	149.24	161.16	160.40	154.08	152.85	161.32	161.22	162.32
8.49	147.83	150.04	161.25	160.39	154.24	152.98	161.35	161.15	162.32
8.52	147.08	149.73	161.24	160.42	154.14	153.04	161.31	161.24	162.32
8.56	146.45	148.73	161.25	160.39	154.08	152.77	161.32	161.18	162.34
8.59	145.85	149.34	161.16	160.43	154.19	152.99	161.39	161.26	162.30
8.62	146.53	150.31	161.16	160.33	154.12	152.85	161.26	161.13	162.30
8.66	145.87	149.36	161.24	160.38	153.97	152.16	161.34	161.21	162.32
8.69	146.04	149.63	161.25	160.42	154.24	153.01	161.41	161.22	162.32
8.72	145.52	149.58	161.23	160.43	154.02	152.62	161.29	161.23	162.32
8.76	146.08	149.71	161.16	160.36	153.98	152.71	161.29	161.12	162.32
8.79	146.25	149.10	161.16	160.33	154.31	153.11	161.39	161.22	162.30
8.82	145.08	148.91	161.20	160.43	153.92	152.55	161.26	161.23	162.32
8.86	145.83	149.99	161.23	160.44	153.96	152.49	161.27	161.23	162.32
8.89	145.81	149.23	161.15	160.32	154.31	153.14	161.28	161.21	162.32
8.92	144.60	149.60	161.15	160.39	154.05	152.85	161.32	161.15	162.32
8.96	144.53	149.60	161.22	160.36	153.91	152.58	161.35	161.15	162.32
8.99	144.60	149.70	161.15	160.36	154.11	152.78	161.38	161.22	162.32
9.02	144.73	149.73	161.15	160.35	154.14	152.94	161.31	161.18	162.32
9.06	144.79	149.56	161.21	160.31	153.80	152.40	161.31	161.21	162.32
9.09	145.30	149.63	161.15	160.32	154.10	153.10	161.38	161.11	162.32
9.12	145.20	149.49	161.15	160.35	154.17	153.00	161.31	161.15	162.32
9.16	144.66	149.69	161.24	160.41	153.97	152.43	161.34	161.21	162.32
9.19	145.56	149.41	161.16	160.40	153.96	152.39	161.30	161.23	162.32
9.22	145.73	149.56	161.14	160.38	154.03	152.60	161.37	161.17	162.32
9.26	145.53	149.45	161.17	160.37	153.96	152.73	161.37	161.24	162.32
9.29	144.77	149.67	161.22	160.39	153.74	152.14	161.28	161.22	162.34
9.32	145.26	149.89	161.28	160.35	154.13	153.00	161.37	161.21	162.30
9.36	144.86	149.62	161.20	160.41	153.96	152.70	161.37	161.14	162.32
9.39	145.50	149.66	161.17	160.35	154.00	152.80	161.37	161.24	162.32
9.42	146.40	149.72	161.20	160.30	153.92	152.49	161.30	161.23	162.32
9.46	147.22	150.20	161.18	160.42	154.21	152.91	161.35	161.18	162.32
9.49	147.30	149.81	161.23	160.43	154.12	152.92	161.29	161.23	162.30
9.52	146.92	149.80	161.19	160.33	154.01	152.51	161.38	161.15	162.32
9.56	144.74	149.44	161.23	160.36	153.75	152.02	161.26	161.16	162.30
9.59	145.32	149.92	161.20	160.38	154.13	152.93	161.34	161.14	162.32
9.62	144.38	149.79	161.24	160.34	153.96	152.73	161.37	161.17	162.32

9.66	144.22	149.62	161.21	160.35	153.87	152.63	161.27	161.21	162.32
9.69	144.17	149.91	161.22	160.43	154.05	152.75	161.35	161.16	162.32
9.72	143.70	149.85	161.16	160.43	153.89	152.25	161.33	161.26	162.32
9.76	143.54	149.48	161.20	160.37	153.83	152.39	161.30	161.23	162.32
9.79	144.05	149.85	161.24	160.34	153.90	152.59	161.37	161.24	162.32
9.82	144.00	149.57	161.22	160.33	153.95	152.42	161.36	161.22	162.34
9.86	143.76	149.13	161.18	160.36	154.14	152.94	161.38	161.25	162.30
9.89	143.51	149.75	161.24	160.31	153.93	152.79	161.37	161.17	162.34
9.92	143.61	150.05	161.13	160.34	153.56	152.49	161.27	161.20	162.32
9.96	143.11	149.73	161.24	160.42	153.84	151.90	161.31	161.14	162.30
9.99	145.33	149.70	161.18	160.42	154.04	153.00	161.35	161.15	162.32
10.02	145.62	149.65	161.16	160.43	153.82	152.65	161.29	161.16	162.32
10.06	145.98	149.94	161.16	160.33	154.01	152.68	161.39	161.26	162.34
10.09	145.94	149.36	161.18	160.42	154.04	152.77	161.31	161.21	162.32
10.12	145.51	149.70	161.18	160.46	154.01	152.78	161.38	161.22	162.30
10.16	147.03	149.75	161.16	160.43	154.09	152.95	161.36	161.20	162.30
10.19	146.83	150.04	161.16	160.43	153.72	152.52	161.29	161.23	162.34
10.22	147.03	150.21	161.29	160.46	153.95	153.05	161.36	161.26	162.32
10.26	147.32	150.00	161.25	160.49	154.17	153.11	161.31	161.18	162.32
10.29	147.04	149.66	161.17	160.38	153.93	152.86	161.34	161.17	162.32
10.32	149.21	149.38	161.23	160.43	154.09	152.69	161.36	161.16	161.96
10.36	126.07	135.28	159.84	157.65	133.72	128.98	156.65	156.25	161.60
10.39	123.39	120.98	155.05	148.40	120.74	115.28	149.88	149.78	160.79
10.42	120.82	111.26	148.75	140.11	111.30	106.55	143.55	144.19	160.18
10.46	116.69	106.11	142.62	133.91	104.74	98.97	137.61	138.76	159.46
10.49	113.97	100.37	136.75	128.55	99.42	96.31	131.93	133.46	158.72
10.52	110.43	96.99	131.35	123.51	96.32	94.44	126.91	128.55	158.05
10.56	107.63	93.69	126.32	118.79	94.29	91.17	122.41	123.92	157.35
10.59	104.41	91.37	121.57	114.14	91.05	87.99	118.16	119.78	156.72
10.62	102.36	88.76	117.08	109.99	89.87	88.19	114.51	115.83	155.98
10.66	99.71	87.15	112.98	106.28	88.86	87.54	111.10	112.32	155.39
10.69	97.45	85.71	109.28	102.98	87.57	86.03	107.95	109.11	154.69
10.72	95.37	84.43	105.86	99.99	86.50	84.86	105.19	106.14	154.09
10.76	93.31	83.18	102.81	97.46	85.15	81.95	102.43	103.27	153.37
10.79	91.84	82.26	99.98	94.93	83.59	82.30	99.98	100.72	152.73
10.82	90.04	81.63	97.42	92.78	82.92	82.35	97.88	98.41	152.15
10.86	88.58	80.58	95.12	90.93	82.38	81.95	95.93	96.29	151.61
10.89	87.04	79.68	92.99	89.14	81.73	81.48	94.09	94.30	151.00
10.92	85.61	78.86	91.11	87.58	81.34	81.02	92.32	92.53	150.39
10.96	84.22	78.24	89.44	86.22	80.51	80.30	90.75	90.97	149.79
10.99	83.40	77.82	88.02	84.95	79.92	79.70	89.45	89.38	149.20
11.02	82.34	77.19	86.57	83.81	79.35	79.10	88.04	88.04	148.64
11.06	80.80	76.83	85.36	82.78	78.64	78.27	86.83	86.79	148.05
11.09	80.17	76.31	84.23	81.93	77.97	77.75	85.74	85.63	147.43
11.12	79.41	76.01	83.11	80.96	77.39	77.31	84.62	84.44	146.86
11.16	78.87	75.58	82.22	80.24	77.07	76.89	83.62	83.48	146.35
11.19	78.31	75.13	81.27	79.43	76.62	76.44	82.67	82.53	145.74
11.22	77.51	74.90	80.46	78.88	76.06	75.88	81.72	81.69	145.22
11.25	76.82	74.46	79.74	78.26	75.66	75.48	80.96	80.89	144.73
11.29	76.34	74.06	79.01	77.64	75.36	75.25	80.24	80.06	144.19
11.32	75.88	73.88	78.44	77.21	75.12	75.04	79.56	79.45	143.65

11.35	75.44	73.52	77.94	76.71	74.86	74.72	78.95	78.77	143.15
11.39	75.10	73.36	77.34	76.26	74.52	74.27	78.32	78.21	142.66
11.42	74.67	73.22	76.84	75.86	73.94	73.91	77.71	77.75	142.16
11.45	74.18	72.95	76.39	75.49	73.67	73.64	77.26	77.11	141.64
11.49	73.83	72.74	75.93	75.02	73.50	73.43	76.80	76.76	141.10
11.52	73.46	72.56	75.49	74.70	73.28	73.17	76.29	76.29	140.63
11.55	73.10	72.37	75.13	74.48	73.03	72.88	75.82	75.82	140.13
11.59	72.90	72.25	74.79	74.14	72.83	72.72	75.51	75.44	139.64
11.62	72.68	72.13	74.49	73.87	72.75	72.53	75.14	75.07	139.17
11.65	72.49	72.05	74.26	73.61	72.45	72.34	74.81	74.77	138.74
11.69	72.39	71.91	73.95	73.40	72.31	72.20	74.49	74.53	138.24
11.72	72.14	71.67	73.63	73.20	72.25	72.07	74.21	74.21	137.73
11.75	71.91	71.66	73.48	72.90	72.02	71.88	73.91	73.91	137.30
11.79	71.85	71.49	73.16	72.83	71.92	71.81	73.67	73.70	136.85
11.82	71.64	71.38	73.06	72.51	71.82	71.68	73.35	73.35	136.36
11.85	71.36	71.29	72.74	72.49	71.73	71.58	73.22	73.14	135.95
11.89	71.11	71.18	72.63	72.20	71.51	71.33	72.89	72.93	135.52
11.92	71.20	71.13	72.51	72.07	71.45	71.31	72.76	72.80	135.03
11.95	71.01	70.97	72.32	71.92	71.30	71.26	72.54	72.68	134.64
11.99	70.88	70.88	72.08	71.90	71.28	71.10	72.45	72.45	134.20
12.02	70.87	70.83	71.92	71.63	71.23	71.09	72.25	72.32	133.75
12.05	70.57	70.75	71.80	71.59	71.11	70.90	72.13	72.13	133.36
12.09	70.54	70.72	71.74	71.48	71.01	70.86	71.96	72.10	132.93
12.12	70.47	70.69	71.53	71.35	71.02	70.84	71.82	71.89	132.53
12.15	70.42	70.56	71.51	71.22	71.00	70.75	71.73	71.77	132.12
12.19	70.32	70.51	71.31	71.20	70.80	70.69	71.71	71.64	131.72
12.22	70.14	70.50	71.19	71.01	70.76	70.54	71.59	71.63	131.32
12.25	70.16	70.45	71.11	70.89	70.67	70.49	71.47	71.47	130.93
12.29	69.96	70.29	70.98	70.80	70.58	70.40	71.38	71.31	130.51
12.32	70.01	70.34	70.92	70.81	70.56	70.37	71.18	71.25	130.12
12.35	69.92	70.17	70.83	70.76	70.50	70.35	71.19	71.16	129.74
12.39	69.70	70.18	70.72	70.69	70.51	70.21	71.09	71.09	129.36
12.42	69.88	70.14	70.69	70.54	70.54	70.32	70.98	71.05	128.98
12.45	69.66	70.06	70.60	70.46	70.35	70.28	70.90	71.01	128.61
12.49	69.70	70.06	70.64	70.42	70.39	70.21	70.90	70.93	128.21
12.52	69.70	70.06	70.57	70.39	70.46	70.21	70.86	70.94	127.87
12.55	69.61	70.01	70.41	70.37	70.41	70.19	70.66	70.74	127.47
12.59	69.56	70.04	70.44	70.25	70.40	70.11	70.76	70.80	127.13
12.62	69.52	70.03	70.43	70.29	70.36	70.14	70.62	70.76	126.77
12.65	69.57	70.08	70.30	70.15	70.37	70.08	70.59	70.63	126.39
12.69	69.44	69.88	70.21	70.10	70.17	70.06	70.50	70.64	126.03
12.72	69.41	69.92	70.28	70.10	70.24	70.14	70.50	70.65	125.69
12.75	69.48	69.95	70.14	70.03	70.32	70.10	70.54	70.54	125.33
12.79	69.38	69.96	70.22	70.04	70.29	70.04	70.51	70.51	125.01
12.82	69.42	69.90	70.15	69.97	70.15	70.04	70.41	70.55	124.63
12.85	69.36	69.87	70.12	69.94	70.20	70.01	70.34	70.38	124.25
12.89	69.38	69.78	70.04	70.00	70.18	70.00	70.33	70.36	123.96
12.92	69.32	69.87	69.94	69.87	70.20	69.98	70.34	70.42	--

SL 7520 Resin Data [3D Systems, 2001]

Liquid Material

MEASUREMENT	CONDITION	VALUE
Appearance		Clear Amber
Density	@ 25°C (77°F)	1.18 g/cm^3
Viscosity	@ 30°C (86°F)	450 cps
Penetration Depth (Dp)		4.9 mils
Critical Exposure (Ec)		9.5 mJ/cm^3
Part building layer thickness*		0.025mm, 0.075mm, 0.150mm (0.001in, 0.003in, 0.006in)

* Dependent upon part geometry and build parameters

Post-cured Material

MEASUREMENT	TEST METHOD	VALUE**	VALUE†
Tensile strength	ASTM D 638	62 – 65 MPa (9.0 – 9.4 ksi)	63 – 69 MPa (9.1 – 10.0 ksi)
Tensile modulus	ASTM D 638	2,937 – 3,158 MPa (426 – 458 ksi)	2,882 – 2,958 MPa (418 – 429 ksi)
Elongation at break	ASTM D 638	5.2 – 7.2 %	2.9 – 3.8 %
Flexural strength	ASTM D 790	97 – 103 MPa (14.1 – 15.0 ksi)	90 – 127 MPa (13.1 – 18.4 ksi)
Flexural modulus	ASTM D 790	2,827 – 2,903 MPa (410 – 421 ksi)	3,785 – 3,854 MPa (549 – 559 ksi)
Impact strength, notched Izod	ASTM D 256	15.5 – 18.1 J/m (0.29 – 0.34 ft-lbf/in)	10.7 – 15.0 J/m (0.20 – 0.28 ft-lbf/in)
Heat deflection temperature	ASTM D 648 @ 66 psi @ 264 psi	54°C (129°F) 49°C (120°F)	89°C (192°F) 72°C (162°F)
Glass transition, T$_g$	DMA, E" peak	68°C (154°F)	87°C (189°F)
Coefficient of thermal expansion	TMA (T < T$_g$)	99 ppm/m-°C	105 ppm/m-°C
Thermal conductivity		0.176 W/m-K (4.20 x 10^{-4} Cal/sec-cm-°C	
Hardness	DIN 53505	86	90
Density		1.24 g/cm^3	

** 90-minute UV post-cure

† 90-minute UV + 160°C Thermal

APPENDIX D-2

700 ND Resin Data [Rapid Prototyping Chemicals, 2001]

Properties

MEASUREMENT	METHOD	VALUE
Penetration Depth (DP)	Window panes	4.6 mils (0.12mm)
Critical Exposure (Ec)	Window panes	10.6 mJ/cm^2
Viscosity of liquid resin	Brookfield @ 30°C	500 cps
Green flex-modulus after 10 min.		130 MPa
Green flex-modulus after 1 hour		270 MPa
Flexural modulus after post-cure		2400 MPa
Tensile modulus after post-cure	ISO 527	2500 MPa
Tensile strength after post cure	ISO 527	71 MPa
Elongation to break	ISO 527	12.5%
Shore D		82
Impact after post-cure, unnotched	ISO 179	30 kJ/m^2
Glass transition, T_g	DSC	81°C

VITA 2

David Eric Roberts

Candidate for the Degree of

Masters of Science

Thesis: FREEFORM FABRICATION OF MULTIFUNCTIONAL COMPOSITE STRUCTURES

Major Field: Mechanical Engineering

Biography:

> Personal Data: Born in Spokane, Washington on March 16, 1977. The son of Kerry L. and Janet M. Roberts.
>
> Education: Graduated from Okmulgee High School, Okmulgee, Oklahoma in May 1995; received a Bachelor of Science degree in Mechanical Engineering with the Aerospace Option in May 1999. Completed requirements for the Masters of Science degree with a major in Mechanical and Aerospace Engineering at Oklahoma State University in August, 2001.
>
> Experience: Technical Intern, Lockheed Martin Tactical Aircraft Systems, 1998, 1999; Teaching Assistant, Oklahoma State University School of Mechanical and Aerospace Engineering, 1999-2001; Graduate Research Assistant, Oklahoma State University School of Mechanical Engineering, 2000-2001.
>
> Professional Memberships: Tau Beta Pi Engineering Honor Society, Pi Tau Sigma Mechanical Engineering Honor Fraternity, Phi Kappa Phi, and Golden Key National Honor Society.